meteorites tektites impactites

meteorites

EDITOR: Tadeusz A. Przylibski

December 2014

Vol. 3
Nos. 1-2

ISSN 2299-1220 (online) DOI: 10.5277/met1401

www.meteorites.pwr.wroc.pl

meteorites

"The first open-access journal focusing exclusively on meteoritics"

Editor: Tadeusz A. Przylibski

Associate editors

Ulrich Ott
Max-Planck-Institut für Chemie
Mainz, Germany

Hasnaa Chennaoui Aoudjehane
Hassan II University Casablanca
Casablanca, Morocco

Dominik Hezel
University of Cologne
Köln, Germany

Philippe Schmitt-Kopplin
Helmholtz Zentrum München
Neuherberg, Germany

Arnold Gucsik
Osaka University
Osaka, Japan

Editorial Board

Łukasz Karwowski
University of Silesia
Sosnowiec, Poland

Andrzej S. Pilski
Nicholaus Copernicus Museum
in Frombork
Frombork, Poland

Ryszard Kryza
Wrocław University
Wrocław, Poland

Andrzej Muszyński
Adam Mickiewicz University
Poznań, Poland

Anna Karczemska
Lodz University of Technology
Łódź, Poland

Stanisław Mitura
Koszalin University of Technology
Koszalin, Poland

Meteorites Publishers

Wrocław University of Technology
Faculty of Geoengineering, Mining and Geology
Wybrzeże S. Wyspiańskiego 27
50-370 Wrocław, Poland

Polish Meteorite Society
ul. Będzińska 60
41-200 Sosnowiec, Poland

Photo on cover: The main mass of Boumdeid chondrite L6, S2, W0
(Photo by Svend Buhl)

Meteorites
Vol. 3, Nos. 1–2, 2014, 1
www.meteorites.pwr.wroc.pl

JOURNAL INFORMATION

Meteorites provides a coherent international forum for the publication of research in the field of meteoritics and its related disciplines. The topics of interest range from, but are not limited to, meteorites and other kinds of extraterrestrial matter and their sources of origin through the examination of the mineral resources of the Solar System, to tektites, impactites, and impact structures.

Meteorites invites the submission of articles covering the broadly defined field of meteorites. In addition to publication of research results, however, authors are encouraged to share and present astronomical, petrological, mineralogical, geochemical, and isotopic data on all groups and types of meteorites. Meteorites is intended to serve as a basic reference source for in-depth analyses and compilations on particular meteorite groups and their parent bodies, as well as the genesis and evolution of the Solar System, as well as other planetary systems.

Considering the progress of human space exploration and conceivable colonization of other planets, this data will likely play an important role in the recognition and exploitation of extraterrestrial mineral resources. Therefore, in light of the potential benefits, Meteorites editors have no intention of rejecting paper submissions pertaining to the research of meteorites with provisional names and pending classifications, esp. prior to their approval by the Committee on Meteorite Nomenclature of the Meteoritical Society.

Meteorites invites the publication of important papers intended as reference sources for other researchers, as well as compilations and interpretations of other works on meteorites of lesser scientific importance and their parent bodies. Not only does Meteorites welcome submissions of research descriptions and results regarding 'rare' meteorites, and topics such as newly-discovered extraterrestrial mineral species, but it also gladly accepts articles covering more common groups of meteorites. Due to their relatively low scientific value in terms of current research trends, many interesting research results are quietly filed away into archives instead of being published in leading scientific journals.

Our intention is not to compete with existing journals, but to add to the currently limited publication space for researches on meteorites. Meteorites editors will gladly accept any reliable research results, including submissions that are virtually impossible to publish in today's existing journals due to the apparent mediocrity of the specimens studied. At Meteorites, we believe that even profoundly studied meteorites can have a significant and relevant bearing on our knowledge and understanding of the Solar System. Meteorites will, in time, develop into a repository of data and knowledge available for everyone with an interest in extraterrestrial matter.

Our purpose is to develop a new interdisciplinary journal covering the multitude of subject matters involved in meteorite research. Due to an insufficient amount of publication space, the increasing number of specimens available for research, and a growing list of research centers, only a small percentage of valuable submissions is ever brought to publication.

Through the Open Access publications, Meteorites aims to support academic work and to act as an accessible research data center. Meteorites is available free of charge in print or digital document. Each paper is thoroughly reviewed by experts in the field. Submissions should be sent directly to the e-mail address of the secretary: meteorites@pwr.wroc.pl. Authors are required to follow the guidelines available at http://www.meteorites.pwr.wroc.pl

Meteorites
Vol. 3, Nos. 1–2, 2014, 3
www.meteorites.pwr.wroc.pl

FROM THE EDITORIAL BOARD

It is with great pleasure that we present the long-awaited double issue of the third volume of *Meteorites*. This volume marks the end of another year of the journal's publication. Despite many challenges, the generous contribution of numerous people has enabled us to continue publishing our journal. The editor-in-chief would like to express his deepest gratitude to everyone who has cooperated with the extended editorial team of *Meteorites*. I would also like to convey words of appreciation to my fellow editors. However, the greatest recognition is owed to all the authors who have decided to publish their research in *Meteorites*. The editorial board makes every possible effort for articles to reach a broad readership across the world. The number of citations of our articles attests to the fact that the rigorous work on the part of the editorial board is yielding the desired results. We likewise owe a debt of gratitude to the reviewers who have played an integral part in ensuring the high standard of our articles. We welcome the steady expansion of our editorial board, as well as new authors and reviewers who cooperate with us. We would like to assure you that the editorial board is committed to the continual improvement of both the quality of articles and the recognition of *Meteorites*. It is imperative to our success that more authors place their trust in *Meteorites* and decide to publish their research in our journal. Therefore, we invite you to submit articles to *Meteorites*. We will never cease our efforts to build and maintain your confidence with our journal.

We hereby present the third volume of *Meteorites*. The articles were being gradually published online in the order of their submission. Consequently, they are available free of charge on our website prior to the publication of the entire volume. This volume includes articles on recently classified ordinary chondrites. One of them was an observed fall in Mauritania in West Africa. A relatively low number of published research papers pertains to meteorites from Mauritania. Therefore, we encourage you to get acquainted with accounts of the witnesses of the fall and the characteristics of the meteorite. The articles also deal with a significant variation between the chemical composition typical for ordinary chondrites of L and LL types and the properties of the chondrites in question. It is an engaging subject matter worthy of further analysis which may have a profound bearing on our knowledge of the chemical composition of the parent bodies of L and LL chondrites. Another article also addresses the significant issue of thermophysical properties of meteorites. The correlation between meteorites and their parent material allows for the development of more precise models of the parent bodies of chondrites and their thermal evolution. It is of fundamental importance to our understanding and ability to identify the underlying processes which shaped the early stages of formation of protoplanetary bodies in the Solar System. Moreover, it may be a starting point for further research which will serve as the basis of proper characteristics of the internal composition of small Solar System bodies which are the source of ordinary chondrites.

We wish you a pleasant reading experience.

The Editorial Board

Meteorites
Vol. 3, Nos. 1–2, 2014, 5–18
www.meteorites.pwr.wroc.pl
DOI 10.5277/met140101

THE METEORITE FALL NEAR BOUMDEID, MAURITANIA, FROM SEPTEMBER 14, 2011

Svend BUHL[1], Cheikhalhoussein TOUEIRJENNE[2], Beda HOFMANN[3], Matthias LAUBENSTEIN[4], Karl WIMMER[5]

[1] Meteorite Recon, Mühlendamm 86, 22087 Hamburg, Germany
[2] Director Complex Scientifique Taleb Ahmed ould Toueirjenne (COMSTAT), Bp 1112 Nouakchott, Dar Naim, Mauritania
[3] Naturhistorisches Museum der Burgergemeinde Bern, Bernastrasse 15, CH-3005 Bern, Switzerland
[4] Laboratori Nazionali del Gran Sasso, S.S.17/bis, km 18+910, I-67100 Assergi (AQ), Italy
[5] Rieskratermuseum, 86720 Nördlingen, Germany

Abstract: On the evening of September 14, 2011 at 21:00 GMT a bright bolide was observed by hundreds of eyewitnesses in the area north and west of the town of Kiffa, in the department of Assaba, in south Mauritania. A terminal fragmentation and sound phenomena were observed near the end point of the trajectory. At least one mass of 3.5 kg was observed to impact and recovered the morning after the fall near Boumdeid (or Bou Mdeid), around 60 km north of Kiffa. Subsequently a large number of eyewitness accounts were recorded and mapped by GPS. The present paper provides a scenario for the trajectory of the Boumdeid (2011) meteorite based on the available parameters and wind data at the relevant altitudes. In addition the paper presents the results of the mineralogical and chemical analysis of the recovered meteorite which is consistent with a classification as ordinary chondrite of type L6, shock stage S2, and a weathering grade of W0. Following its analysis and classification, the meteorite was published under the official name Boumdeid (2011) in Meteoritical Bulletin, no. 100, MAPS 49(8), (2014). Gamma-ray spectroscopy was conducted 84 days after the fall and the detection of short-lived radionuclides such as ^{56}Co and ^{46}Sc confirmed the recency of the event. Derived from the data of ^{60}Co, ^{54}Mn and ^{22}Na the approximate preatmospheric radius of the meteorite body was 10–20 cm. The report is also intended to serve as a case example for post-event data recovery and trajectory reconstruction in areas not covered by sky-camera networks and with limited scientific infrastructure.

Keywords: Boumdeid (2011); meteorite fall; Mauritania; trajectory scenario; L6 chondrite; cosmogenic radionuclides

INTRODUCTION

Although Mauritania has a land surface that is triple the size of the neighbouring Western Sahara, and double the size of Morocco, Mauritania's meteorite finds are only a fraction of the two countries. Prior to the Boumdeid (2011) event, a total of only 18 meteorites were known for Mauritania. Among the latter were 14 finds and four falls. In comparison, the data base of the Meteoritical Bulletin currently lists 879[1] meteorites for Morocco (including 6 falls), and 106 meteorites for Western Sahara (including 3 falls). The reasons for the disparity in meteorite finds are manifold. While geological and geomorphologic differences are relevant to some extent, the actual cause is determined by social factors such as population density, education level, limited access to modern information technology, lack of infrastructure, and the absence of an established commercial market for rocks, minerals and fossils in Mauritania. In combination, these conditions provide an environment in which the general interest in the subject is low, and in which the scientific potential of Mauritania's meteorite heritage is yet be recognized. Thus, one of the objectives of this work is to raise the awareness for meteorites in Mauritania and to offer an example for the future investigation of meteorite falls and finds within the country.

Corresponding author: Svend BUHL, SvendBuhl@web.de

[1] This number includes meteorites with NWA (Northwest Africa)-designation for which no find locations are recorded. It is widely assumed that some of these undocumented finds were found in neighboring countries.

GEOGRAPHY, GEOLOGY AND TOPOGRAPHY OF THE FALL AREA

Assaba region and department are located in southern Mauritania and governed by its capital Kiffa, one of the larger Mauritanian department towns with currently around 36,000 inhabitants (The mean population density in Mauritania is 1.7 persons per km^2). The Assaba department borders the neighbouring departments of Brakna and Tagant to the north, the department of Hodh El Gharbi to the east, the border to Mali to the south, and the Mauritanian departments of Gorgol and Guidimaka to the west. Kiffa is also a major local market place with the important east-west road from Mauritania's capital Nouakchott to the city of Nema passing through its center. Boumdeid is located around 93 km north of Kiffa and connected to it by the Tidjikja – Kiffa road (Fig. 1a).

Kiffa, and Boumdeid, are situated in the Taoudeni Basin, the largest sedimentary basin in Northwest Africa, which covers two thirds of the West Africa craton. The basin that makes up most of Mauritania's east and northeast is composed of a sequence of essentially flat-lying, undeformed Upper Proterozoic and Palaeozoic sedimentary rocks with total thickness reaching 6 km. In the Assaba region, the Taoudeni Basin is masked by overlying Mesozoic to Cenozoic sandstone sediments (Blanchot, 1975; Mattick, 1982). West of Boumdeid, the Taoudeni Basin borders the Palaeozoic Maurita-

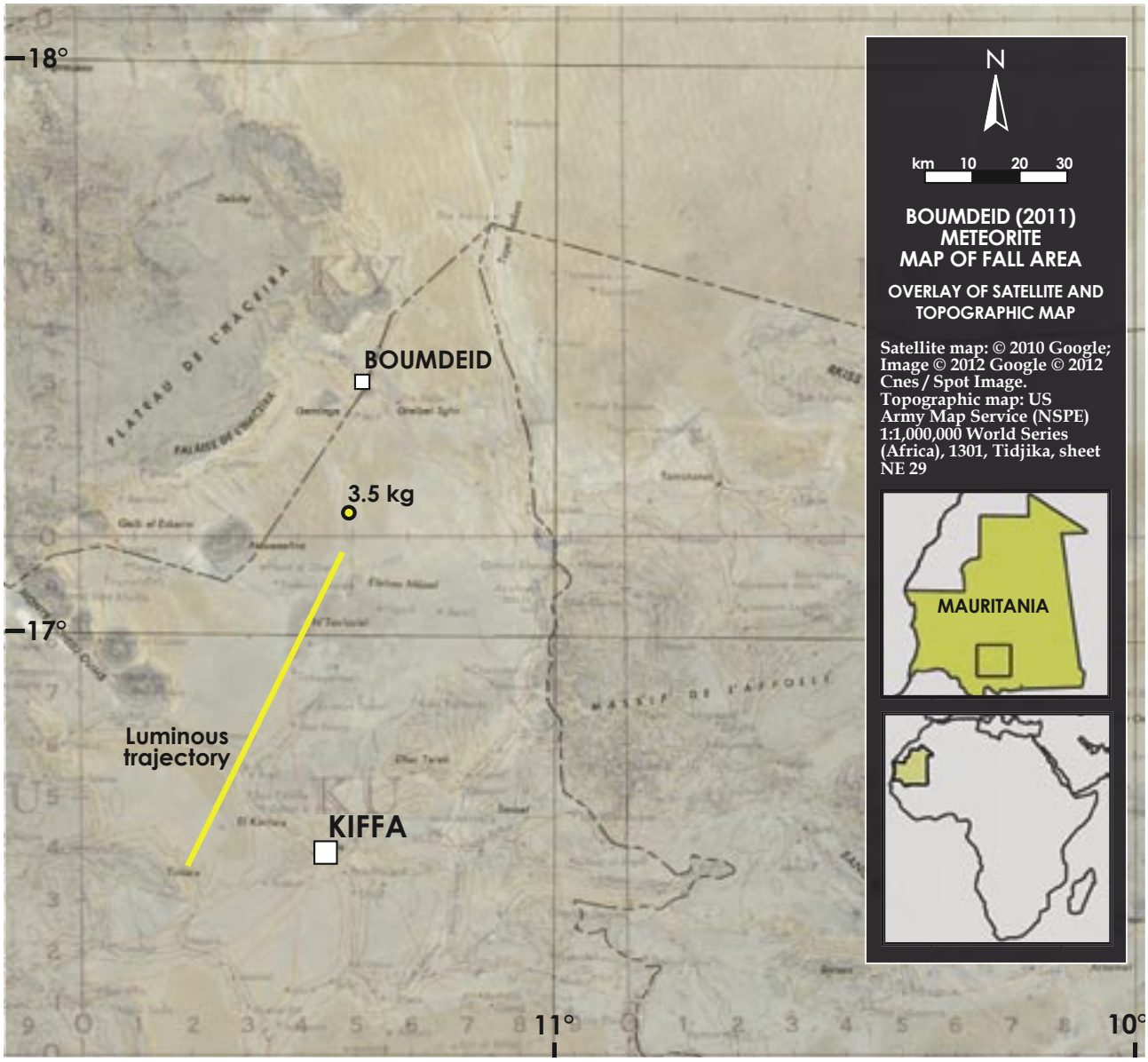

Fig. 1a. Boumdeid (2011) meteorite, map of fall area. Overlay of satellite chart and topographic map, compiled by S. Buhl. Satellite map: © 2010 Google; Image © 2012 Google © 2012 Cnes / Spot Image. Topographic map: US Army Map Service (NSPE) 1:1,000,000 World Series (Africa), 1301, Tidjika, sheet NE 29.

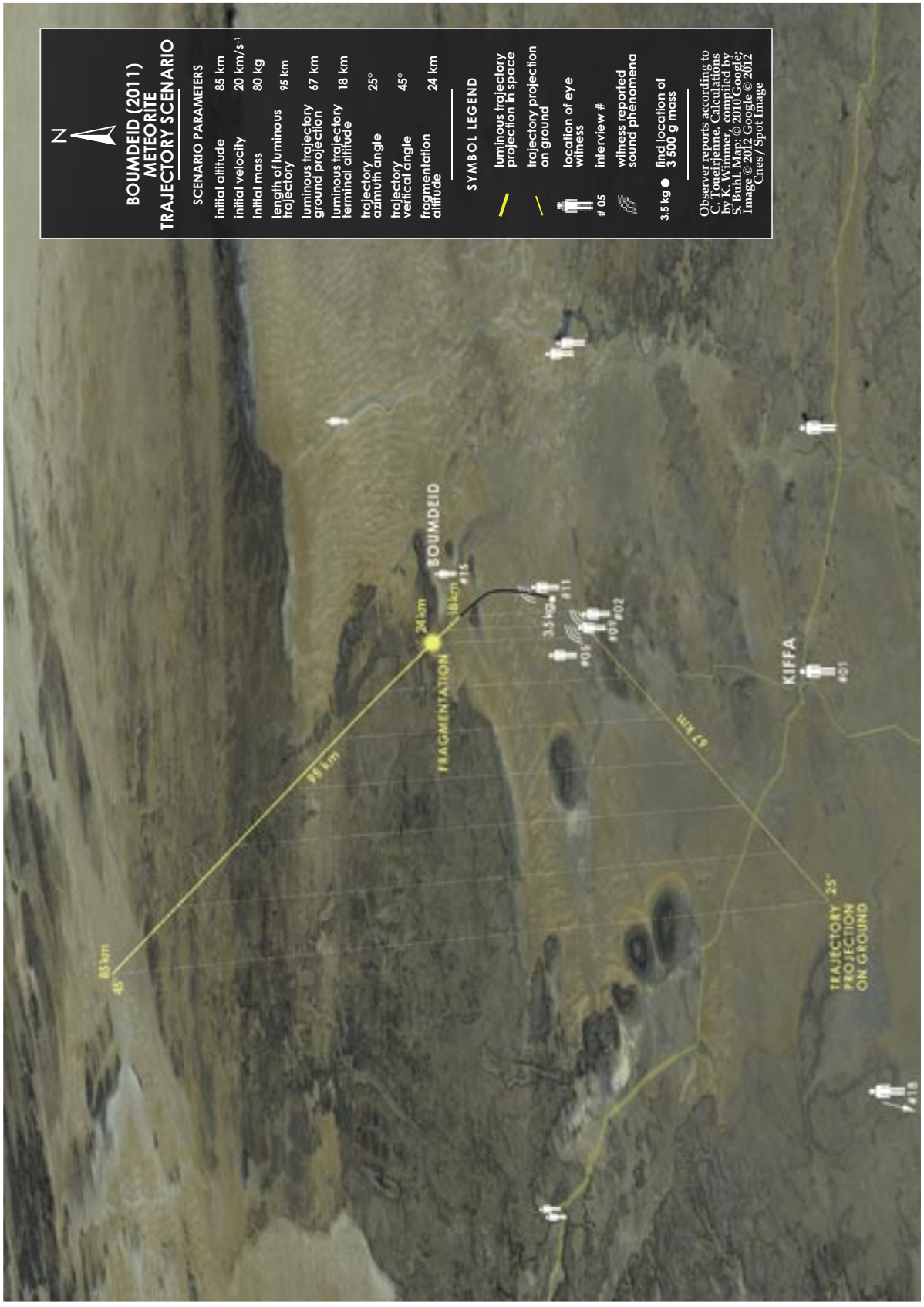

Fig. 1b. 3D-trajectory scenario of the Boumdeid (2011) meteorite fall of September 14, 2011, 21:00 GMT. For further parameters and comments see table 1. Observer reports according to C. Toueirjenne. Calculations by K. Wimmer, compiled by S. Buhl. Map: © 2010 Google; Image © 2012 Google © 2012 Cnes / Spot Image

nides chain (or greenstone belt), mainly composed of deformed sedimentary, igneous and metamorphic rocks of the Precambrian to Palaeozoic age. Boumdeid is situated between the inselbergs of the Mauritanides chain and near a seasonal drainage system extending from the plateaus in the west into the lower plains of the basin. The topography of the closer Boumdeid area is dominated by a cover of continental sands and shales as well as Holocene desert deposits which cover much of the Palaeozoic sequence in a nonconforming manner (Mattick, 1982).

The surface geomorphology of the immediate fall area is determined by Pleistocene alluvial deposits and Holocene Ergs with abundant SW-NE oriented barchan systems. Most of the topography of the Boumdeid area is flat, dipping gently to the SE, with the exception of the isolated mesas in the northwest and south of the town. The Assaba region is extremely arid with very little annual rainfall. At Kiffa, the mean annual rainfall is 350 mm, however, slightly farther north at Tidjikdja only 140 mm falls per year (Hughes & Hughes, 1992).

The vegetation at the fall site is sparse. The most abundant plants are Ziziphus Mauritania, the grass Panicum turgidum, the desert melon Calotropis procera and the small tree Capparis decudea. Acacia species are confined to the rocky beds of wadis and the gravel alluvium of outwash fans (Wickens, 1995). Migrating flocks of camel and goats are frequently abundant and litter the surface with their excrements, which, as reported by locals, makes the visual recognition of the very similar looking recently fallen meteorites particularly difficult.

FIRST MEDIA REPORTS

A very early note on the incident was released by the national press agency of Mauritania, Agence Nouakchott d'Information (2011), on September 15, 2011, one day after the fall. According to the report, a luminous body fell from the sky near Boumdeid on the evening of September 14. It was observed from as far as Kiffa and near its endpoint, explosions were heard that terrified the local population (ANI, 2011, see appendix no. 1).

The news of the event spread quickly among local media and found its way on several websites and blogs within hours. According to the website of *Carrefour de la République Islamique De Mauritanie* (CRIDEM), the "large meteorite that fell in the vicinity of Boumdeid" illuminated a large area "before causing a loud explosion", which created "panic among the population." According to the source, the event remained unclear at the time of publication whether it was caused by "a meteor or a piece of a satellite"(CRIDEM, 2011, see appendix no. 1).

WITNESS ACCOUNTS

While in Kiffa and Nouakchott speculations on the cause of the event were still ongoing, one of the authors, Cheikhalhoussein Toueirjenne, Director of COMSTAT, decided to investigate the event in person to collect and record first hand accounts in the field. It is due to Mr. Toueirjenne's diligent and thorough efforts, that this recent meteorite fall in Mauritania could be comprehensively documented in the week following the event.

The evening of Wednesday, September 14, was cloudless and bright, being just the second night after full moon. The nomads in the Boumdeid area had lit their campfires and most people were still outside their tents preparing dinner. In Kiffa, 93 kilometers south of Boumdeid, the streets were busy with traffic on the main roads and many people who enjoyed the cool evening breeze were outside. At 21:00 UTM, people west of Kiffa and in the city spotted an intensely bright object that appeared in the west and that was quickly moving to the north, illuminating the streets "like during the brightest day" (witness #01, see appendix no. 2). Observers located further north and closer to the trajectory reported a south to north moving body that "exploded" along its path, after which "three smaller stars" continued in slightly diverging directions (witness #02, see appendix no. 2). The trajectory azimuth and general direction reported for the fan shaped spreading of the detonation fragments was later found consistent with the find location of the single mass recovered. Other observers located near the endpoint of the trajectory reported explosive sounds. One group of witnesses camping in close proximity of the fall site reported "three or four explosions from the south" and the swishing noise of a falling object followed by the sound of its impact (witness #11, see appendix no. 2).

In total 30 interviews were conducted and 18 accounts were recorded in detail (see appendix no. 2).

With the exception of witnesses #05 and #09, those observers that gave a direction of movement for the light phenomenon reported a south to north trajectory. One witness who observed the bolide directly overhead was unsure about its direction.

TRAJECTORY AND STREWNFIELD

It is well established practice to predict strewn fields by model calculations based on at least two independent camera records. In contrast it is virtually impossible to do the same based on visual observations alone. Eye witness reports, even by astronomically experienced observers, are rarely precise enough and sometimes even contradictory (e.g. Bronshten, 1999; Pugh et al., 2004; Beech et al., 2007). Thus, additional facts are required, like the coordinates of the recovered meteorites, to enable at a minimum a fall scenario and strewn field constraints.

Fortunately, that is the case with the Boumdeid (2011) fall where the location of one recovered meteorite is well documented. This position serves as an anchor point for the analysis of visual and acoustic observations (Fig. 1b). One of the first steps in building an accurate trajectory model is to account for wind drift during the dark flight of the meteorite. All available wind data was collected from sounding stations as far as 500 to 730 km from the fall area (mainly stations 61442 GQNN Nouakchott, 61291 GABS Bamako and 61641 GOOY Dakar at 12:00 and 00:00 GMT) as obtained from the NOAA/ESRL Radiosonde Database Archive. Therefore, the interpolation in space and time is subject to an element of uncertainty. The resulting scenario, however, appears to be quite consistent. The model shows very little wind in the high atmosphere, predominant wind direction from nearly east (from about 100°) and an average wind speed of 7 ms^{-1} in the relevant altitudes.

With these data, a dark flight calculation based on the single body theory (Ceplecha et al., 1998) yields an offset from the projected trajectory of only about 1 km from the actual impact location of the 3.5 kg mass. The shift defines a point about 1 km east of the find location through which the ground projection of the extrapolated trajectory has to go.

The next parameter necessary for a reconstruction of the trajectory is its azimuth angle. The combination of visual observations #1 and #2 with acoustic observations #2 and #9 leads to a SSW to NNE directed trajectory with an azimuth angle around 25°. Interestingly, and in contrast to the other observers, the two witnesses #5 and #9 report an incident direction "from North to South". These conflicting reports are very common in similar scenarios where observers directly under the trajectory have difficulty perceiving the true direction of movement. Also there is the possibility that their description may refer to the direction of observation rather than to the direction of the meteor movement, a misunderstanding that occurs frequently with non-standardized interviews. From personal experience (K. Wimmer), another explanation might be that the shadow movement on the ground dominated the observer's perception, who, surprised by the extremely fast phenomenon overhead and out of normal visual range, looked up too late.

The initial height of fireballs of comparable size is typically in between 80 km and 90 km (e.g. Popova et al., 2009). Assuming a statistically average height of 85 km and combining it with observation #1 from Kiffa the vertical angle of the trajectory can be estimated to be approximately 45°. Using these values, the resulting total length of the luminous trajectory is about 95 km and its ground projection about 67 km. Assuming a typical initial velocity of 20 kms^{-1} this corresponds to a meteor duration of about 5.9 s.

According to observer #2 the fireball released three major fragments upon its explosion. This fragmentation happened at an altitude of about 24 km or below as indicated by the locations where the sonic boom was perceived (Fig 1b). The fragment becoming the recovered meteorite was visible down to 18 km. Due to the lack of data regarding precise velocity and direction of flight we have no information about the total mass on the ground or the mass of other fragments. Derived from radionuclide measurements of ^{60}Co, ^{54}Mn and ^{22}Na, the preatmospheric meteoroid radius can be constrained to 10-20 cm. With a bulk density of 3500 kgm^{-3} this corresponds to an initial mass between 14 kg and 114 kg for a spherical body. Allowing for a non-spherical shape the upper limit may be up to about 150 kg.

The mass loss by ablation during the atmospheric passage increases strongly with the meteoroid velocity. Using the maximum initial mass of 150 kg and a minimum final mass of 3.5 kg, i.e. the recovered meteorite, we can constrain the upper limit for the initial velocity. With the typical ablation coefficient of $1.4 \cdot 10^{-8}$ s^2m^{-2} for ordinary chondrites we find an initial velocity lower than 23 kms^{-1}, compatible with our assumption.

With one meteorite already found, the strewnfield with the highest probability for meteorites in the mass

range from 100 g to 10 kg with typical drag and shape factors (Wimmer, 2009) can be constrained to an area of 8 km × 2.5 km.

No information on time delays between the termination of the fireball, the visible fragmentation and the observed sound phenomena were reported. Those eyewitnesses reporting sound phenomena explained though, that the explosion noise and the hissing sound of a falling object were perceived subsequent to the visible fragmentation and termination of the fireball. Also, no durations for these sounds were given.

Despite the lack of data, the resulting deductions are plausible as they are consistent and similar to other well-understood meteorite falls. Due to the lack of objective records, however, these results are considered to only be the most likely scenario based on existing assumptions and uncertainties. Table 1 gives an overview over its parameters with their most probable ranges.

THE FIND

The encampment of Sidi Mahmoud Ould Belkheir Ould Eabeid (witness #11), a camel herdsman in the service of Sidi Ould Sidibrahim of Tejkanet, is situated 31 km south of Boumdeid at 17°10'29.748"N, 11°20'28.8"W. It was in his family's "backyard" that the recovered mass fell, amidst a flock of camels, and just seven meters from where he and his company were camping (Fig. 2).

This is how Sidi Ould Eabeid described the event: "We were preparing dinner when suddenly the torch I was holding was no longer necessary as night had become bright day. We became very frightened as it appeared that the day of the last judgement had begun. Just after the light had passed there were three or four explosions from the South, and after this we heard an *ishshsh*-like sound that terminated in a big thud. We searched for the object that obviously had fallen upon us but we only discovered a hole in the soil." On the morning following the event, a man named Sidi Mohamed Ould Alharthi, called Albadad, arrived and said he had found the meteorite. The 3.5 kg stone was then broken apart and pieces of it were distributed as souvenirs "to everybody who asked for one." (witness #11, see appendix no. 2)

The find location of the single recovered mass was some 30 meters downhill from the camp in the direction of flight. No photos of the complete mass are known. The mass of the recovered stone prior to breaking it apart was given with around 3.5 kg. It was described as an angular stone with smoothly rounded edges covered in a dull black skin showing several thumbprint-like indentations. According to the finder the main fragment of around 1.6 kg was handed over to local authorities that kept the stone for further investigation. The second large fragment of 1.59 kg was later obtained by one of the authors (S. Buhl) and is shown in Fig. 3.

EXTERIOR MORPHOLOGY

Fragments of the Boumdeid (2011) meteorite reveal a thin but well developed (0.4 mm) primary fusion crust and on one surface a less thick (0.1 mm) secondary fusion crust. The surfaces indicating primary

Table 1. Values and probable ranges of the Boumdeid fall scenario parameters.

Parameter	Value	Range	Comment
Initial altitude	85 km	80 – 90 km	assumption, typical range
Initial velocity	20 kms^{-1}	< 23 kms^{-1}	assumption, upper limit calculated from mass loss
Initial radius		10 – 20 cm	^{60}Co, ^{54}Mn and ^{22}Na data
Initial mass	80 kg	14 – 150 kg	assumption, range derived from initial radius with bulk density 3500 kgm^{-3}
Trajectory azimuth angle	25°	15° – 35°	
Trajectory vertical angle	45°	35° – 55°	
Fragmentation altitude	24 km	25 – 19 km	from sonic boom observation
Luminous trajectory terminal altitude	18 km	17 – 19 km	from recovered meteorite mass
Length of luminous trajectory	95 km		
Length of luminous trajectory ground projection	67 km		
Meteor duration	5.9 s		based on assumptions above
Dark flight duration	157 s	135 – 175 s	for the recovered meteorite

Fig. 2. Find location of the 3.5 kg Boumdeid (2011) meteorite. The car marks the spot where the camp of Sidi Mahmoud Ould Belkheir Ould Eabeid (witness #11) was located in the night of September 14/15. The meteorite was found on the opposite slope of the ridge, approx 30 m behind the tall acacia next to the car. Photo: A. Mohamed

Fig. 3. Image of the 1.59 kg fragment that was broken from the 3.5 kg mass recovered near Boumdeid on the morning of September 15, 2011. Fractions are caused by the finder who broke the individual meteorite apart to look inside. Note the prominent impact marks on the right of the specimen. Scalecube is 1 cm. Photo: S. Buhl

atmospheric ablation show few distinct regmaglypts with an average diameter of 12 mm and an average depth of 6 mm. No visible oxidation is present on the fusion rind and only minor rust spots are visible on the fragmented surfaces.

The largest fragment remaining from the shattered ~3.5kg mass shows an elongated and rounded shape with one angular-edged surface as an exception. The flat fusion crusted fragmentation plane indicates that the meteorite broke apart along a pre existing fracture plane prior to or during atmospheric ablation. The large size of the fraction plane indicates that at least one other fragment detached from the initial mass prior or during the ablation phase. This observation is consistent with the eyewitness report, which stated that the meteor parted into 3 fragments.

COSMOGENIC AND PRIMORDIAL RADIONUCLIDES

Of the fragments broken from the ~3.5 kg stone, several were obtained by one author (S. Buhl) and submitted to institutions in Italy and Switzerland for further analysis. The head of the Special Techniques Service at the Gran Sasso National Laboratory, Matthias Laubenstein, conducted measurements of cosmogenic radionuclides. Beda Hofmann from the Natural History Museum in Bern subsequently conducted the chemical and petrological analysis and classification. Both institutes worked with the same 53.60 g partially crusted sample fragment (NMBE 41388).

The concentrations of short-lived cosmogenic radionuclides, as well as long-lived cosmogenic ^{26}Al and natural radioactivity, were measured using non-destructive gamma-ray spectroscopy. One fragment of the ordinary, L6 chondrite Boumdeid (2011) was measured in the STELLA (SubTerranean Low Level Assay) facility of the underground laboratories at the Laboratori Nazionali del Gran Sasso (LNGS) in Italy, using a high-purity germanium (HPGe) detector of ca. 400 cm^3 (Arpesella, 1996). The specimen was measured at LNGS 84 days after the fall, so that short-lived radionuclides such as ^{56}Co (half-life = 312.13 d) and ^{46}Sc (2.6027 y) could still be detected. The counting time was 12.616 days. The counting efficiencies were calculated using a Monte Carlo code. This code is validated through measurements and analyses of samples of well-known radionuclide activities and geometries. The uncertainties in the radionuclide activities are dominated by the uncertainty in the counting efficiency, which is conservatively estimated at 10%. The average density and composition were taken from Britt and Consolmagno (2003), and from Jarosewich (1990), respectively.

Table 2 lists the measured activity concentrations for the detected short- and medium-lived cosmogenic radionuclides (^{7}Be, ^{58}Co, ^{56}Co, ^{46}Sc ^{57}Co, ^{54}Mn, ^{22}Na, ^{60}Co, ^{44}Ti, ^{26}Al). The given activities are already calculated back to the date of fall following the simple decay law, and taking into account the time that passed between the fall of the meteorite and its measurement. In order to derive an approximate size of the meteorite body, the data of ^{60}Co, ^{54}Mn and ^{22}Na were used. Assuming the ^{59}Co concentration in Boumdeid

Table 2. Summary table for the detected cosmogenic radionuclides in the specimen of the Boumdeid (2011) L chondrite

Sample Weight [g]		NMBE 41388 55.2
radionuclide	half-life	specific activity [dpm·kg^{-1}]
^{7}Be	53.22 d	91 ± 20
^{58}Co	70.38 d	4 ± 1
^{56}Co	77.236 d	4 ± 1
^{46}Sc	83.788 d	9.0 ± 0.8
^{57}Co	271.8 d	8.9 ± 1.4
^{54}Mn	312.13 d	71.7 ± 7.3
^{22}Na	2.6027 a	91.9 ± 9.5
^{60}Co	5.27 a	< 0.47
^{44}Ti	60 a	< 2.5
^{26}Al	7.17×10^{5} a	57.1 ± 6.1

(2011) to be 600 ppm (Jarosewich, 1990), the resulting specific activity was directly compared to the calculations of Eberhardt et al. (1963), and Spergel et al. (1986). This comparison gave a possible range for the radius of <20 cm. The ^{22}Na data was compared to the calculations of Bhandari et al. (1993) for H chondrites, correcting obviously for the differences between L and H chondrites in composition. The resulting possible range in the radius is (10–15) cm. Finally, the data of ^{54}Mn was normalised to the concentration of its main target Fe and then compared to the calculations of Kohman and Bender (1967), giving a range for the radius of ≤13 cm. Combining the radius estimates from the three radionuclides tests results in a conservative range for the radius of a spherical meteoroid of 10 to 20 cm. This range corresponds to a parent meteoroid mass of 14 to 114 kg. Assuming the production rates in L chondrites for ^{26}Al to be that of Leya and Masarik (2009), the expected saturation values for the above determined size range are 48 dpm·kg^{-1} and 62 dpm·kg^{-1}, respectively, for the radii 10 cm and 20 cm. Thus, taking the measured value for ^{26}Al of 57.1 ± 6.1 dpm·kg^{-1}, the results fall well within the range obtained for the radius. Since no noble gas data is available, these estimates have to be taken as preliminary. Additionally, given the stringent low value of ^{60}Co in the specimen, the sample could also have come from the outermost surface of a bigger parent body.

Table 3. Results for the naturally occurring radioactive elements Th, U, and K in the sample of the Boumdeid (2011) L chondrite. The reported uncertainties are expanded uncertainties, the upper detection limits are given with a confidence level of ca. 68%

Sample Weight [g]	NMBE 41388 55.2
radionuclide	concentration [ng·g^{-1}]
^{238}U	14 ± 2
^{232}Th	38 ± 5
radionuclide	total K concentration [mg·g^{-1}]
^{40}K	0.89 ± 0.09

The decay of the short-lived radioisotopes, with half-lives less than the orbital period, represents instead the production integrated over the last segment of the orbit. The fall of the Boumdeid (2011) L chondrite occurred in the preparatory phase of the current solar cycle 24 as indicated by the publicly available neutron monitor data (Bartol, 2012). As in the case of e.g. the Jesenice L chondrite (Bischoff et al., 2011), the galactic cosmic ray flux was therefore moderately high in the six months before the fall. The activity for the very short-lived radionuclides ^{57}Co and ^{54}Mn are expected to be close to maximal following the sunspot number as reported in Bischoff et al. (2011) and the references cited therein. This is confirmed by our measured values for ^{57}Co and ^{54}Mn, normalised to their primary targets of Co, and Fe/Ni respectively.

The specific activities are given in dpm (decays per minute, 60 dpm = 1 Bq) per kg. The reported uncertainties are expanded uncertainties, the upper detection limits are given with a confidence level of ca. 68%. Radionuclide concentrations are normalised to the date of fall (September 14th, 2011). The concentrations of the natural radionuclides ^{232}Th and ^{238}U as well as for ^{40}K in the meteorite specimens are listed in Table 3. They are well in accordance with the average concentrations given in Wasson and Kallemeyn (1988) for L chondrites.

CHEMICAL AND PETROLOGIC ANAYLYSIS AND CLASSIFICATION

Boumdeid (2011) is an ordinary chondrite of type L6, shock stage S2, weathering grade W0. In thin section, Boumdeid (2011) shows a brecciated texture (Fig. 4). Both breccia matrix and clasts are strongly recrystallized (Fig. 5a, b) with only few well outlined chondrules preserved, and feldspar is coarse-grained (up to 100 μm), indicating petrologic type 6. The recognition of former chondrules is made difficult by both metamorphism and brecciation. However, several quite well preserved chondrules of barred olivine, porphyritic olivine and radial pyroxene type are visible (Fig. 6). The strong brecciation of this chondrite is quite difficult so see on broken surfaces, but is very evident in thin section. Individual clasts are up to 10 mm in size and are well delimited against a clastic, but well recrystallized matrix.

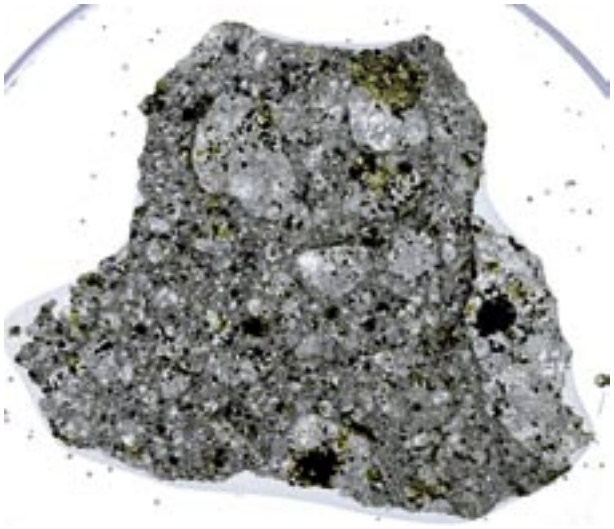

Fig. 4. Scan of polished thin section showing the brecciated nature of Boumdeid (2011) with only marginally visible chondrules. The dark grain (middle right) is the Cr-Al-rich chondrule, all other opaque grains are metal/troilite. Maximum width of section is 19 mm. Mosaic of images taken with digital microscope (Keyence VHX). Image: B. Hofmann

A single Cr-Al-rich chondrule (1.0 mm) with sodium-rich plagioclase (An_{25}), spinel-chromite solid solutions, ilmenite-geikielite and micron-sized baddeleyite is present in the largest clast of the analyzed thin section. Near the center of this chondrule, spinel is Al-rich, with increasing Cr-concentration to the rim (Fig. 7). Similar Cr-rich chondrules have been reported from a number of ordinary chondrites (e.g. Brearley et al., 1991; Krot & Ignova, 1992) but appear to be quite rare.

Electron microprobe analyses and backscattered electron images showed that olivine is homogeneous and has a mean composition of $Fa_{23.9}$ (identical value confirmed by XRD), homogeneous orthopyroxene has a composition of $Fs_{20.2}Wo_{1.6}$. The mineral chemistry is consistent with equilibrated ordinary chondrites of type L. Shock effects are generally minor, and the only common effect observed is the weak undulatory extinction of olivine. Some olivines show a partially recrystallized texture reminiscent of mosaicism, and some remnants of planar fractures are also visible, indicating a pre-metamorphic shock event largely masked by recrystallization. A single narrow shock vein cuts the thin section, showing melting of troilite. A cut metal grain shows an offset of ~250 μm. This vein appears to be younger than the metamorphism causing silicate recrystallization.

Metal grains reach 1 mm in size and often represent intergrowths of kamacite and taenite, sometimes with numerous troilite inclusions. Troilite (typically 100-200 μm), generally monocrystalline, and chromite (100-300 μm) are common accessories. Ilmenite

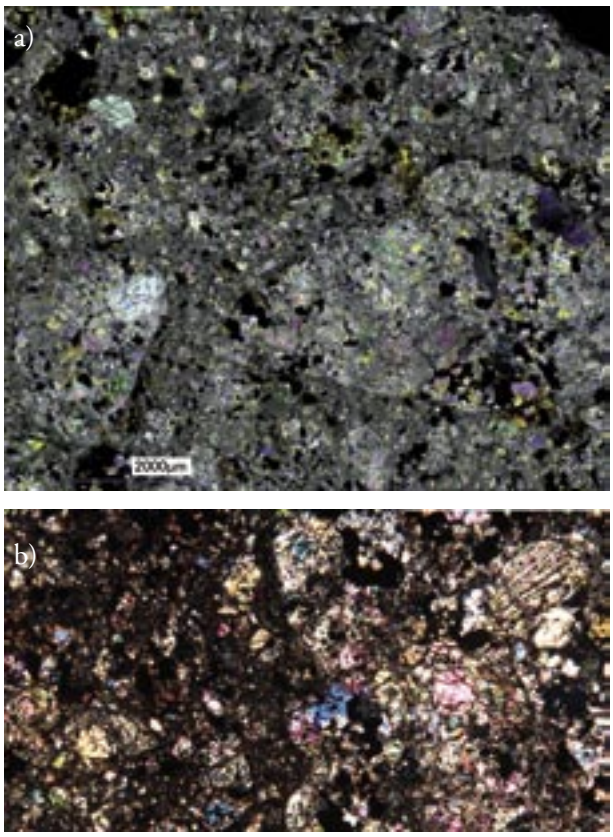

Fig. 5. a) Transmitted light image (cross polarized light) of thin section of Boumdeid (2011) at low magnification showing brecciated texture with well-delineated clasts. No chondrules are visible. Mosaic of images taken with digital microscope (Keyence VHX). Image: B. Hofmann; b) Transmitted light image showing the transition from matrix to a breccia clast. Transmitted light, crossed polarizers, image width is 4.9 mm. Photo: B. Hofmann

was observed in contact with metal. Native copper is very rare and was observed at kamacite-taenite and metal-troilite contacts (Fig. 8).

Besides some minor rusty specks up to 2.5 mm in diameter around metal grains, observed macroscopi-

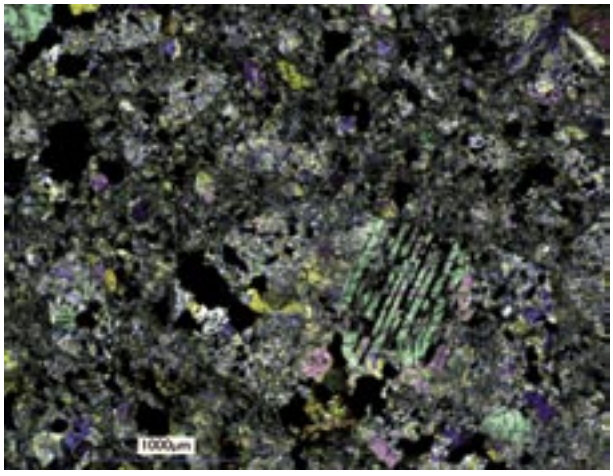

Fig. 6. Transmitted light image (cross polarized light) of thin section of Boumdeid (2011) showing brecciated texture and well-preserved barred olivine chondrule. Mosaic of images taken with digital microscope (Keyence VHX). Image: B. Hofmann

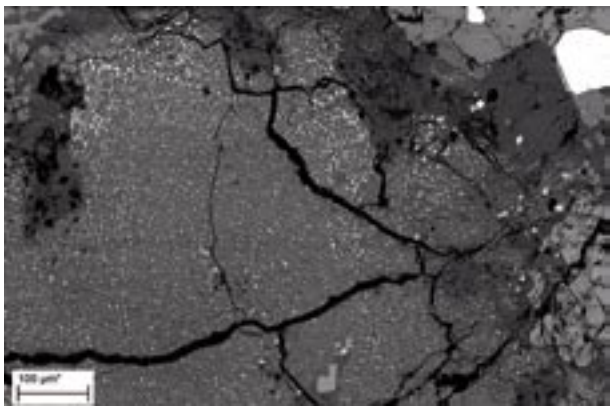

Fig. 7. Backscattered electron image showing a section of the Cr-Al-rich chondrule. Dark groundmass is feldspar, bright inclusions are spinel with increasing Cr-concentrations to the rim of the chondrule (indicated by higher brightness in BSE-image). Bright inclusions include metal, ilmenite-geikielite and baddeleyite. Image: N. Greber

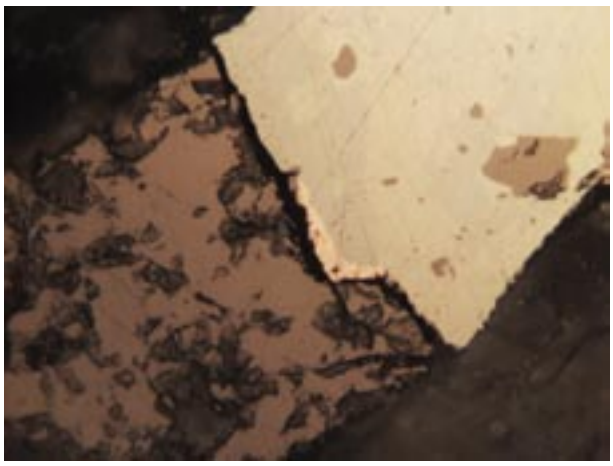

Fig. 8. Reflected light image (oil immersion) showing native copper at the border between metal and troilite. Image width 120 micron. Photo: B. Hofmann

cally and in thin section, the meteorite is unaltered (W0). In a single grain of kamacite, corrosion to an apparent depth of 15 µm was observed, while bordering taenite was unaffected.

Parallel to the completion of this paper, the meteorite was submitted to the Nomenclature Committee by one of the authors (B. Hofmann) and subsequently published under the official name Boumdeid (2011)[2] in Meteoritical Bulletin (Ruzicka et al., 2014).

DISTRIBUTION

- ~1600 g Mauritania [seized by local authorities, unconfirmed]
- 752.00 g S. Buhl, Hamburg, Germany
- 735.80 g M. Jost, Brügg, Switzerland
- 53.60 g Naturhistorisches Museum der Burgergemeinde Bern, Switzerland
- 50.20 g Don Hurkot, Monarch, Canada
- 8.60 g K. Wimmer, Nördlingen, Germany
- Fragments of unknown weight distributed by the finder

The TKW is reported by the finders with around 3500 g (one single mass recovered).

One author of this report (S. Buhl) contacted the department of Earth Sciences at the University of Nouakchott repeatedly with a request for further information on the recovered mass and with the offer to share the collected data as well as sample material. However, as of August 2013, no reply was received.

CONCLUSION

Boumdeid (2011) is the 5th confirmed meteorite fall in Mauritania. Prior to the Boumdeid (2011) event a total of two crater structures and 18 meteorites were known for Mauritania. Among the latter are 14 finds and only four falls. Aioun el Atrouss, a polymict diogenite weighing 1 000 g fell at Gounquel in south-east Mauritania on April 17 in 1974 (Lomena et al., 1976, Graham, 1979). Kiffa, an ordinary chondrite with a TKW of 1 500 g fell on October 23, 1970 at 14:55 hrs, not far from the recent event (Clarke, 1971). Boumdeid (2003), a mass of 190 g, fell ~30 km north of the village of Boumdeid and was also classified as an L6 chondrite. Despite sharing the same petrologic type, month of the fall and, despite the fact that the fall location differs by only 59 kilometers, both meteorite falls, Boumdeid (2003) and Boumdeid (2011) are separate events and the similarities are based on coincidence only. Bassikounou, the fourth registered fall in Mauritania, an ordinary chondrite (H5) with

[2] Following nomenclature protocol, the year 2011 was added to the meteorite's name in order to distinguish it from Boumdeid (2003), a mass of 190 gram that fell on September 24, 2003, 30 km north of the village of Boumdeid (Ruzicka et al., 2014).

a confirmed total known weight of 93.8 kg, fell on October 16, 2006, 04:00 UTC, and is at present the largest witnessed fall in the history of the country (Conolly et al., 2007; Buhl et al., 2008). While the Bassikounou meteorite can be considered a well documented fall, particularly in terms of the recording of the recovered material, only a few eye witness reports were collected and only very little information on the trajectory of the detonating fireball is known.

Boumdeid (2011) is presently the second largest meteorite fall in the country and, due to the efforts of Mr. Toueirjenne, a substantial number of eye witness accounts were collected. These were sufficient to constrain a scenario for the trajectory of the bolide that is consistent with the find location of the recovered 3.5 kg mass and the values derived from the measurements of cosmogenic radionuclides. In this scenario the incident direction of the bolide is within a range between 15° and 35° and its vertical angle between 35°–55°. The luminous track started in 85 km altitude and ended in 18 km altitude, with a fragmentation event occurring at 24 km altitude. The luminous trajectory has a most probable length of ~95 km, its projection on the ground has a length of ~67 km. The impact site of the recovered 3.5 kg mass is shifted ~1 km to the west of the trajectory due to wind drift.

The mineralogy, texture and mineral chemistry of Boumdeid (2011) is fully consistent with a classification as ordinary chondrite of type L6, shock stage S2, and no weathering (W0). The meteorite is brecciated and contains Al-Cr-rich chondrules. Remnants of stronger shock metamorphism indicate strong recrystallization with near complete obliteration of older shock metamorphic features.

The availability of a 56 g sample shortly after the fall enabled the measuring of cosmogenic radionuclides 84 days after the event and facilitated the retrieval of a new suite of radionuclide values of a freshly fallen chondrite. The data obtained from the measurements of the short-lived radioisotopes are consistent with a fall event on September 14 and confirm that the meteoroid underwent its last orbital segment during a period with a moderately high cosmic ray flux due to the preparatory phase of the current solar cycle 24. Based on previously determined production rates in L chondrites for ^{26}Al the measured values for ^{26}Al in the Boumdeid (2011) meteorite are well within the expected saturation values for preatmospheric radii of 10–20 cm.

REFERENCES

Agence Nouakchott d'Information (ANI), 2011 – Mauritanie: L'explosion d'un corps étrange secoue la ville de Boumdeid. Press release, Nouakchott, Sept. 15.

Arpesella C., 1996 – A low background counting facility at Laboratori Nazionali del Gran Sasso. *Applied Radiation and Isotopes* 47, 991–996.

Bartol Neutron Monitors, 2012. http://neutronm.bartol.udel.edu/.

Beech M., Wenshuang N., Coulson I.M., 2007 – The Chassigny Meteorite and Fireball: a forensic study. *Journal of the Royal Astronomical Society of Canada* 101(4), 139.

Bhandari N., Mathew K.J., Rao M.N., Herpers U., Bremer K., Vogt S., Wölfli W., Hofmann H.J., Michel R., Bodemann R., Lange H.-J., 1993 – Depth and size dependence of cosmogenic nuclide production rates in stony meteoroids. *Geochimica et Cosmochimica Acta* 57 (10), 2361–2375.

Bischoff A., Jersek M., Grau T., Mirtic B., Ott U., Kučera J., Horstmann M., Laubenstein M., Herrmann S., Řanda Z., Weber M., Heusser G., 2011 – Jesenice – A new meteorite fall from Slovenia. *Meteoritics & Planetary Science* 46, 793–804.

Blanchot A.J., 1975 – Plan minéral de la République Islamique de Mauritanie. Republique Islamique de Mauritanie Ministere de la planification et du developpement industriel, Direction des mines et de la geologie.

Brearley A.J., Casanova I., Miller M.L., Keil K., 1991 – Mineralogy and possible origin of an unusual Cr-rich inclusion in the Los Martinez (L6) chondrite. *Meteoritics* 26 (4), 287–300.

Britt D.T., Consolmagno G.J., 2003 – Stony meteorite porosities and densities: A review of the data through 2001. *Meteoritics & Planetary Science* 38, 1161–1180.

Bronshten, V.A., 1999 – Trajectory and orbit of the Tunguska meteorite revisited. *Meteoritics & Planetary Science*, 34, 137–143.

Buhl S., Baermann M., Hofmann B., Weber P., Gnos E., 2008 – Account of a meteorite fall near Bassikounou, Mauritania, on October 16, 2006, Part I: The fall and recovery of the Bassikounou meteorite. *Meteorite* 14 (3), 7–14.

Buhl S., Baermann M., Hofmann B., Weber P., Gnos E., 2008 – Account of a meteorite fall near Bassikounou, Mauritania, on October 16, 2006, Part II: The Bassikounou meteorite. *Meteorite* 14 (4), 10–14.

Buhl S., Baermann M., 2007 – The Bassikounou Meteorite Fall. Descriptive Catalog of the Recovered Masses, Vol. 1, until June 30, 2007. Electronic paper published on www.meteorite-recon.com.

Carrefour de la République Islamique De Mauritanie (CRIDEM), 2011 – Chute d'une grosse météorite dans les environs de Boumdeid. Sept. 15, published on http://www.cridem.org/C_Info.php?article=59988.

Ceplecha Z., Borovička J., Elford W.G., Revelle D.O., Hawkes R.L., Porubčan V., Šimek M., 1998 – Meteor phenomena and bodies. *Space Science Reviews* 84 (3–4), 327–471.

Clarke R.S. Jr., 1971 – Fall of the Kiffa, Mauritania, Stony Meteorite. *Meteoritical Bulletin* No. 50, *Meteoritics* Vol. 6, 114–115.

Connolly H.C., Jr., Smith C., Benedix G., Folco L., Righter K., Zipfel J., Yamaguchi A., Chennaoui Aoudjehane H., 2007 – The Meteoritical Bulletin, No. 92, 2007 September. *Meteoritics & Planetary Science* 42 (9), 1647–1694.

Eberhardt P., Geiss J., Lutz H., 1963 – Neutrons in meteorites. Earth Science and Meteoritics (Geiss J., Goldberg E.D., eds.), North-Holland, Amsterdam, 143–168.

Graham A. L., 1979 – The Meteoritical Bulletin No. 56. *Meteoritics* 14, 161–174.

Hughes R.H., Hughes J.S., 1992 – A Directory of African Wetlands. IUCN, Gland, Switzerland and Cambridge, UK, UNEP, Nairobi, Kenya and WCMC, Cambridge, UK.

Jarosewich E., 1990 – Chemical analyses of meteorites: A compilation of stony and iron meteorite analyses. *Meteoritics* 25, 323–337.

Kohman T.P., Bender M.L., 1967 – Nuclide production by cosmic rays in meteorites and on the Moon. High-Energy Nuclear Reactions in Astrophysics. In: High-Energy Nuclear Reactions in Astrophysics – A collection of articles, edited by Shen B.S.P. and Benjamin W.A., New York, N.Y., 169–245.

Krot A.N., Ignova M.A., 1992 – Cr-rich chondrules and inclusions in ordinary chondrites. *Abstracts of the 23rd Lunar and Planetary Science Conference*, 23, 729.

Leya I., Masarik J., 2009 – Cosmogenic nuclides in stony meteorites revisited. *Meteoritics & Planetary Sciences* 44, 1061–1086.

Lomena I.S.M., Touré F., Gibson E.K., Jr., Clanton U.S., Reid A.M., 1976 – Aioun el Atrouss – A new hypersthene achondrite with eucritic inclusions. *Meteoritics* 11, 51–57.

Mattick R.E., 1982 – Project report West African states (ECOWAS) region investigation, (IR)WA-5. Assessment of the petroleum, coal, and geothermal resources of the economic community of West African states (ECOWAS) region. United States Department of the Interior, US Geological Survey.

Popova O., Borovička J., Hartmann W.K., Spurný P., Gnos E., Nemtchinov I., Trigo-Rodríguez J.M., 2011 – Very low strenghts of interplanetary meteoroids and small asteroids. *Meteoritics & Planetary Science* 46 (10), 1525–1550.

Pugh R., Ruzicka A., Hutson M., Schmeer B., 2004 – Eyewitness reports for the June 3, 2004 Pacific Northwest fireball. http://astrowww.phys.uvic.ca/-tatum/fireball/, June 3, 2004.

Ruzicka A., Grossman J.N., Garvie L., 2014 – The Meteoritical Bulletin, No. 100, 2014 June. *Meteoritics & Planetary Science* 49 (8), E1–E101.

Spergel M.S., Reedy R.C., Lazareth O.W., Levy P.W., Slatest L.A., 1986 – Cosmogenic neutron-capture-produced nuclides in stony meteorites. 16th Proceedings of the Lunar & Planetary Science Conference, *Journal of Geophysical Research*, Supplement: 91, D483–D494.

Wasson J.T., Kallemeyn G.W., 1988 – Compositions of Chondrites. In: *Philosophical Transactions of the Royal Society of London*. Series A, Mathematical and Physical Sciences: 325, (1587), The Solar System: Chemistry as a Key to Its Origin, 535–544.

Wickens G.E., Seif El Din A.G., Sita G., Nahal I., 1995 – Role of Acacia Species in the rural economy of Dry Africa and the Near East. FAO Conservation guide no. 27.

Wimmer K., 2009 – Studies of meteorite drag-shape factors during dark flight. Bolides and Meteorite Falls, Prague, May 10–15, abstract, 25.

APPENDIX 1. MEDIA REPORTS

Agence Nouakchott d'Information (ANI): Mauritanie: **L'explosion d'un corps étrange secoue la ville de Boumdeid**, Nouakchott Sept. 15, 2011

Mauritanie: L'explosion d'un corps étrange secoue la ville de Boumdeid

Selon des témoins oculaires, l'explosion d'un « corps étrange et lumineux tombé du ciel » a secoué la ville de Boumdeid, dans la soirée du mercredi [Sept. 14]. Un habitant de la ville a précisé qu'il « s'agit d'un corps, dont émanait une lumière aveuglante, ayant chuté non loin de Boumdeid et dont l'explosion a secoué les habitants et provoqué chez eux une psychose».

Ce témoin a souligné que les habitants de kiffa ont également pu observer la lumière émanant de ce corps « étrangement terrifant »

English translation:

Mauritania: Explosion of a strange body shakes city of Boumdeid

According to eyewitnesses, the explosion of a "strange and luminous body which fell from the sky" shook the city of Boumdeid, on the evening of Wednesday [Sept. 14]. A local resident said it was "a body, which gave off a blinding light, falling near Boumdeid and whose explosion shook the people and caused in them a psychosis." This witness said that the inhabitants of Kiffa have also observed light from this "strangely terrifying" object.

Carrefour de la République Islamique De Mauritanie (CRIDEM): **Chute d'une grosse météorite dans les environs de Boumdeid**. Sept. 15, 2011, published on http://www.cridem.org/C_Info.php? article=59988, 2011

Le village de Boumdeid, en Assaba risque d'être la destination prisée les prochains de experts et des passionnés des secrets du cosmos. Selon le site alakhbar, citant des sources dans cette localité, une grosse météorite est tombée dans les alentours de Boumdeid, illuminant dans sa chute la zone avant de faire une forte explosion, suivie d'une forte panique chez les populations.

S'agit-il d'une, foudre, d'une météorite ou d'un morceau d'un satellite désintégré dans l'espace ? En attendant de savoir au juste de quoi il s'agit, seul les gens du cosmos peuvent éclairer l'opinion sur un événement qui attire les scientifiques comme les éclipses et qui est très rare.

Est-on également en présence d'une nouvelle météorite comme celle du Nord de l'Adrar découverte par Théodore Monod. Notons qu'on ne sait pas encore si cette présumée météorite a fait des dégâts.

NAM (Stagiaire)

English translation:

Fall of a large meteorite near Boumdeid

The village of Boumdeid in Assaba may be the next popular destination of experts and enthusiasts researching the secrets of the cosmos. According to the site Alakhbar, citing sources in this locality, a large meteorite fell in the vicinity of Boumdeid, illuminating in its fall the surrounding area before causing a loud explosion, followed by a sharp panic among the population.

Is this a lightning, a meteor or a piece of a satellite disintegrated in space? Until we know exactly what it is, only people of the cosmos can enlighten public opinion on an event that attracts scientists similar like eclipses, and which is very rare.

Is it also in the presence of another meteorite like the one discovered in northern Adrar by Theodore Monod. Note that we do not yet know whether the alleged meteorite did damage.

NAM (Intern)

APPENDIX 2. EXCERPTS FROM WITNESS ACCOUNTS

Ahmed Ould Ahmedwali (witness #01) observed the event from 16°35'33"N, 11°23'4.908"W, just south of the town Kiffa: "I was looking to the north and saw the star during its complete duration from when it appeared in the west until it ended in the northeast. Everything was lighted like during the brightest day."

Limam Ould Ekhou (witness #02) camped with his brother Mohamed Lemine Ould Ekhou and his sons short east of the dirt track from Kiffa to Boumdeid at position 17°3'46.752"N, 11°21'26.784"W. His report, which is confirmed by his brother, is particularly interesting, because it describes the fragmentation of the Boumdeid bolide from a location relatively close to the trajectory: "Suddenly the night became day and we saw a flying star crossing the sky from south to north until the star exploded. After the explosion three smaller stars continued in slightly diverging directions." Witness #02 described the movement of the three fragments as "fan-shaped".

Mohamed Ould Enebbie (witness #05), located 36 km southwest from Boumdeid at 17°8'22.968"N, 11°24'46.272"W, stated that: "The fireball came from north to south". Mr. Ould Enebbie also reported a second observation by Dedahi Ould Chamad (witness #16), a young boy who saw the bolide approaching "almost above his head" and moving in a steep angle towards the zenith. No precise coordinates for the location of Ould Chamad are reported, but from the description of Mr. Ould Enebbie his position can be estimated – 15 km southeast of Boumdeid, which places the boy approximately on the axis of the trajectory, but north of the end point of the luminous path.

Salem Elbooussaty Abou Cheikh (witness #09) and his family camped west from the dirt track leading from Kiffa to Boumdeid at 17°3'55.572"N, 11°22'30.792"W, not far from the position of witness #02: "We saw it move from north to south and when it disappeared we heard a big explosion". This report was later confirmed by the son and the sister of Mr. Abou Cheikh, although no direction of movement was mentioned.

Sidi Mahmoud Ould Belkheir Ould Eabeid (witness #11) gave the following account: "We were preparing dinner when suddenly the torch I was holding was no longer necessary as night had become bright day. We became very frightened as it appeared that the day of the last judgement had begun. Just after the light had passed there were three or four explosions from the South, and after this we heard an *ishshsh*-like sound which terminated in a big thud. We searched for the object that obviously had fallen upon us but we only discovered a hole in the soil. In it was some kind of ash-like dust which we could also smell, and which was different from the camel's urine [which soaked the ground around the animals]. Early the next morning I told the story to Eli who in turn told it to Albadad [Sidi Mohamed Ould Alharthi]. Albadad arrived later during the day and actually found the stone, broke it apart, and gave pieces of it as souvenirs to everybody who asked for one."

List of other witnesses:

- Mohamed Lemine Ould Ekhou, brother of Limam Ould Ekhou (witness #03),
- Edaya Ould [?] from Aoulad Boumalek (witness #04),
- Cheikh Ould Aabda from Hseytinne: (witness #06),
- Brother of Cheikh Ould Aabda, also from Hseytinne (witness #07),
- Mohamedvadel Ould Cheikh Saadbouh (Cheikhna), who witnessed the event with the finder of the meteorite (witness #08),
- Son (Cheikh Ould Salem) and sister of Salem Elbooussaty Abou Cheikh (witnesses #10 and 10b)
- Ould Sidbrahim (witness #12),
- Sidi Ahmed Ould Sweidy and family (witness #14),

- Dhahbi Ould Alaarbi Ould Moulay Zeine and brother who witnessed the event in Boumdeid (witness #15),
- Mohamed Ould Elhassen Ould Adermaz (witness #17),
- Mahfoudh Ould Naha who witnessed the event in Selibabi (witness #18).

Publishers: Wrocław University of Technology, Faculty of Geoengineering, Mining and Geology
Polish Meteorite Society

Meteorites
Vol. 3, Nos. 1–2, 2014, 19–32
www.meteorites.pwr.wroc.pl
DOI 10.5277/met140102

A NEW CLASSIFICATION OF NYIRÁBRANY, AN ORDINARY CHONDRITE FROM HUNGARY

Marianna MÉSZÁROS[1], Ákos KERESZTURI[2], Zuárd DITRÓI-PUSKÁS[3]

[1] Physics Institute, Space Research and Planetary Sciences, University of Bern, Sidlerstrasse 5, CH-3012 Bern, Switzerland
[2] Research Center for Astronomy and Earth Sciences, Konkoly Astronomical Institute, Astrophysical and Geochemical Laboratory, H-1121 Budapest, Konkoly Thege Miklós út 15-17, Hungary
[3] Department of Petrology and Geochemistry, Eötvös Loránd University, Pázmány Péter Sétány 1/C, Budapest 1117, Hungary

Abstract: The Nyirábrany meteorite is an ordinary chondrite from Hungary that fell in 1914 and, to date, has been studied very little. The aim of this work was to carry out a more detailed examination of this meteorite (using optical polarization microscope, energy dispersive X-ray spectroscopy and Raman microspectroscopy) and re-investigate its previous classification as an LL5 type ordinary chondrite, moreover to complete its classification with a shock stage and a weathering grade. Our new results indicate that Nyirábrany could be a transition type between the L and LL chondrites. The main mineral phases of Nyirábrany are olivine, pyroxene and opaque minerals (e.g. Fe-Ni metal, troilite, chromite), minor constituents are plagioclase, Cl-apatite, cristobalite and glass. The Fe-Ni metal content (1.32 vol%) of Nyirábrany is typical of the LL group, the Fa-content of olivines (26.71 mol%) is between the range of the L and LL types, while the Fs-content of the low-Ca pyroxenes (20.51 mol%) is typical of the L-chondrites. Chondrules appear in different sizes, mineral compositions and textures. The textural and mineralogical features (e.g. mostly homogeneous silicate minerals, dominance of clinopyroxenes, recrystallized matrix, well-defined chondrules) indicate petrological type 4-5 for Nyírábrány. The shock stage and the weathering grade of this meteorite were examined for the first time. On the basis of the observed optical and textural features of the olivine grains (e. g. sharp optical extinction, irregular and planar fractures) Nyirábrany has an S2 shock stage. About 30–40% of the opaque phases are affected by oxidation, which shows a W2 weathering grade.

Keywords: chondrite, classification, L and LL chondrites.

INTRODUCTION

The aim of this study is the re-analysis of the ordinary chondrite called Nyirábrany. We present the results on its classification according to chondrite groups based on the Fe-Ni metal content, and the chemical composition of olivine and low-Ca pyroxene. The assignment of the petrologic type was based on the van Schmus and Wood (1967) petrologic type scheme. The shock stage of Nyirábrany was defined by using the shock classification of Stöffler et al. (1991) and the weathering grade was defined according to the weathering scale of Wlotzka (1993). Using up-to-date methods, we present new details and characterization of this meteorite. The results here could be used to target further analysis.

Nyirábrany is one of the 27 meteorite falls and finds from the Carpathian Basin. It fell on the 17th of July, 1914 on the north-western part of Hajdú-Bihar County, Hungary (N 47°33', E 22°1'30") (Fig. 1) and was named after the village in the vicinity of which it fell. The meteorite was recovered right after the fall by an eyewitness as a single stone with a mass of 1104 g. Nyirábrany is a poorly studied meteorite whose first investigation was undertaken by Sztrókay et al. (1977). At that time no advanced instrumental analysis methods were available, the chemical composition of the main silicate phases was determined by optical methods. Kubovics et al. (2004) re-investigated Nyirábrany together with five other meteorites from

Corresponding author: Ákos KERESZTURI, kereszturi.akos@csfk.mta.hu

Fig. 1. Map of the Carpathian Basin showing the meteorite falls and finds from this area. The location of Nyirábrany is marked by an ellipse (Kubovics et al., 2004)

the Carpathian Basin, but no detailed analyses were made on its mineralogical and chemical composition. Nyirábrany was mentioned in other publications in connection with its reflectance spectra as one among other meteorite samples (Paton et al., 2011), and another work mentioned its chromium and manganese content (Yates et al., 1968), while most of this meteorite's basic properties have remained unexplored.

ANALYTICAL METHODS

Due to the limited availability of Nyirábrany samples, only one polished thin section of the meteorite was used for the investigation – as a result, our findings are not absolutely representative for the whole meteorite, but still provide important insights into its properties. The polished thin section was studied with an optical microscope in transmitted light to identify the main mineral phases and chondrules, and to observe the textural features. The semi-quantitative chemical analysis and BSE imaging was undertaken on the same thin section of the meteorite to identify minor components, to determine the chemical composition of the main mineral phases and to observe the textural features in details. This measurement was conducted using energy dispersive X-ray spectroscopy on an AMRAY 1830i scanning electron microscope with up to 4 nm spatial resolution at the Petrology and Geochemistry Department of Eötvös Loránd University. During the analysis 20 kV acceleration voltage and 1 nA beam current intensity were used. Counting time was 100 s and the ZAF procedure was used to correct matrix effect. The Raman measurement was made by HORIBA JobinYvon LabRAM HR type Raman-microspectrometer, equipped with Olympus BXFM type optical microscope, and thermoelectrically cooled CCD detector, 532 nm wavelength excitation, recording spectra between about 895 and 1080 cm^{-1} with 2×30 second intervals, 1800 line/mm optical lattice and 100-times magnification.

The estimation of shock level is important to evaluate the past collisional history of any meteorite and their parent bodies. Various micro- and macroscopic structural changes, specific phases and mineral assemblages in meteorites are related to the shock produced deformation and transformation, and could be used to estimate the shock level. These shock indicators include deformation bands, planar deformation features (Stöffler, 1967; Nagy et al., 2008), mosaicism,

twin lamellae formation, isotropization (Stöffler et al., 1986), recrystallization (Ostertag et al., 1986), formation of new minerals (Bridges et al., 2001), or melt veins (Gillet et al., 2000), transformation of plagioclase to jadeite (Kubo et al., 2010) and olivine to spinel structures (Putnis & Price, 1979). The methods to identify these shock markers include nuclear magnetic resonance (Stöffler & Langenhorst, 1994), cathodoluminescence (Kayama et al., 2009), Raman spectroscopy (Miyamoto & Ohsumi, 1995; Gucsik et al., 2004, 2010), refractive index (Lambert, 1981; Fritz et al., 2003), X-ray diffraction (Nakamura et al., 2011) analysis. A recently emerging new field is the alkali feldspar analysis by cathodoluminescence as shock barometers in meteorites (Kayama et al., 2012), what looks as an universal tool to estimate wide pressure range between about 4.5 and 40.1 GPa.

Due to equipment availability and various technical reasons, the shock stage was estimated using the simple method of polarization microscopy. Here we use the Stöffler et al. (1991) classification system developed for ordinary chondrites with six distinct shock stages labelled from S1 to S6. The aim was an improved classification of this meteorite in order to better target future investigations. The authors would like to conduct detailed shock analysis in the future on this meteorite.

RESULTS

In this section we give an overview of the analysis of the meteorite, focusing on the general microscopic appearance, including petrography, mineralogy, chemical composition of mineral phases, and the shock stage and weathering, to support a more precise classification and characterization.

Macroscopic description

For the macroscopic description, we used a ~50×35×5 mm rock slice of Nyirábrany (Fig. 2a), which was investigated with a stereomicroscope. The sample has a dark fusion crust along its surface which was produced during the transport trough the atmosphere. The fusion crust is usually ~50 μm thick (Fig. 2b), but the thickness can go up to ~400 μm at certain locations. The meteorite has a light grey coloured matrix in which different sized chondrules, chondrule-fragments and usually sub-millimeter sized opaque constituents are embedded. Porphyritic and radial textures of some of the chondrules are also vis-

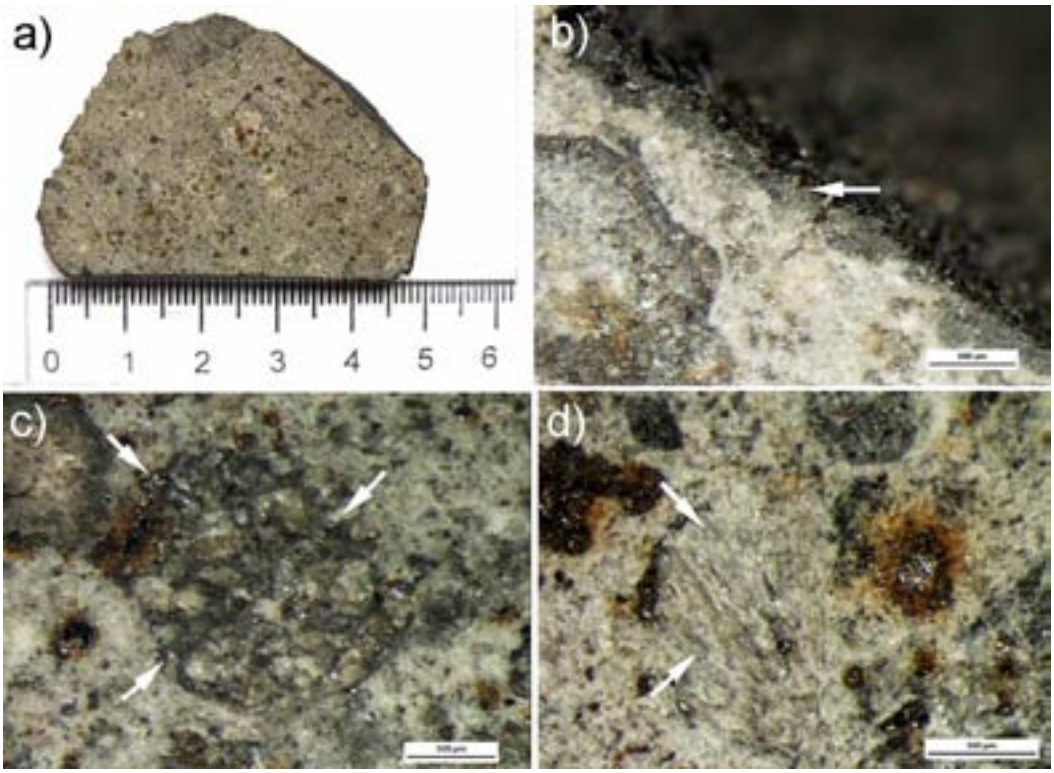

Fig. 2. General images of the Nyirábrany meteorite: a) cross section of the meteorite with bright reflecting opaque minerals; b) fusion crust on the surface of the meteorite; c) porphyritic textured chondrule; d) radial textured chondrule

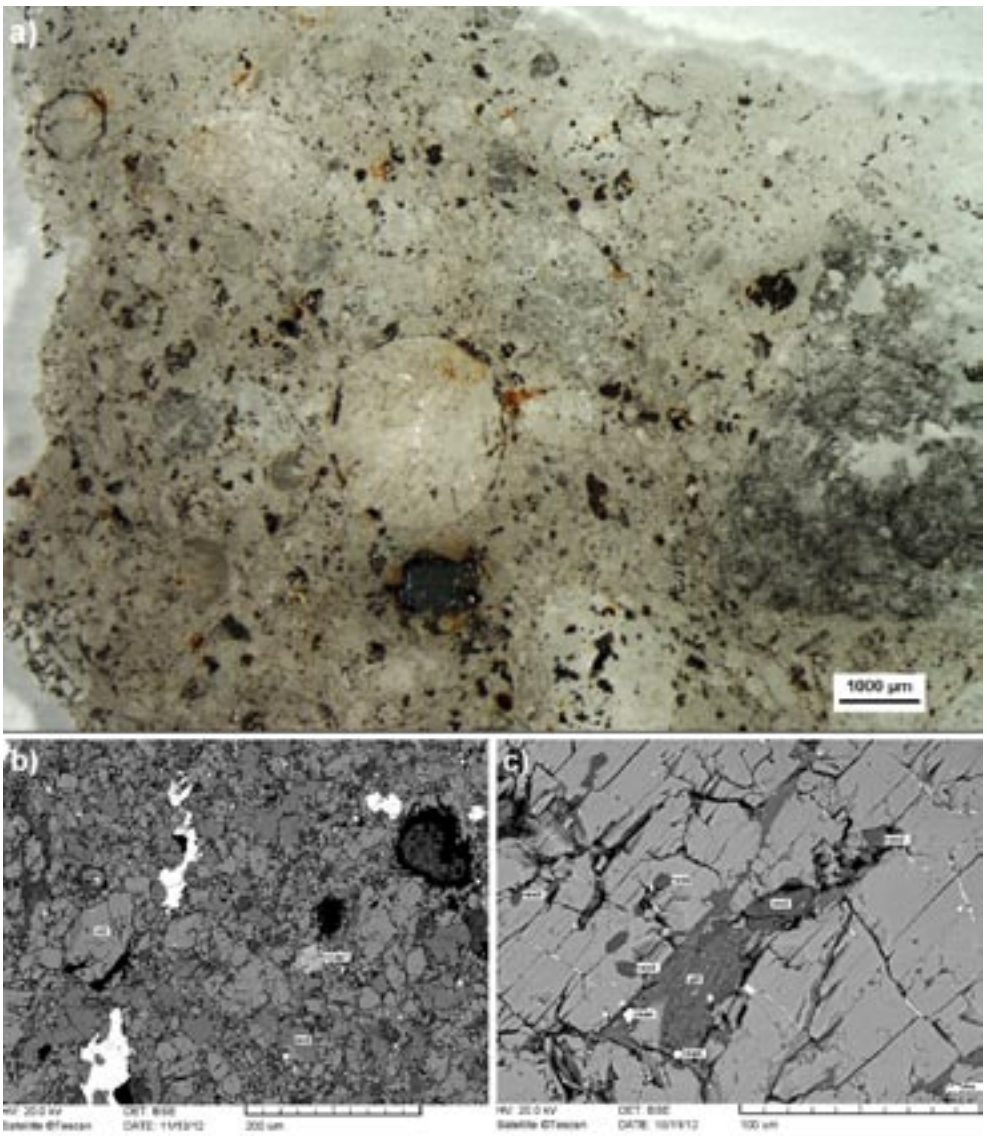

Fig. 3. Images of Nyirábrany: a) overview image of the examined thin section of Nyirábrany with well-defined and diffuse chondrules; b) Cl-apatite (light gray) in the crystallized matrix of the meteorite (cl-ap-chloroapatite, ol-olivine, px-pyroxene); c) cristobalite (middle gray) in the pyroxene crystals of a radial textured chondrule (acronyms: SiO_2-cristobalite, gl-glass, kam-kamacite, tro-troilite)

ible with stereomicroscope (Fig. 2c and d). Reddish-brown weathering products occur around the opaque phases as a result of terrestrial alteration.

Petrography

The matrix is composed of fine (5–50 µm) grains and is completely crystalline as can be seen on the BSE images (Fig. 3b). Chondrules appear in diverse sizes, mineral compositions and textures, like radial pyroxene, porphyritic olivine, poikilitic pyroxene-olivine and barred pyroxene chondrules. In some cases, chondrules are well-defined, in other cases they are diffuse, which makes difficult to define their exact abundance (Fig. 3a). The size of the well-defined chondrules ranges from ~560 µm to ~2200 µm. Most of the chondrules are fractured and some of them are broken too. We have selected eight well-defined chondrules in the thin section of Nyirábrany to illustrate the main, characteristic chondrule types and their features (Fig. 4), that listed in Table 1. The various types of chondrules provide evidence for different cooling speed values. Refractory inclusions were not identified in the thin section of Nyirábrany.

Mineralogy

The main mineral phases of Nyirábrany are olivine, pyroxenes and opaque constituents. Minor amount of plagioclase, Cl-apatite, cristobalite and recrystallized glass were also identified.

Olivine is the most abundant mineral phase of Nyirábrany, it has an amount of ~58.5% (Sztrókay et al., 1977).

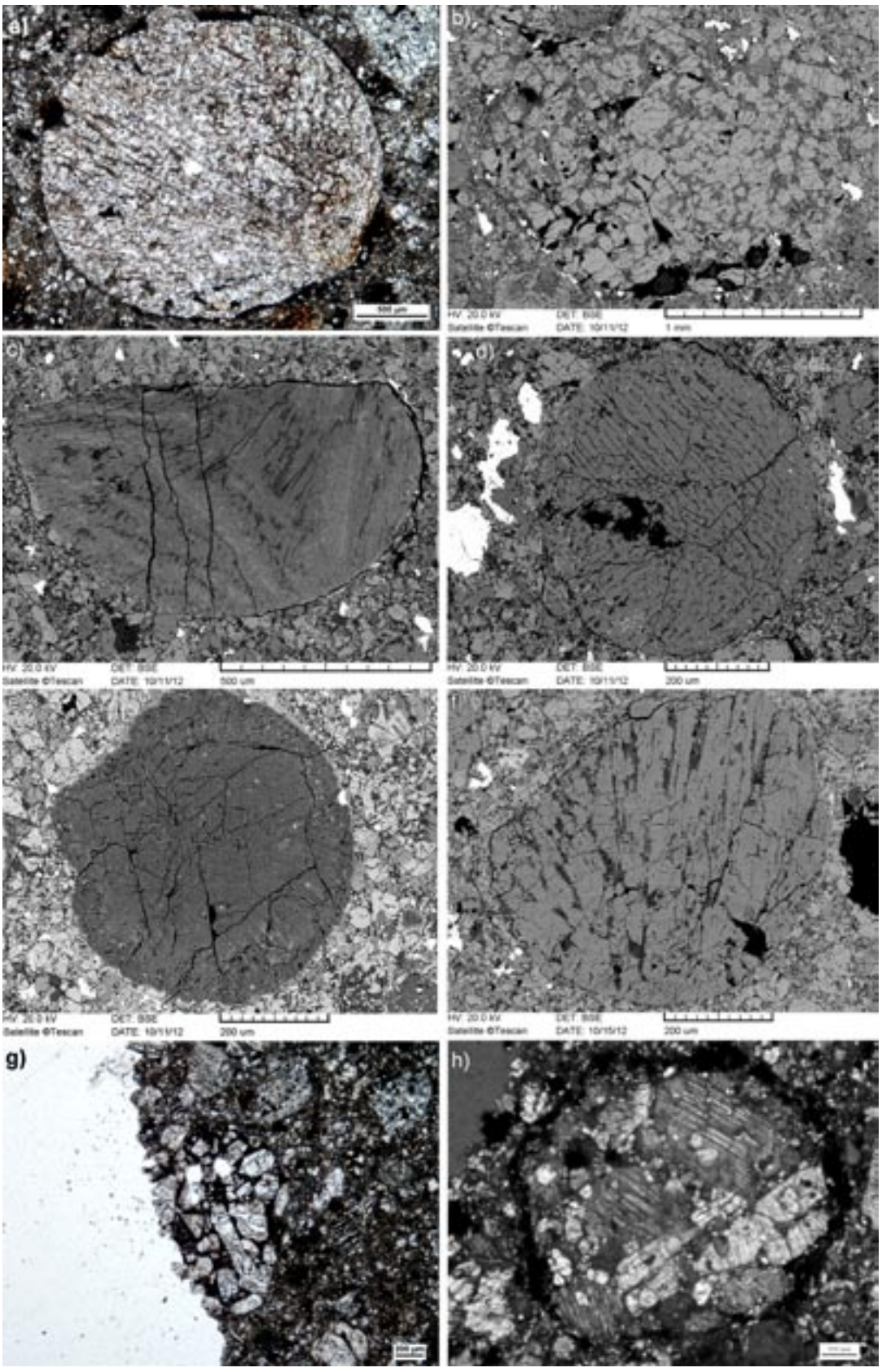

Fig. 4. Main chondrule types of Nyirábrany showing the following features: a) radial pyroxene chondrule (Ch1) (optical microscope image with 1 polar); b) porphyritic olivine chondrule (Ch2) (BSE image); c) fractured radial pyroxene chondrule fragment (Ch3) (BSE image); d) fractured barred pyroxene chondrule (Ch4) (BSE image); e) fractured barred pyroxene chondrule (Ch5) (BSE image); f) radial pyroxene chondrule fragment (BSE image) (Ch6); g) porphyritic olivine chondrule with euhedral crystals (Ch7) (optical microscope image with 1 polar); h) poikilitic pyroxene-olivine chondrule (Ch8) (optical microscope image with crossed polars)

Table 1. Main chondrule types and their characteristic features

	Size (μm)	Texture	Main mineral phase	Minor components	Outline	Comments
Ch1	2200	radial	pyroxene	opaque, cristobalite, glass	well-defined	-
Ch2	2000	porphyritic	olivine	plagioclase, pyroxene, glass, opaque	moderately delineated	-
Ch3	1000*	radial	pyroxene	olivine, opaque	well-defined	fractured and broken
Ch4	560	barred	pyroxene	opaque, glass	moderately delineated	fractured
Ch5	570	barred	pyroxene	opaque, glass	moderately delineated	fractured
Ch6	700*	radial	pyroxene	plagioclase	well-defined	broken
Ch7	1200*	porphyritic	olivine	glass	moderately delineated	broken
Ch8	1000	granular/poikilitic	pyroxene-olivine	opaque	moderately delineated	-

Ch – chondrule
* – estimated original size

Pyroxenes are the second most abundant mineral phases in the meteorite.

Opaque minerals in the meteorite include Fe-Ni metal, troilite and chromite. The amounts of Fe-Ni metal and troilite are ~1.32% and ~2.5%, respectively, which were calculated by analyzing the BSE images of the thin section using a software called "ImageJ". Opaque constituents can be found inside chondrules, at the chondrules' rims and in the matrix (Fig. 5).

The amount of plagioclase is ~2.5% (Sztrókay et al., 1977). It is present in the mesostasis (Fig. 6) of some of the chondrules, in the matrix and in the melt veins of some olivine crystals.

Traces of cristobalite and Cl-apatite were also identified in the meteorite. Cristobalite was identified first as an SiO_2 phase by the SEM-EDX analysis, the Raman microspectroscopic study showed, this phase is cristobalite, regarding to the crystal structure. Cristobalite can be found as rounded grains in pyroxene crystals in a radial chondrule (Ch1) (Fig. 3c). Observations and modelling show cristobalite could form by metamorphic processes (example: ALHA 76003, Olsen et al., 1981) and high temperature (example: Parnallee and Farmington meteorite, Bridges et al., 1994) from silica melt and by inversion from stishovite or coesite, always at high temperature (Heaney et al., 1994). Cl-apatite was identified by SEM-EDX analysis in the matrix (Fig. 3b).

Mineral compositions

In the following section we present the characteristics of minerals and their chemical composition. The main mineral phases of Nyirábrany are olivine, pyroxenes and opaque constituents. Minor amount of plagioclase, Cl-apatite, cristobalite and recrystallized glass were also identified.

Olivine

Olivine is the most abundant mineral phase of Nyirábrany, it has an amount of ~58.5% (Sztrókay et al., 1977). It is present in chondrules and in the matrix. Olivine grains are homogeneous, no zoning was observed. The crystals have sharp optical extinction. Irregular fractures (Fig. 5) were visible in the grains, but no planar deformation features or any hint of undulatory extinction could be identified, possibly due to the relatively low shock level.

The chemical composition of olivines was measured at 22 points of the thin section by SEM-EDX, out of which 16 were in the chondrules and 6 in the matrix. Olivine grains were selected randomly in the matrix. The chemical composition and Fa-content of olivines are summarized in Table 2. The matrix olivines are a little more fayalitic in composition, compared to the olivines in the chondrules. In chondrules, the average Fa-content is 25.99 mol% with a standard deviation of 1.15 mol%, while in the matrix these values are 27.44 and 0.18 mol% respectively. The measured Fa-contents are relatively close to each other but some difference is visible in the standard deviation. Smaller standard deviation for matrix olivines, compared to chondrule olivines is present and it fits well with the expectation that chondrules formed in different regions of the solar nebulae, while the components of the matrix were formed at the same location and under the same conditions. The calculated average Fa-content for Nyírábrány is 26.71 mol%, which falls between the range of L and LL type ordinary chondrites. For comparison, the mean Fa-content of olivines measured in the preliminary studies were 25 mol% (Sztrókay et al., 1977) and 27–28 mol% (Kubovics et al., 2004), which are typical of the L and LL group ordinary chondrites.

Table 2. The chemical composition of olivines in chondrules and matrix of Nyirábrany measured by SEM-EDX

	Oxide content (wt%)						Fa-content
	SiO_2	FeO	MnO	MgO	total		(mol%)
Ch2_ol1	37.68	23.89	0.46	37.68	99.71		26.24
Ch2_ol2	38.29	23.77	0.36	37.59	100.01		26.19
Ch2_ol3	37.97	24.25	0.42	37.35	99.99		26.70
Ch2_ol4	38.26	23.69	0.48	37.56	99.99		26.14
Ch2_ol5	38.10	23.93	0.39	37.58	100.00		26.32
Ch7_ol1	38.33	23.79	0.52	37.36	100.00		26.32
Ch7_ol2	38.19	24.20	0.46	37.15	100.00		26.77
Ch7_ol3	37.95	24.50	0.30	37.25	100.00		26.96
Ch7_ol4	38.38	23.82	0.33	37.47	100.00		26.29
Ch7_ol5	38.12	24.03	0.35	37.50	100.00		26.45
Ch8_ol1	38.54	21.48	0.46	39.52	100.00		23.37
Ch8_ol2	38.36	21.85	0.35	39.45	100.01		23.71
Ch8_ol3	38.67	22.06	0.32	38.95	100.00		24.11
Ch9_ol1	38.20	24.18	0.32	37.30	100.00		26.67
Ch10_ol1	38.01	24.18	0.58	37.23	100.00		26.71
Ch10_ol2	38.19	24.28	0.48	37.05	100.00		26.88
						Mean	25.99
						σ	1.15
M_ol1	37.94	24.71	0.46	36.89	100.00		27.32
M_ol2	38.10	24.74	0.27	36.88	99.99		27.35
M_ol3	37.95	24.74	0.41	36.90	100.00		27.34
M_ol4	37.79	24.92	0.56	36.72	99.99		27.58
M_ol5	37.78	25.08	0.51	36.63	100.00		27.75
M_ol6	37.94	24.67	0.54	36.86	100.01		27.30
						Mean	27.44
						σ	0.18
	Average olivine composition for Nyirábrany						26.71
						σ	0.80

Ch = chondrule
M = matrix
ol = olivine
σ = standard deviation

Pyroxene

Pyroxenes are the second most abundant mineral phases in the meteorite. According to the first study of Nyirábrany, the amount of orthopyroxene is ~25% (Sztrókay et al., 1977). The extinction features of pyroxene crystals were investigated under an optical microscope. In contradiction to earlier findings, we identified clinopyroxene in many chondrules, based on the inclined extinction of the crystals. Pyroxenes are presented as main mineral phases in a number of chondrules, or in the chondrules' mesostasis, but can be also found as single crystals in the matrix. Ca-poor clinopyroxenes (clinohypersthene, clinobronzite) make up the radially structured no. 1 chondrule, and the barred no. 4 chondrule. Normal zoning was observed at the pyroxenes of the no. 5 chondrule, while inverse zoning was present in some cases at the pyroxenes of the no. 1 chondrule. Ca-poor pyroxenes make up the radially textured no. 6 chondrule, and orthopyroxenes can be found in the poikilitic structured no. 8 chondrule.

Pyroxenes are present in a wide compositional variation in Nyirábrany. The chemical composition of pyroxenes was measured at 25 points of the thin

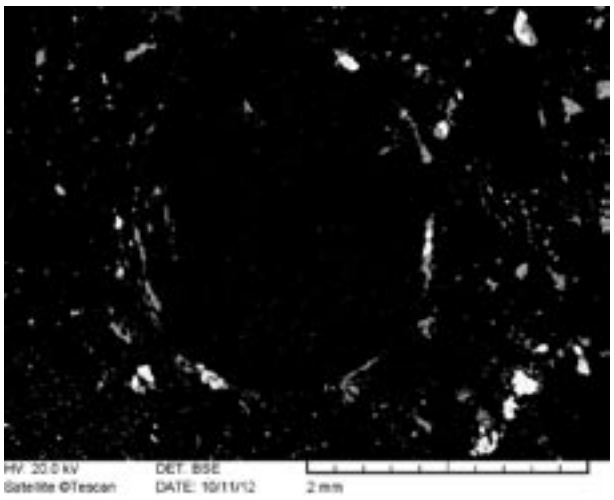

Fig. 5. FeNi-metal (white) and troilite (grey) at the rim and inside of Ch1. Opaque phases can be found in the matrix as well

section by SEM-EDX, out of which 19 were in the chondrules and 6 in the matrix. Pyroxene grains were selected randomly in the matrix. Although pyroxenes appear in diverse chemical compositions in the meteorite, most of them belong to the group of the low-Ca pyroxenes ($Wo_{1.61}$), both monoclinic and rhombic in structure, but most of them are clinopyroxenes, as mentioned above. The Fs-content of low-Ca pyroxenes are summarized in Table 3. There is also a small group of Ca-rich pyroxenes ($Wo_{36.03}$) and pyroxenes with intermediate composition ($Wo_{10.99}$). The average Fs-content of Ca-poor pyroxenes is 20.51 mol%, which is typical for L type chondrites. The average (and standard deviation values in parentheses) of enstatite and wollastonite in Nyirábrany are: 77.97 (11.65), 1.31 (1.14) mol%, respectively; while these values in the matrix are: 77.78 (9.95), 1.92 (0.74) mol%, re-

Table 3. The chemical composition of low-Ca pyroxenes in chondrules and matrix measured by SEM-EDX

	Oxide content (wt%)										En	Wo	Fs
	SiO_2	TiO_2	Al_2O_3	Cr_2O_3	FeO	MnO	MgO	CaO	total			(mol%)	
Ch1_px1	54.23	n.d.	n.d.	0.25	20.45	0.72	23.87	0.49	100.01		66.11	0.98	32.91
Ch1_px2	55.68	n.d.	n.d.	0.16	14.48	0.47	28.62	0.60	100.01		76.44	1.15	22.41
Ch1_px3	51.81	n.d.	1.97	0.84	22.69	0.79	19.81	2.09	100.00		57.43	4.36	38.21
Ch1_px4	53.86	n.d.	n.d.	0.53	20.86	0.62	23.38	0.75	100.00		64,99	1.50	33.51
Ch1_px5	55.97	n.d.	n.d.	n.d.	14.26	0.41	29.07	0.28	99.99		77.51	0.54	21.95
Ch4_px1	54.15	n.d.	n.d.	0.50	14.82	0.45	29.50	0.57	99.99		76.66	1.06	22.27
Ch4_px2	55.05	n.d.	n.d.	0.16	14.96	0.29	28.99	0.56	100.01		76.39	1.06	22.55
Ch5_px1	58.89	n.d.	n.d.	0.54	2.73	0.25	37.31	0.28	100.00		95.21	0.51	4.27
Ch5_px2	59.03	n.d.	n.d.	0.47	2.28	n.d.	38.03	0.19	100.00		96.41	0.35	3.24
Ch6_px1	54.64	n.d.	2.56	0.54	11.26	0.27	29.29	1.45	100.01		79.58	2.83	17.58
Ch6_px2	55.74	n.d.	n.d.	0.16	14.59	0.36	28.82	0.33	100.00		76.96	0.63	22.41
Ch8_px1	58.80	n.d.	n.d.	0.31	3.09	0.25	37.38	0.17	100.00		94.93	0.31	4.76
Ch9_px1	55.46	0.23	n.d.	0.16	14.90	0.49	27.88	0.89	100.01		75.03	1.72	23.25
										Mean	77.97	1.31	20.72
										σ	11.65	1.14	11.09
M_px1	52.82	0.29	3.44	1.09	14.53	0.40	26.20	1.22	99.99		73.89	2.47	23.63
M_px2	59.52	n.d.	n.d.	n.d.	0.63	0.16	39.21	0.48	100.00		98.03	0.86	1.11
M_px3	55.44	n.d.	n.d.	n.d.	15.16	0.49	27.66	1.25	100.00		74.07	2.41	23.52
M_px4	55.35	n.d.	n.d.	0.25	15.72	0.50	27.62	0.56	100.00		74.39	1.08	24.52
M_px5	55.17	n.d.	n.d.	0.18	16.25	0.45	26.75	1.19	99.99		72.34	2.31	25.35
M_px6	55.47	n.d.	n.d.	n.d.	15.37	0.36	27.58	1.22	100.00		73.97	2.35	23.68
										Mean	77.78	1.92	20.30
										σ	9.95	0.74	9.43
Average low-Ca pyroxene composition for Nyirábrany											77.88	1.61	20.51
										σ	9.95	0.74	7.58

Ch = chondrule
M = matrix
px =pyroxene
σ = standard deviation
n.d. = not detected

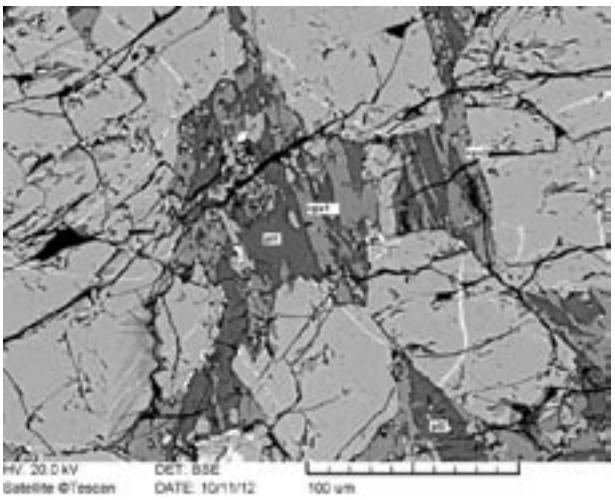

Fig. 6. Plagioclase (pl) and pyroxenes (px) in the mesostasis of a porphyritic olivine chondrule (Ch2)

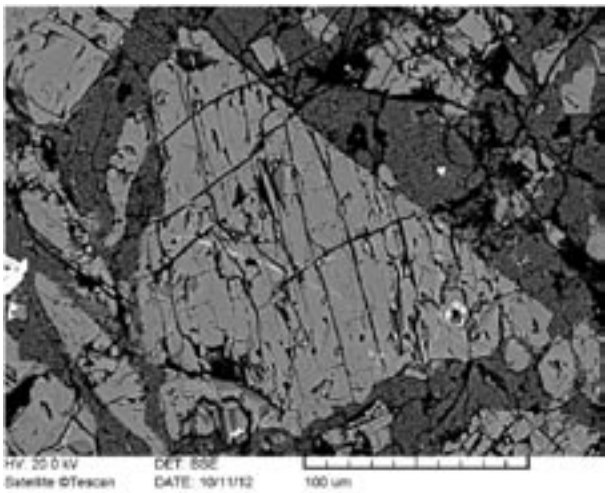

Fig. 7. BSE image of a planar fractured olivine crystal in a porphyritic olivine chondrule

spectively. To compare the diversity of pyroxenes regarding the chondrules and matrix values, the standard deviations for the above mentioned two pyroxenes are (chondrules/matrix): 11.65/9.95, 1.14/0.74. The same trend is visible and expected as in the case of olivine where the chondrules formed under more diverse conditions and larger deviations can be observed than in the matrix.

Plagioclase

The amount of plagioclase is ~2.5% (Sztrókay et al., 1977). It is present in the mesostasis of some of the chondrules, in the matrix and in the melt veins of some olivine crystals. Plagioclase crystals are present as xenomorph grains, mostly between other silicate crystals (Fig. 6), in the matrix or inside melt veins of olivine grains. Sztrókay et al. (1977) identified An-content between 14 and 23 mol%, while Kubovics et al. (2004) identified only sodic plagioclase and measured 11 mol% An-content of the plagioclase. In addition to the above mentioned compositions, we also identified mafic plagioclase in a small quantity with an An-content of 78.6 mol%, however this composition was measured only in the mesostasis of chondrule no. 2. During our SEM-EDX investigation, we also analyzed sodic plagioclase with average $An_{23.7}$ and $An_{10.4}$ in chondrule no. 6 and in another, diffuse chondrule (not mentioned in the text).

Opaque minerals

The main opaque minerals in the meteorite are Fe-Ni metal and troilite, beside these phases minor amount of chromite is also present. These opaque constituents were identified by opaque microscopy and SEM-EDX. The amount of Fe-Ni metal and troilite are ~1.32% and ~2.5%, respectively, which were calculated by analyzing the BSE images of the thin section using a software called "ImageJ". Opaque constituents can be found inside chondrules, at the chondrules' rims and in the matrix (Fig. 5). They appear as xenomorph crystals or crystal agglomerates, or as tiny round grains with a diameter of a few μm.

The Ni content of the metal grains was measured by SEM-EDX. Fe-Ni metal is arranged in an inhomogeneous pattern with highly variable Ni content. The Ni contents of kamacite varies between 3.19 and 5.10 wt% with an average of 4.4 wt% (σ = 0.77) and the Ni content of taenite varies between 27.36 and 54.28 wt% with an average of 40.67 wt% (σ = 10.75).

Shock stage and terrestrial weathering

We characterized the shock metamorphic stage of Nyirábrany using the 6 level scale for ordinary chondrites developed by Stöffler et al. (1991) and presented in Table 4. It was the first time that such an analysis was conducted on this meteorite.

Fragmented chondrules were identified in the meteorite, suggesting early shock events, but their analysis does not give exact information on the characteristics of these shocks. During the optical study, we searched for shock markers in olivine and plagioclase crystals, as referred previously by Stöffler et al. (1991). Due to its small quantity, plagioclase was identified only with SEM-EDX analysis, so we only used the optical and textural features of the olivine crystals for this purpose. Most olivine grains show sharp optical extinction in transmitted, plane polarized light, with irregular fractures in most of them. Planar fractures were visible only in very few cases (Fig. 7), and undulatory optical extinction could not be observed in

Table 4. Characteristics of shock stages by Stöffler et al. 1991

Shock stage	Olivine	Plagioclase	Local Scale effects	Pressure (GPa)
S1 (completely unshocked)	sharp extinction, regular fractures	sharp extinction, regular fractures	–	<4–5
S2 (very weakly shocked)	undulating extinction, irregular fractures	undulating extinction, irregular fractures	–	5–10
S3 (weakly shocked)	undulating extinction, planar and irregular fractures	undulating extinction	melt veins	15–20
S4 (moderately shocked)	weak mosaicism, planar deformational fractures	undulating extinction, planar deformation features, partially isotropic behaviour	melt pockets, melt veins crossing each other	30–35
S5 (strongly shocked)	strong mosaicism, planar deformational fractures	maskelynite	melt pockets, extended melt veins system	45–55
S6 (very strongly shocked)	solid phase recrystalization, melting, Ringwoodite	melting, glass formation	melt pockets, extended melt veins system	75–90

any crystals, including those with planar deformation fractures.

These findings suggest that the shock stage of Nyirábrany is around S2, but some of its signatures show that it could rarely reach the S3 level. Although the former presence of S3 or even higher shock level cannot be excluded (as post shock thermal event might overprint them), presenting observable signatures of only lower shock levels (Rubin, 2004), for the whole meteorite we could estimate only a very low degree of shock which is consistent with an S2 shock level in general.

There are chromite minerals in the meteorite that might be also produced by shock effects. Chromite is present as small opaque crystals in chondrules but also in the matrix, often in the form of anhedral clusters or as tiny isometric grains. Chromite could be produced by moderate level of thermal metamorphism (Rubin, 2003; Huss et al., 2006) and its presence also suggests shock event(s) (Lauretta et al., 2005) in the history of the meteorite.

Terrestrial alteration was determined by analyzing mineralogical changes and identification the oxidation of different mineral groups. For such an observation, a 7 level scale can be used, originally proposed by Wlotzka (1993).

Analyzing Nyirábrany with naked eye, reddish-brown oxidation products could already be observed at several locations around opaque phases. Using polarizing microscope, the reddish-brown weathering rind was even more evident around many minerals. While the weathering process influenced about 30 – 40% of the metal and sulfides in Nyirábrany, no similar features were present on the silicates. Based on this observation, we classified Nyirábrany in the W2 class of Wlotzka's scale.

Cristobalite and Cl-apatite

Cristobalite can be found as rounded grains in pyroxene crystals in a radial chondrule (Ch1) (Figure 3c). Observations and modelling show cristobalite could form by metamorphic processes (example: ALHA 76003, Olsen et al., 1981) and high temperature (example: Parnallee and Farmington meteorite, Bridges et al. 1994) from silica melt and by inversion from stishovite or coesite, always at high temperature (Heaney et al., 1994).

Cl-apatite was identified by SEM-EDX analysis in the matrix (Fig. 3b). The presence of cristobalite indicates that the cristobalite-bearing chondrule could have experienced a temperature as high as ~2000 K during its formation (Hezel et al., 2006). The presence of Cl-apatite could be the evidence that halogene-rich fluids affected the chondritic material inside the parent body (Jones et al., 2011).

CLASSIFICATION

Chondrite Group

To define the chondrite group of Nyirábrany, Fe-Ni metal content was calculated using BSE images, and the chemical composition of olivines and low-Ca pyroxenes were analyzed by SEM-EDX in the thin section. Unfortunately, detailed bulk chemistry analysis was not possible due to the limited access to the sample, but such measurement has been done before, details can be seen in the Table 5 and 6. According to Sztrókay et al. (1977) Nyirábrany was classified as an

Table 5. Bulk chemical composition of Nyirábrany by H. B. Wiik (Sztrókay et al., 1979)

Element/sulfide/ oxide	wt%	Element	atom%
Fe	2.34	Fe_{total}	20.38
Ni	1.04	Ni	1.04
Co	0.0085	Co	0.08
FeS	5.70	Si	18.76
SiO_2	40.09	Ti	0.09
TiO_2	0.15	Al	1.16
Al_2O_3	2.19	Cr	0.49
Cr_2O_3	0.72	Mn	0.22
FeO	18.55	Ca	1.25
MnO	0.28	Mg	15.45
MgO	25.63	K	0.12
CaO	1.77	Na	0.90
K_2O	0.09	S	2.08
Na_2O	1.21	P	0.10
P_2O_5	0.24	C	0.12
H_2O	0.10		
C	0.12		
Total	100.30		

Table 6. Trace element content of Nyirábrany (Sztrókay et al., 1979)

Trace element	ppm
Ag	25
B	16
Ba	1000
Cu	60
Sr	900
Zn	1000
Li	600
Pb	<10
V	<10

LL type ordinary chondrite. Our results showed that Nyirábrany can't be classified clearly as an LL chondrite, because some of its main chemical features are typical of L group chondrites (Fig. 8):

- On the basis of the 1.32% Fe-Ni metal content, Nyirábrany belongs to the LL group chondrites.
- The average Fa-content of olivines ($Fa_{26.71}$) falls between the ranges of the L and LL type ordinary chondrites (Fig. 8).
- The average Fs-content of low-Ca pyroxenes ($Fs_{20.51}$) falls within the value of the L chondrites, however the composition varies between 1 and 38 mol%.

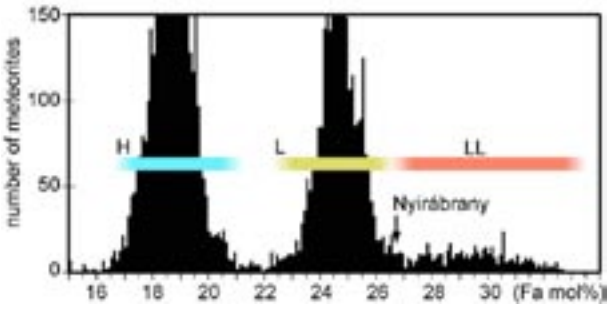

Fig. 8. Visualization of the average Fa-content of olivines (mol%) in Nyirábrany that puts this meteorite between the L and LL groups. The data for the ordinary chondrite groups (H, L, LL) is from Rubin (1990), the data for the histogram is selected from Met-Base (Koblitz, 2005 in Trigo-Rodríguez et al., 2009)

Petrologic type

On the basis of the van Schmus and Wood (1967) petrological type scheme, Nyirábrany was previously classified by Sztrókay et al. (1977) as petrologic type 5 ordinary chondrite. Our investigation showed that some of Nyirábrany's mineralogical and textural features indicate a smaller degree of thermal metamorphism:

- all the olivines and the majority of pyroxenes are homogeneous, the inhomogeneity of zoned pyroxene crystals is usually less than 5%, indicating petrologic type 4,
- monoclinic pyroxenes dominate in the sample, which is typical for petrologic type 4; the majority of chondrules contain only a small amount of recrystallized glass, which indicates petrologic type 4–5,
- some chondrules are well-defined, while others have diffuse outline, indicating petrologic type 5.
- the matrix is crystalline, it is composed of mineral grains with different size, which is typical for petrologic type 4-5.

Shock stage and weathering grade

The optical and textural features of olivines, like sharp optical extinction, irregular and a few planar fractures, but no observed undulatory extinction, suggest S2 shock stage for Nyirábrany, which is consistent with a very low degree of shock metamorphism.

The terrestrial alteration affected only the opaque phases of the meteorite. About 30–40% of the metal and sulfide minerals were oxidized, which is consistent with a W2 weathering grade.

COMPARISON TO OTHER CHONDRITES

To exploit the gained data and also provide suggestions for future research directions for this meteorite, we compared our results to other well studied LL5/6 meteorites below. Such comparison might give insight into the general properties of this meteorite group, and also to identify differences between them. The main goal would be to improve the knowledge of the parent bodies of these meteorites in the future.

In the case of Bensour LL6 chondrite, signatures of probably impact induced compaction and brecciation was observed (Gattacceca et al., 2003) with shock remnant magnetization. Bensour is possibly connected to Kilabo meteorite that also fell in Africa, this later one shows thick, black shock veins, and its shock stage was determined to be S3 (Gorin & Alexeev, 2006). The Ni and Co concentration both in Bensour and Kilabo was high together with relatively small bulk metal content (The Ni content of Nyírábrany can be seen in Tab. 5). Bensour and Kilabo meteorites are probably among the most oxidized ones (Cole et al., 2007). Both meteorites show the same fayalite content ($Fa_{30.7}$ for Bensour, and $Fa_{30.9}$ for Kilabo), and they show a microbrecciated structure with very few chondrules, though relict chondrules could be identified. These two meteorites might come from the same parent body, although the different cosmic exposure ages suggest complex history. A possible source candidate for them is the 3628 Boznemcova asteroid (Ustinova et al., 2008). The Ensisheim meteorite (fell in 1492), an LL6 chondrite, is also important target for comparison.

The average chondrule abundance in both L and LL chondrites varies between 60 and 80%. In Nyirábrany, because of the 4-5 petrologic type, the identification of chondrules was not evident in every cases, but their total amount was around 65%, and their size ranged between ~560 μm and ~2200 μm in diameter. The metal abundance for L chondrites is between 4-9%, while in LL chondrites around 0.3-3% (Weisberg et al., 2005), in Nyírábrany it was around 1.32%. The fayalite content in Nyírábrany is between the characteristic L and LL values, suggesting intermediate situation among these two groups.

Mineral composition suggests that LL chondrites especially thermally metamorphosed LL5 and LL6 like Tuxuac (Matsumoto et al., 2012), where the ratio of poly/mono-mineralic particles and the characteristic grain size (Tsuchiyama et al., 2012) resemble to the small samples acquired by Hayabuse mission from the surface of asteroid Itokawa (Matsumoto et al., 2012; Nagano et al., 2012; Yakame et al., 2012). This observation enhances the importance of LL chondrites and other objects that are close to them in properties, including Nyirábrany, as they could provide insight into the geological evolution of Itokawa-like asteroids. Such comparison is important as LL chondrites present a wide range of thermal metamorphism, also presenting decreasing mineral variability from LL4 to LL7 (Reid, 1997).

CONCLUSION

Our new petrological, mineralogical and chemical results show that the Nyirábrany meteorite can be classified as an L/LL type ordinary chondrite, which has undergone a moderate to high degree of thermal metamorphism and has equilibrated to petrologic type 4-5. Moreover, it has experienced a very low degree of shock metamorphism and weak terrestrial alteration. In summary, Nyirábrany can be designated as an L/LL4-5, S2, W2 ordinary chondrite. In the future, we are planning to investigate more the shock stage of the meteorite using Raman microspectroscopy that could support to draw conclusions on the formation and early history of this meteorite's parent body.

Comparing Nyírábrany to other meteorites, Nyírábrany is a well metamorphosed object representing a section of its parent body that differentiated substantially and lost substantial part of its metal content. However, impact processes did not erase the much earlier formed features. It is known that peak temperature during metamorphism increases from petrologic type 4 to 5 to 6, while the cooling times are poorly known (Dodd, 1981). Nyírábrany might provide useful information on the ancient process, above all impact and thermal driven alteration in parent bodies that is connected to the geological evolution of asteroids. The importance of Nyirábrany as being an intermediate type between L and LL groups, just like Bjurböle, Cynthiana, Knyahinya, Qidong, Xi Ujimgin meteorites (Weisberg et al., 2005) is increased after the Itokawa asteroid sampling event by Hayabusa spacecraft, as some mineral features in the LL group resemble to those found in that asteroid samples.

ACKNOWLEDGMENT

This work is based on the MSc thesis of M. Mészáros, and supported by T. Váczi, Zs. Bendő, Sz. Nagy, Gy. Buda, Cs. Szabó, L. Patkó, Á. Szabó.

REFERENCES

Bridges J.C., Franchi I.A., Hutchison R., Alexander C.M. O'd., Morse A.D., Pillinger C.T., Long V.P., 1994 – Petrographic, isotopic, and chemical studies of cristobalite- and tridymite-bearing chondrules and clasts in ordinary chondrites. *Meteoritics* 29, 448–449.

Bridges J.C., Catling D.C., Saxton J.M., Swindle T.D., Lyon I.C., Grady M.M., 2001 – Alteration Assemblages in Martian Meteorites: Implications for Near-Surface Processes. *Space Science Reviews* 96, 365–392.

Cole K.J., Schultz L., Sipiera P.P., Welten K.C., 2007 – Kilabo and Bensour, Two LL6 Chondrite Falls from Africa with Very Similar Mineralogical Compositions but Different Cosmic-Ray Exposure Histories. 38th Lunar and Planetary Science Conference, League City, Texas, abstract no. 1477.

Dodd R.T., 1981 – Meteorites – A Petrologic-Chemical Synthesis. Cambridge, New York.

Fritz J., Greshake A., Stöffler D., 2003 – Launch Conditions for Martian Meteorites: Plagioclase as a Shock Pressure Barometer. 34th Annual Lunar and Planetary Science Conference, League City, Texas, abstract no. 1335.

Gattacceca J., Rochette P., Bourot-Denise M., 2003 – Magnetic properties of a freshly fallen LL ordinary chondrite: the Bensour meteorite. *Physics of the Earth and Planetary Interiors* 140, 343–358.

Gillet P., Chen M., Dubrovinsky L., El Goresy A., 2000 – Natural $NaAlSi_3O_8$-Hollandite in the Shocked Sixiangkou Meteorite. *Science* 287, 1633–1636.

Gorin V.D., Alexeev V.A., 2006 – Radionuclides in the Bukhara CV3 and Kilabo LL6 chondrites. 37th Lunar and Planetary Science Conference, abstract no. 1034.

Gucsik A., Nishido H., Ninagawa K., Okumura T., Toyoda S., 2010 – Micro-Raman spectroscopy of anomalous planar microsctructures in quartz from Mt. Oikeyama: discovery of a probable impact crater in Japan. *Meteoritics & Planetary Science* 45, 2022–2035.

Gucsik A., Ming Z., Koeberl C., Salje E., Redfern S.A.T., Pruneda J.M., 2004 – Infrared and Raman spectroscopy of experimentally shocked zircon. *Mineralogical Magazine* 68, 801–811.

Heaney P.J., Prewitt C.T., Gibbs G.V., 1994. Silica: behavior, geochemistry and physical applications. *Reviews in Mineralogy and Geochemistry* 29, Mineralogical Society of America.

Hezel D.C., Herbert P., Lutz N., Frank E.B., 2006 – Origin of SiO_2-rich components in ordinary chondrites. *Geochimica et Cosmochimica Acta* 70, 1548–1564.

Huss G.R., Rubin A.E., Grossman J.N., 2006 – Thermal metamorphism in Chondrites. Meteorites and the Early Solar System II, Univ. of Arizona Press, Tucson, 943, 567–586.

Jones R.H., McCubbin F.M., Dreeland L., Guan Y., 2011 – Phosphate minerals in type 4-6 LL chondrites: The nature of fluids on the LL chondrite parent body. 42nd Lunar and Planetary Science Conference, abstract no. 2464.

Kayama M., Nishido H., Sekine T., Nakazato T., Gucsik A., Ninagawa K., 2012 – Shock barometer using cathodoluminescence of alkali feldspar. *Journal of Geophysical Research* 117(E9), CiteID E09004 , doi:10.1029/2011JE004025

Kayama M., Gucsik A., Nishido H., Ninagawa K., Tsuchiyama A., 2009 – Cathodoluminescence and Raman Spectroscopic Characterization of Experimentally Shocked Plagioclase. AIP Proceedings of the International Conference. 1163, 86–96.

Koblitz J., 2005 – MetBase version 7.1 for Windows. CD-ROM.

Kubo T., Kimura M., Kato T., Nishi M., Tominaga A., Kikegawa T., Funakoshi K.-I., 2010 – Plagioclase breakdown as an indicator for shock conditions of meteorites. *Nature Geoscience* 3, 41–45.

Kubovics I., Ditrói-Puskás Z., Gál-Sólymos K., 2004 – Re-evaluation of meteorites from the Carpathian Basin: Preliminary results from Kisvarsány, Knyahinya, Mezőmadaras, Mike, Mócs and Nyírábrány. *Acta Geologica Hungarica* 47/2–3, 269–285.

Lambert P., 1981 – Reflectivity applied to peak pressure estimates in silicates of shocked rocks. *Journal of Geophysical Research*, 86, 6187–6204.

Lauretta D.S., Nagahara H., Alexander C.M. O'd, 2005 – Petrology and origin of Ferromagnesian Silicate Chondrules. In: Meteorites and the Early Solar System II, Lauretta D. S. and McSween Jr. H. Y. (eds.), University of Arizona Press, Tucson, 943, 431–459.

Matsumoto T., Tsuchiyama A., Gucsik A., Noguchi R., Matsuno J., Nagano T., Imai Y., Shimada A., Uesugi M., Uesugi K., Nakano T., Takeuchi A., Suzuki,Y., Nakamura T., Noguchi T., Mukai T., Abe M., Yada T., Fujimura A., 2012 – Micro-structures of particle surfaces of Itokawa regolith and LL chondrite fragments. 43rd Lunar and Planetary Science Conference, The Woodlands, Texas, abstract no. 1969.

Miyamoto, M., Ohsumi, K., 1995 – Micro Raman spectroscopy of olivines in L6 chondrites: Evaluation of the degree of shock. *Geophysical Research Letters* 22, 437–440.

Nakamura T., Noguchi T., Tanaka M., Zolensky M.E., Kimura M., Tsuchiyama A., Nakato A., Ogami T., Ishida H., Uesugi M., Yada T., Shirai K., Fujimura A., Okazaki R., Sandford S.A., Ishibashi Y., Abe M., Okada T., Ueno M., Mukai T., Yoshikawa M., Kawaguchi J., 2011 – Itokawa Dust Particles: A Direct Link Between S-Type Asteroids and Ordinary Chondrites. *Science* 333, 1113.

Nagy S.,Okumura T., Gucsik A., 2008 – A cathodoluminescence characterization of shocked K-feldspar from Bosumtwi meteorite crater, 71st Annual Meteoritical Society Meeting, Matsue, Japan, abstract no. 5028.

Nagano T., Tsuchiyama A., Shimobayashi N., Seto Y., Noguchi R., Imai Y., Matsumoto T., Matsuno J., 2012 – Homogeneity of LL5 and LL6 Chondrites in Relation to Hayabusa Sample Analysis. 43rd Lunar and Planetary Science Conference, The Woodlands, Texas, abstract no. 2500.

Olsen E.J., Mayeda T.K., Clayton R.N., 1981 – Cristobalite-pyroxene in an L6 chondrite – Implications for metamorphism. *Earth and Planetary Science Letters* 56, 82–88.

Ostertag R., Stöffler D., Bischoff A., Palme H., Schultz L., Spettel B., Weber H., Weckwerth G., Wänke H., 1986 – Lunar meteorite Yamato-791197: Petrography, shock history and chemical composition. The Tenth Symposium on Antarctic Meteorites, Proceedings of the 1985 conference. Edited by Keizo Yanai, Hiroshi Takeda and Akira Shimoyama. Memoirs of the National Institute of Polar Research, Special Issue No. 41. Tokyo: National Institute of Polar Research, 17.

Paton M., Muinonen K., Pesonen L.J., Kuosmanen V., Kohout T., Laitinen J., Lehtinen M., 2011 – A PCA study to determine how features in meteorite reflectance spectra vary with the samples' physical properties. *Journal of Quantitative Spectroscopy & Radiative Transfer* 112, 1803–1814.

Putnis A., Price G.D., 1979 – High-pressure $(Mg, Fe)_2SiO_4$ phases in the Tenham chondritic meteorite. *Nature* 280, 217–218.

Reid A.M., 1997 – Workshop on Parent-body and Nebular Modification of Chondritic Materials, LPI Tech. Rept. 97-12 Part 1, 50–51.

Rubin A.E., 1990 – Kamacite and olivine in ordinary chondrites: Intergroup and intragroup relationships. *Geochimica et Cosmochimica Acta* 54, 1217–1232.

Rubin A.E., 2003 – Chromite-Plagioclase assemblages as a new shock indicator, implications for the shock and thermal histories of ordinary chondrites. *Geochimica et Cosmochimica Acta* 67, 2695–2709.

Rubin A.E., 2004 – Postshock annealing and postannealing shock in equilibrated ordinary chondrites: Implications for the thermal and shock histories of chondritic asteroids. *Geochimica et Cosmochimica Acta* 68, 673–689.

Stöffler D., 1967 – Deformation und Umwandlung von Plagioklas durch Stoßwellen in den Gesteinen des Nördlinger Ries. *Contributions to Mineralogy and Petrology* 16, 51–83.

Stöffler D., Ostertag R., Jammes C., Pfannschmidt G., Sen Gupta P.R., Simon S.B., Papike J.J., Beauchamp R.H., 1986 – Shock metamorphism and petrography of the Shergotty achondrite. *Geochimica et Cosmochimica Acta* 50, 889–903.

Stöffler D., Keil K., Scott E.R.D., 1991 – Shock metamorphism of ordinary chondrites. *Geochimica et Cosmochimica Acta* 55, 3845–3867.

Stöffler D., Langenhorst F., 1994 – Shock metamorphism of quartz in nature and experiment: I. Basic observations and theory, *Meteoritics* 29, 155–181.

Sztrókay K.I., Wiik H.B., Buda Gy., 1977 – Ein Amphoterit-Chondrit aus Ungarn. *Chemie der Erde* 36, 287–298.

Trigo-Rodríguez J.M., Llorca J., Rubin A.E., Grossman J.N., Sears D.W.G., Naranjo M., Bretzius S., Tapia M., Guarín Sepúlveda M.H., 2009 – The Cali meteorite fall: A new H/L ordinary chondrite. *Meteoritics & Planetary Science* 44, 211–220.

Tsuchiyama A., Uesugi M., Uesugi K., Nakano T., Noguchi R., Matsumoto T., Matsuno J., Nagano T., Imai Y., Shimda A., Takeuchi A., Suzuki Y., Nakamura T., Noguchi T., Mukai T., Abe M., Yada T., Fujimura A., 2012 – Three-Dimensional Structures of Itokawa Particles Using Micro-Tomography: Comparison with LL5 and LL6 Chondrites. 43rd Lunar and Planetary Science Conference, The Woodlands, Texas, abstract no. 1870.

Ustinova G.K., Alexeev V.A., Gorin V.D., 2008 – Orbits and Probable Parent Body of the Kilabo and Bensour LL6-Chondrites. 39th Lunar and Planetary Science Conference, League City, Texas, abstract no. 1011.

van Schmus W.R., Wood J.A., 1967 – A chemical-petrologic classification for the chondritic meteorites. *Geochimica et Cosmochimica Acta* 31, 747–765.

Weisberg M.K., McCoy T.J., Krot A.N., 2005 – Systematics and Evaluation of Meteorite Classification. In: Meteorites and the early Solar System II. Eds: Lauretta D.S., McSween H.Y., Dotson R. joint book project of the University of Arizona Press and the Lunar and Planetary Institute.

Wlotzka F., 1993 – A weathering scale for the ordinary chondrites (abstract). *Meteoritics* 28, 460.

Yakame S., Uesugi M., Karouji Y., Ishibashi Y., Yada T., Okada T., Abe M., Fujimura A., 2012 – Observation of Shock Textures in Fragments of Kilabo (LL6). 75th Annual Meeting of the Meteoritical Society, Cairns, Australia. *Meteoritics and Planetary Science* 47, Supplement s1, A424 (5169.pdf).

Yates A.M., Tackett S.L., Moore C.B., 1968 – Chromium and manganese in chondrites. *Chemical Geology* 3, 313–322.

Publishers: Wrocław University of Technology, Faculty of Geoengineering, Mining and Geology
Polish Meteorite Society

Meteorites
Vol. 3, Nos. 1–2, 2014, 33–44
www.meteorites.pwr.wroc.pl
DOI 10.5277/met140103

NWA 6255 METEORITE – THERMOPHYSICAL PROPERTIES OF INTERIOR AND THE CRUST

Katarzyna ŁUSZCZEK[1], Radosław A. WACH[2]

[1] Wroclaw University of Technology, Faculty of Geoengineering, Mining and Geology, Wybrzeże S. Wyspiańskiego 27, 50-370 Wrocław, Poland
[2] Lodz University of Technology, Institute of Applied Radiation Chemistry, Wróblewskiego 15, 93-590 Łódź, Poland

Abstract: Differences in the thermophysical properties of NWA 6255 meteorite samples obtained from various locations with respect to the distance from the surface of the meteorite were evaluated by a differential scanning calorimetry (DSC). DSC is a perfect tool to experimentally verify theoretically predicted thermophysical properties of extraterrestrial matter. The specific heat capacity of the crust and the interior of meteorite were determined to be in the temperature range of 223−823 K. Measured *Cp* values at room temperature for crust and for the interior of this meteorite were 602 and 668 $J \cdot kg^{-1} \cdot K^{-1}$, respectively. In addition, the phase transition of troilite from: (a) the fusion crust samples, (b) the edge part of the meteorite (1−2 mm below the crust), and (c) the interior (over 10 mm below the fusion crust) was examined. It is shown that the shift of α/β transition peak of the troilite exhibits the temperature gradient evolved during atmospheric passage of a meteoroid. Moreover, the enthalpy changes of α/β transition were used to determine the troilite content in the meteorite samples (3.6 wt.%). Obtained data are in agreement with previous Leco method's results, since NWA 6255 is relatively fresh find (W1) and troilite tends to oxidized quickly.

Keywords: NWA 6255, DSC, thermophysical properties of meteorite, specific heat capacity, troilite phase transition, troilite cosmothermometer

INTRODUCTION

The NWA 6255 meteorite was found in Morocco in 2009. The exact place of find and the coordinates are unknown, so the meteorite belongs to a large group of meteorites represented under the dense collection area name "North West Africa (NWA)" and was registered under the number of 6255 (it was 6255th meteorite from the region to be classified and assigned a number). The total mass of the two pieces of NWA 6255 was 3.2 kg. It was classified as an L-type ordinary chondrite, due to its low metal content with the petrographic type L5, shock stage S4, and weathering grade of W1 (www.lpi.usra.edu, 2014).

NWA 6255 is an interesting meteorite not only because it is really fresh (Fig. 1), unique or especially distinctive object, but also because it is a very common meteorite type. It is one of 5565 approved meteorites, classified as L5 type chondrite (www.lpi.usra.edu, 2014), and therefore representative of typical S-type asteroid material (Sears, 2004).

The bulk chemical composition of NWA 6255 has been previously analyzed by Inductively Coupled Plasma Mass Spectrometry (ICP MS) (Łuszczek, 2012) and the content of volatile elements, such as sulphur was determined by the Leco method. It was found that NWA 6255 contains ca. 1.65 ± 0.02% of sulphur. This indicates that the meteorite may have sufficient content of troilite (FeS) for precise determination of its thermophysical transitions. Since NWA 6255 is a relatively fresh desert find and considering the fact that troilite is prone to relatively fast oxidation (Velbel, 2014), the meteorite is a good representative rock of its L-chondrite parent body. NWA 6255 was not evaluated in terms of thermophysical properties before.

Corresponding author: Katarzyna ŁUSZCZEK, katarzyna.luszczek@pwr.edu.pl

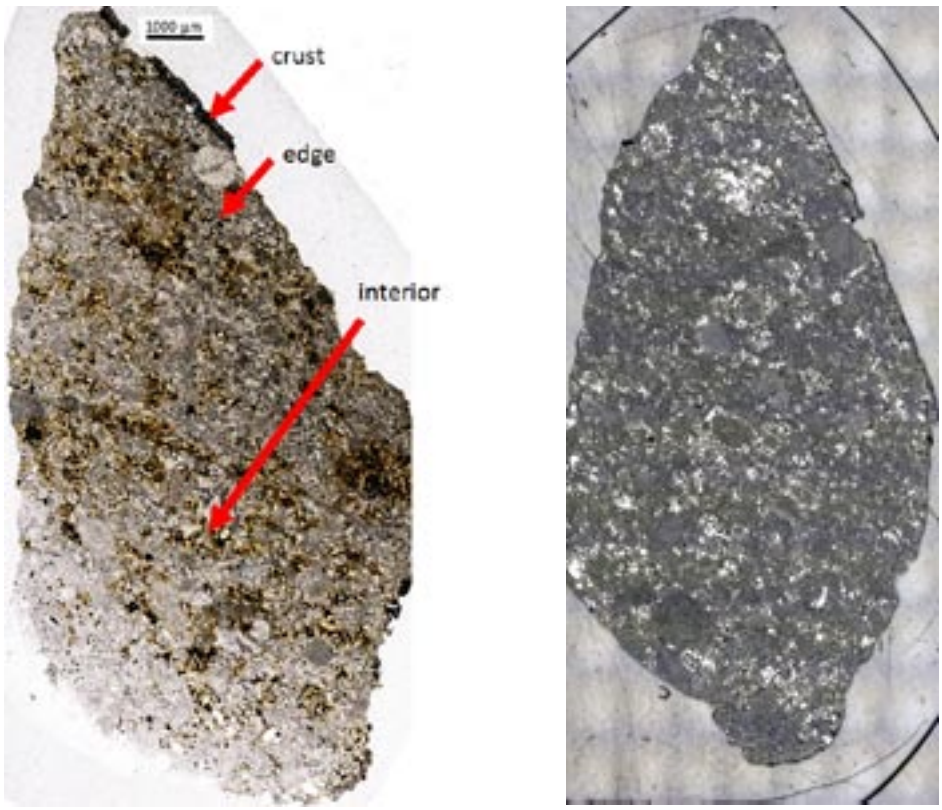

Fig. 1. Microscopic view of NWA 6255 chondrite; transmitted (left picture) and reflected light (right picture)

Thermophysical properties data of meteorites can seldom be found in the literature. However, as they represent principal features of the extraterrestrial matter it is fundamental to identify them. Knowledge of thermophysical properties of meteorites is extremely important for modeling the cooling rate of their parent bodies after accretion and the heat flow resulting from the decay of short-lived isotopes, mainly ^{26}Al.

The Yarkovsky and YORP (Yarkovsky-O'Keefe-Radzievskii-Paddack) effects on asteroid orbital and spin perturbations depends on the inverse thermal inertia, which varies with the square root of thermal conductivity and heat capacity. Thermal properties of meteorites, besides their importance for modelers, also provide important information on the meteorite's composition and its physical state (Opeil et. al, 2011). In many cases to date thermophysical properties were estimated and not measured directly (Gosh & Mc-Sween, 1999; Henke et al., 2012). In addition, the temperature of α/β transition of troilite (T_α), a mineral regularly present in ordinary chondrites in a few wt.% (ca. 5 wt.%), reflects its thermal history (Allton et al., 1993). Due to this fact, the troilite transition was proposed to be used as cosmothermometer (Lauer & Gooding, 1996) based on shift of the peak temperature indicating α/β transition of troilite.

Significant efforts have been made to determine thermal properties of meteorites, representing rocks on their parent bodies, in recent years by Szurgot (2003; 2011a, b; 2012a, b, c, d), and Szurgot and coworkers (Szurgot et al., 2008; Szurgot & Wojtatowicz, 2011; Szurgot & Polański, 2011; Szurgot et al., 2012). Valuable research was also conducted in Japanese and American laboratories by Matusi & Osako (1979), Yomogida & Matsui (1981, 1983), Gosh & Mc Sween (1999), Beach et al. (2009), Opeil et al. (2011), Consolmagno et al. (2013).

The aim of this study was to apply differential scanning calorimetry to evaluate thermal properties of NWA 6255 meteorite, especially to determine specific heat capacity and analyze troilite phase transition in various locations in the meteorite bulk, and to determine troilite content. Through investigations of meteorite fragments selected from different locations of the meteorite cross-section (Fig. 1), we expected to identify differences in troilite α/β transition, which can provide evidence of a temperature gradient generated during its atmospheric passage. To date, troilite α/β transitions have been measured only by thermoluminescence method and only for a few meteorites (Vaz, 1971, 1972; Sears, 1975). It is important to know the thermal effect (heating) that develops during entry, e.g. for estimating bolide brightness, and consequently its impact on the Earth surface, as a function of the meteoroid size.

PHASE TRANSITIONS OF TROILITE

Troilite is a nonmagnetic iron sulfide (FeS) and belongs to the pyrrhotite group. It was first discovered in 1766 in a meteorite (Albareto), and later in terrestrial rock. The name of this common extraterrestrial mineral is derived from the name of the discoverer, Italian scientist Domenico Troili (www.mindat.org, 2014).

A great deal of work has gone into discovering the nature of this mineral. FeS adopts three distinct temperature-dependent crystallographic and magnetic structures (Fig. 2) in which the Fe atoms occupy octahedral positions with varying degrees of distortion. Hexagonal troilite with space group $P\bar{6}2c$ is stable at low temperatures (Evans, 1970). In this structure, which has only been reported so far for FeS (King & Prewitt, 1982), all Fe atoms are combined in triangular clusters of three atoms in planes perpendicular to *c*. Half of the Fe-Fe bonds along *c* are parallel, whereas half are inclined to the *c* axis. Sulfur atoms may be regarded as forming triangles about these Fe-Fe bonds. The normals to the planes of these triangles tend to align with the Fe-Fe bonds; thus, half of the planes are perpendicular to *c* and half are tilted (Kruse, 1992). The structure can be derived from the NiAs structure. Based on the NiAs subcell axes A and C, the troilite supercell axes are given as $a = \sqrt{3}A$ and $c = 2C$ (Hägg & Sucksdorff, 1933).

At the α transition (named also α/β transition), the troilite structure, including its clusters, break down. Troilite transforms into the orthorhombic MnP-type structure with space group *Pnma* on the heating trough T_α (King & Prewitt, 1982). In this structure the Fe-Fe bonds form zigzag chains and all S triangles are tilted. Various values of T_α have been reported for ambient pressure: 413 K, based on electrical resistivity measurements on synthetic FeS (Ozawa & Anzai, 1966); 425 K based on DTA of syntetic samples (Moldenhauer & Brückner, 1976); and 388–423 K, according to TEM of meteoritic troilite (Töpel-Schadt & Müller, 1982).

However, Haraldsen (1941) found X-ray supercell reflections of synthetic samples to be weaker at 375 K than at 293 K. Thus, the α transition is indicated to be gradual with an onset detectable at 375 K. Kruse and Ericsson (1988) obtained a completed transition at 413 K on heating, using Mössbauer spectroscopy with meteoritic troilite. The reverse transition started at 410 K and was not completed even after 15 d of slow cooling to 280 K, where 20% of the Fe still was included in the MnP-type structure (Kruse, 1992).

Susceptibility measurements on a synthetic $Fe_{0.996}S$ single crystal by Horwood and coworkers (1976) showed that antiferromagnetically coupled spins of the Fe atoms point along the *c* axis of the NiAs subcell (c_{NiAs}) below the spin-flip temperature ($T_s \approx 445$ K), where the spin flipped reversibly by 90°. Values for T_s, include 458 K for synthetic FeS using neutron diffraction (Andresen & Torbo, 1967) and the intervals 410–470 K (heating) and 450–360 K (cooling) for meteoritic troilite (Kruse & Ericsson, 1988); the specific behavior depended on the sample pretreatment.

On heating at 483 K FeS transforms into the NiAs-type structure with the space group $P6_3/mmc$ (Fig. 2) (Töpel-Schadt & Müller, 1982), where the Fe-Fe bonds form a straight line along *c*; all S triangle planes are perpendicular to *c*. At $T_N \approx 600$ K the antiferromagnetic order in FeS breaks down into paramagnetism (Horwood et al., 1976).

Despite the voluminous literature on iron sulfides in meteorites, quantitative information on FeS properties above room temperature is rather rare. Troilite undergoes two phase transitions upon heating to the temperature below its melting point (Allton et al., 1993). Besides α/β there is a β/γ transition, which occurs at 598 ± 3 K (Chase et al., 1985).

The experimentally measured α/β onset temperature shows a systematic decline with the maximum experienced temperature, suggesting that high onset temperature is indicative of only low temperature in the natural history of the troilite samples (Allton et al., 1993). That trend is at least quantitatively consistent with the petrographic rankings of the meteorites in which troilite from the relatively unmetamorphosed L3 chondrites show a higher onset temperature than the troilite from either a highly metamorphosed L7 or an iron octrahedrite (Allton et al., 1993). Troilite was proposed to be a cosmothermometer for this reason.

The purpose of the present work was also to use troilite as the cosmothermometer and investigate the effect of temperature produced during atmospheric passage. Therefore, troilite α/β transitions in samples from different parts of the meteorite were investigated.

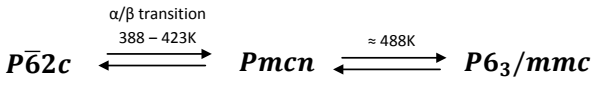

Fig. 2. Sequences of transitions of crystal structure observed in troilite from subsolidus phase (Töpel-Schadt & Müller, 1982; adapted by authors)

METHODOLOGY

A thermoanalytical technique of differential scanning calorimetry (DSC) is commonly used for following a phenomenon or a reaction occurring in a specimen that is accompanied by a change in its enthalpy whether temporal or permanent. DSC measures the temperatures and heat flows associated with transitions in materials as a function of time and temperature in a controlled manner. The measurements provide qualitative and quantitative information about physical and chemical changes that involve exothermic or endothermic processes or changes in heat capacity (Höhne et al., 1996). The technique is regularly utilized for polymers, textiles, food, adhesives, composites, packaging and for many other materials. Beside evaluation of thermal effects of various chemical reactions, the most general physical phenomena or material properties that can be determined with DSC include physical phase transitions and specific heat capacity of a specimen. Melting, crystallization, boiling, and glass transition (for polymers) are the primary examples of applications of the DSC technique.

All measurements were conducted with a Differential Scanning Calorimeter (Q200 TA Instruments). The instrument used was a heat flux type; the power compensation method (temperature of specimen and a reference should be the same) underlay the other common DSC type. In the heat flux DSC, two thermocouple integrated sensors in a furnace allow a sample pan (crucible) and the reference pan (usually empty) placed on them (Fig. 3) to be simultaneously heated/cooled at the same rate. Absolute temperatures of both are recorded in real time. Due to the heat capacity of the examined material the sample pan temperature is a bit lower (in the heating mode) or delayed with respect to the empty reference pan. At a constant heating rate the temperature increases linearly, in parallel for two pans – the difference, ΔT can be translated into heat flow due to performed calibration.

The instrument was calibrated for both temperature and heat flow using respectively indium (melting temperature 429.75 K) and the synthetic sapphire standard with well characterized *Cp* in the broad range of temperatures.

$$\Delta H = Cp_{sp}\,\Delta T \tag{1}$$

ΔH – measured heat flow rate
Cp_{sp} – a specific heat capacity of sapphire
ΔT – measured heating rate

Sample preparation

DSC measurements can determine thermal properties of relatively small samples of even a few mg (for chondrites it will be ca. 1.0–1.5 mm^3 for troilite phase transition, and ca. 5 mm^3 for *Cp* determination), therefore one can get information on the variation of measured property as a function of locations of a particular portion of the specimen. Sampling every mm is possible for precisely cut samples. However, this is also the main drawback of this method since a small sample mass requires multiple measurements in order to get an indication of the complete specimen. This is especially important when the specimen is heterogeneous in mm scale, like in ordinary chondrites. Therefore, while examining the chondritic meteorite with respect to troilite transitions or specific heat capacity, evaluation of few samples from all selected locations in essential. Another way to solve the problem of heterogeneity is by grinding a bigger piece of chondritic rock in order to homogenize it. Moreover, grinding has another advantage – the influence of physical state of the rock (porosity) is neglected, thus enabling instant heat transfer.

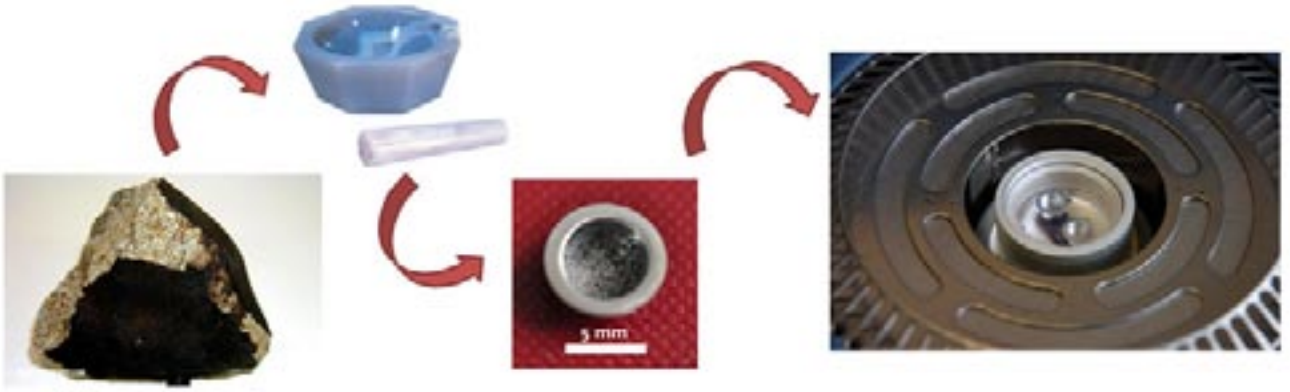

Fig. 3. Samples preparation for DSC measurements: choosing the crust, edge and interior part of meteorite (left), grinding the selected part in the agate mortar (middle top), preparing 5 mg of homogenized sample in the pan (middle bottom), putting the pan in the DSC – left pan with reference material, right with sample (right)

EXPERIMENTAL

Specific heat capacity

Specific heat capacity, *Cp* of two samples, representing the fusion crust, and the interior was determined. In DSC measurements of *Cp* of NWA 6255 samples the following equation applies:

$$C_p = C_{p_{sp}} \frac{H}{H_{sp}} \frac{m_{sp}}{m_m} \quad (2)$$

where Cp_{sp} is a specific heat capacity of the sapphire standard at a particular temperature, m_{sp} is the mass of the sapphire standard, and H is the heat flow of the meteorite specimen. Samples, with approximately the same mass as the sapphire (ca. 20 mg of grounded matter), were sealed in aluminum pans and analyzed in the temperature range between 223 and 823 K at a heating rate of 20 K·min^{-1} under nitrogen flow of 50 ml·min^{-1}. In the current investigations relative error in the measurement of *Cp* of NWA 6255 meteorites was 3–4%.

α/β phase transition of troilite

If the sample undergoes thermal transition, the measured heat flow rate momentarily changes at the endothermal α/β transition of troilite. Seven samples (with mass ca. 5–6 mg) from different parts of the meteorite were selected: three from the fusion crust, two comprising of the fusion crust and the edge of the meteorite (1–2 mm below the crust) and two from the interior of the meteorite (10 mm below the crust). They were analyzed in temperature range of 373 to 473 K to observe the α/β phase transition (Fig. 4). The conditions of the experiment, except the temperature range and the sample mass, were the same as for the measurement of the specific heat capacity. The α/β and β/γ phase transitions are also recorded during *Cp* measurements. In principle, examination of samples with lower sample mass provides more accurate results in precise determination of temperature transition T_α. This correlates with the contact area of the samples with the bottom of the crucible, which greatly influences the speed of response. In samples of higher mass, where the entire specimen cannot connect with the bottom of the crucible, detection of a thermal effect is delayed, or unsatisfactory in resolution (wider) due to prolonged heat transfer through a bulky specimen. In this work we focused on the α/β transition due to its importance as a cosmothermometer.

RESULTS

Specific heat capacity

The heat capacity of two samples from different regions: one from the crust, and one from the interior was determined. The mass of the samples was 20.3 and 20.9 mg, respectively. Table 1 compiled, calculated with equation 2, *Cp* of these samples at various temperatures. Temperature 423 K is omitted because of the α/β phase transition of troilite occurs in this region displaying endothermic heat effect disturbing proper determination of the *Cp*.

The values of *Cp* for the interior are higher than those for the crust. An increase of *Cp* value with the increase of temperature was observed for both samples. However, from 393 K the *Cp* for the interior in-

Table 1. Specific heat capacity *Cp* [J·kg^{-1}·K^{-1}] of NWA 6255 meteorite samples at various temperatures

T [K]	T [°C]	*Cp*	
		crust	interior
223	–50	476	532
263	–10	546	607
283	10	577	641
300	27	602	668
323	50	634	705
373	100	701	784
398	125	740	840
448	175	759	862
473	200	774	880
523	250	805	929
573	300	830	965
623	350	842	986
673	400	855	997
723	450	868	1007
773	500	876	1008
823	550	–	1017

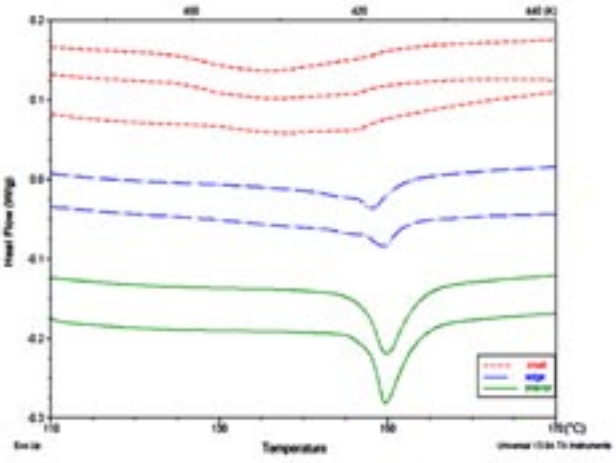

Fig. 4. Endothermic peaks of α/β transition of troilite from different parts of the NWA 6255 meteorite. DSC scan showing the heat flow during heating of the meteorite samples (dash line – crust, dash dot line – edge, solid line – interior)

creases a bit more steeply than for the crust (Fig. 5). From 573 K for the crust, and from 623 K for the interior the increase rate of *Cp* become slower, only about 10 $J \cdot kg^{-1} \cdot K^{-1}$ for 50 K.

α/β transition

Figure 4 shows the heat flow during heating of the meteorite samples. An intense endothermic peak indicates α/β phase transition of troilite. The enthalpy changes $\Delta H_{\alpha/\beta}$ and the onset of T_α were determined by using the TA Analysis software (dedicated to DSC of TA Instruments). The $\Delta H_{\alpha/\beta}$ is calculated as the area under the peak, whereas the peak temperature is regarded as the temperature of α/β phase transition.

The masses of analyzed samples, the temperature transition and the transition enthalpy are shown in Table 2. The average value and standard deviation were calculated for specimens of crust, edge and interior of the meteorite.

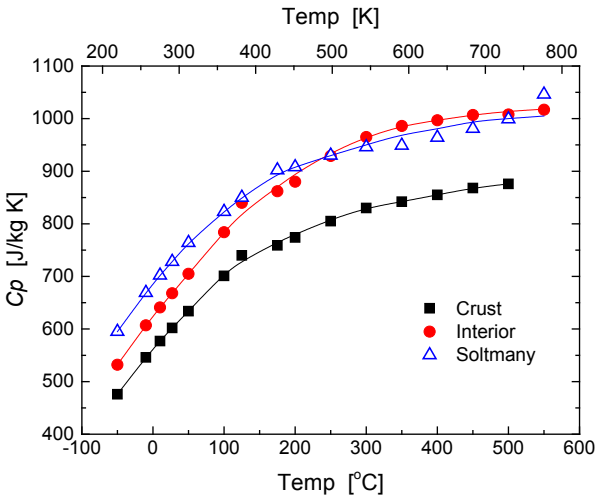

Fig. 5. *Cp*(*T*) dependence for crust and interior of NWA 6255 in comparison with bulk of Sołtmany (Szurgot et al., 2012)

Temperature of α/β transition of troilite in the meteorite exhibits an increase, from the crust (ca. 414.4 K) inward, through the edge, 1–2 mm part below the crust (422.25 K) to the interior (ca. 422.9 K). Despite small difference in T_α between the edge and the interior it becomes obvious that the edge has different characteristics than the interior when comparing offset temperature (T_{off}). T_{off} indicates the early stage of the transition or, as in this case, presence of various crystallographic types of the troilite. The T_{off} of the edge is 1.4 K less than that of the interior.

Despite the fact that the T_α of the edge differs slightly as compared to the interior, significant changes of enthalphy ($\Delta H_{\alpha/\beta}$) are observed. Therefore, the content of FeS in the edge part of the same crystallographic form as in the interior is three times lower than in the interior. The edge experienced rapid but intense elevation of temperature during atmospheric passage.

Troilite concentration

Troilite content in chondrites is about 5 wt.% (Hutchison, 2006; McSween & Huss, 2010). Our preliminary data on the bulk chemical composition established by Leco method indicate that NWA 6255 contains about 1.65 ± 0.02 wt.% of sulphur (Łuszczek, 2012). Knowing the molar mass of troilite (m_{molFeS} = 87.91) and that sulphur constitutes 36.5% in FeS, and assuming that the all sulphur crystallized in the form of FeS troilite, we calculated the troilite content in NWA 6255 samples to be ca. 4.5 wt.%.

We can compare the results obtained by Leco method with that from DSC measurements. The $\Delta H_{\alpha/\beta}$ of the interior part is representative, as the interior of the meteorite was not changed by either the temperature experienced during atmospheric passage, or the weathering of the meteorite after fall. The mean enthalpy change determined for α/β transition

Table 2. Temperature of α/β transition (the T_{off} is an offset temperature), transition enthalpy and estimation of FeS content of samples from different part of NWA 6255 meteorite

part of meteorite	mass [mg]	T_{off} [K]	mean T_{off} (SD)	T_α [K]	mean T_α (SD)	$\Delta H_{\alpha/\beta}$ [$J \cdot g^{-1}$]	mean $\Delta H_{\alpha/\beta}$ (SD)	FeS content [%]	mean FeS content [%]
crust	5.4	-	-	410.25*	414.4 (3.52)	0.44	0.44 (0.06)	1.0	1.0 (0.12)
	5.2	-		414.15*		0.37		0.9	
	3.7	-		418.85*		0.51		1.2	
edge	5.5	418.35	418.9 (0.55)	421.55	422.25 (0.7)	0.55	0.50 (0.06)	1.3	1.15 (0.15)
	6.1	419.45		422.95		0.44		1.0	
interior	5.7	419.95	420.3 (0.35)	422.95	422.9 (0.5)	1.57	1.53 (0.04)	3.7	3.6 (0.1)
	5.1	420.65		422.85		1.49		3.5	

* Peak positions were determined at temperatures between 410 to 418.85 K however, for these samples there was a broad depression indicating two effects of partially oxidized troilite and its *α/β* transition combined.

(1.53 $J \cdot g^{-1}$) shows that troilite is present in NWA 6255 as a small fraction of the overall mass.

We estimated the mean troilite content in the samples by measuring enthalpy change for the α/β transition. According to Allton and co-workers, enthalpy change for α/β transition of troilite is equal to 42.5 $J \cdot g^{-1}$ at transition temperature 423 K (Allton et al., 1994), i.e. at the mean transition temperature established for the NWA 6255 meteorite. Therefore, based on measurements of the interior, the content of troilite was estimated to be 3.6 wt.%. Current estimation of troilite content seems to be correct since values of enthalpy changes 1.49–1.57 $J \cdot g^{-1}$ are in agreement with those obtained by Lauer and Gooding (1996).

Moreover, the enthalpy of the fusion crust is much lower in the case of the edge as compared with that of the interior part. The lower value of $\Delta H_{\alpha/\beta}$ indicates that the sample contains less troilite. Therefore, troilite content in the crust part is much lower than in the interior. The range of troilite content is, however, much broader, between 0.9 and 3.7 wt.% (Tab. 2). It should be added that results obtained based on DSC measurements determined only the troilite in the crystallographic form undergoing α/β transition.

DISCUSSION

Thermophysical properties of the specific heat capacity and the temperature of α/β phase transition of troilite of the interior and the crust of NWA 6255 meteorite were determined by means of DSC measurements and are presented in this paper. The results for the fusion crust, the edge of the meteorite (1–2 mm below the crust), and for the meteorite interior (10 mm below the crust) were compared. By using small samples obtained from various locations in the meteorite, we are able to determine how the thermophysical properties change with respect to the sample location and the heating it experienced during atmospheric passage.

Heat capacity

The values of *Cp* of ordinary chondrites are similar to terrestrial rocks, thus proving the uniformity of mineral composition of the matter constituting the universe. The assumption that the heat capacity of a rock sample equals the sum of *Cp* of constituent minerals with respect to their weight fractions (Gosh & McSween, 1999) was supported by Opeil and co-authors (2011). Consequently, theoretical calculations of heat capacity can be directly compared with the experimentally obtained values of *Cp*, based for instance on DSC measurements. Using theoretical data of the constituent minerals of ordinary chondrites to calculate total heat capacity of a sample gave results that correspond well with experimentally determined values (Opeil et al., 2011 after Yomogida and Matsui, 1983). Calculation of *Cp* for Braunschweig (L6) based on *Cp* values of constituting minerals gave reliable values of *Cp* for this meteorite (704 ± 20 $J \cdot kg^{-1} \cdot K^{-1}$) at room temperature (Szurgot et al., 2014). They are nearly identical with the experimental values of *Cp* = 682 ± 15 $J \cdot kg^{-1} \cdot K^{-1}$ measured by DSC (Szurgot et al., 2014). Similary, the theoretical calculation of *Cp* for Sołtmany (L6) at room temperature (674 $J \cdot kg^{-1} \cdot K^{-1}$) (Szurgot, 2014) is close to the experimental values of *Cp* = 671 $J \cdot kg^{-1} \cdot K^{-1}$ (Wach et al., 2013). Moreover, results presented in this paper for NWA 6255 (*Cp* = 668 $J \cdot kg^{-1} \cdot K^{-1}$ at room temperature) show good agreement with theoretically predicted value of *Cp* for L group chondrites (*Cp* ≈ 700 $J \cdot kg^{-1} \cdot K^{-1}$) (Gosh & McSween, 1999).

As specific heat capacity is the inherent property of the matter, the results obtained experimentally by DSC measurements may be used to more accurately model the thermal history of asteroids as well as predict their future state. The heat capacity should be determined at various temperatures as the *Cp* is temperature-related. Moreover, *Cp* depends of the chemical composition of the sample, and since the interior and the crust have different composition, this should be measured for specimens obtained from various locations of the meteorite with respect to the distance from its surface. Therefore, measuring the samples from different places in the meteorite cross-section provides valuable data. It may be a useful tool for determining the heat gradient in the meteorite during its atmospheric passage. In fact, to come to more precise conclusion the exact distance from the fusion crust should be known. It will also be pivotal to estimate the chemical and the mineralogical composition of each sample as the *Cp* value depends on both. This will also influence the temperature of the troilite transition, T_α. Karwowski (2012) performed interesting work reporting the mineralogical composition of the fusion crust for an analogous chondrite, the Sołtmany (L6) meteorite. There is a need for similar examination of NWA 6255 (and other meteorites) in order to verify the conclusions.

About 80% of a meteoroid composed of an ordinary chondrite is lost during atmospheric entry. This loss was proven by measurements of $^{22}Ne/^{21}Ne$ isotopic ratio which then enabled the pre-atmospheric radius of a meteoroid (Bhandari et al., 1980) to be estimated. It is well known that refractory elements tend to survive high temperatures, whereas volatile el-

ements are the first to be mobilized firstly as the temperature increases. Therefore, the refractory elements are mostly to remain in the fusion crust. Refractory elements are in most cases also siderophile or chalckophile elements (from a geological point of view), so they will substitute in Fe-Ni alloy or in sulfides. Sulfides have a lower melting temperature compared to metals alloys, so they tend to sublimate from the outer region of the fusion crust (Karwowski, 2012). Elements such as metals will decrease the specific heat capacity value (Waples & Waples, 2004). Enrichment of the crust with metals may explain why the *Cp* value of the crust is lower, over the entire measured temperature range, than for the interior of the NWA 6255 meteorite.

Water bonded in the hydroxide group influences the specific heat capacity in an opposite way than metals. It will increase the *Cp* value, as water has one of the highest *Cp* value (Waples & Waples, 2004). Water is only present in asteroids beyond the snow line, in the outer part of the asteroid belt orbits, such as carbonaceous asteroids with water-rich, clay-like minerals. By contrast, ordinary chondrites originated from the inner part of the asteroid belt dominated by rocky, siliceous and dry bodies (Lang, 2011). Nevertheless, due to the fact that ordinary chondrites come from the region of the Solar System where water is absent, this consideration should be neglected.

Data of experimentally determined *Cp* values at room temperature of L-chondrites are listed in Table 3. Results obtained in this work are in good agreement with Alexeyeva's data (1958) for Kharhov (L6), but lower than for Elenovka (L5). The *Cp* value for Kukschin is much higher than that for NWA 6255 and also exceeds the theoretical value of *Cp* for L-chondrites of 700 $J \cdot kg^{-1} \cdot K^{-1}$ (Ghosh & McSween, 1999) or 770 $J \cdot kg^{-1} \cdot K^{-1}$ (Matsui & Osako, 1979). It is well known that specific heat is related to the content of metallic and sulfide minerals. So the differences exhibited in *Cp* values of Kukschin (Alexeyeva, 1958) are probably due to the differences in the mineral composition of the measured samples. On the other hand, the Y-74191 has very low *Cp*, which may be due to the fact that smaller sample evaluated (m = 10 mg) might not have been representative of the complete meteorite mass as the experimental value of *Cp* does not meet the theoretical value for L group chondrites. Currently obtained results of *Cp* are in the same range as those for Sołtmany (L6) and Braunschweig (L6).

Table 3. Heat capacity of L group chondrites at room temperature

meteorite	type	*Cp* $J \cdot kg^{-1} \cdot K^{-1}$	source
Kukschin	L6	1000	Alexeyeva (1958)
Kharhov	L6	707	Alexeyeva (1958)
Elenovka	L5	762	Alexeyeva (1958)
Yamoto-74191	L3	603	Matsui & Osako (1979)
Sołtmany	L6	671	Wach et al. (2013)
		705–769	Szurgot et al. (2012)
Braunschweig	L6	682	Szurgot et al. (2014)
NWA 6255	L5	668	this work

The comparison of heat capacity values at various temperature of NWA 6255 with Sołtmany (Szurgot et al., 2012) is depicted in Fig. 5. In the temperature range of 223–523 K, the *Cp* values of Sołtmany are slightly higher (ca. 40–50 $J \cdot kg^{-1} \cdot K^{-1}$) than these for the interior samples of NWA 6255. However, over 523 K the heat capacity of both meteorites are nearly identical (within experimental error). Since the masses of the samples of both meteorites are similar, and the procedure to determine the *Cp* values is exactly the same, the differences in *Cp* values may reflect heterogeneity in mineral and chemical composition of both meteorites.

α/β transition

The enthalpy of α/β transition could be used to estimate the troilite content in the sample (Szurgot et al., 2012). After heating of the samples containing troilite, the thermal effect ($\Delta H_{\alpha/\beta}$) of α/β transition is reduced and the peak of the transition shifts to a lower temperature. This fact is not surprising as the T_α depends on the relict temperature that the material experienced during its thermal history (Allton et al., 1993). It is known that T_α is inversely proportional to the relict temperature of troilite. The current results are in good agreement with this consideration, as the lowest values of T_α for crust (Tab. 2) show the evidence of the highest temperature experienced during atmospheric passage. However, differences in T_α with regards to the distance from the meteorite surface inward provides evidence that the meteoroid experienced increased temperatures due to friction in the atmosphere as well as heat flow. Sampling the cross-section of a meteorite from crust to the interior (precisely defined fractions) may give valuable information. Therefore, differences in temperature of α/β transition of troilite, as a representative constituent, in crust, edge and interior of NWA 6255 (Tab. 2) indicate the temperature gradient that the meteorite experienced. Accurate data representing thermophysical characteristics of a meteorite or its parent body can be obtained only by examination of a fresh fall as troilite tends to oxidize quickly.

The reduction of thermal effects is dependent on both the temperature experienced and the time of

heating. The crust reaches its maximum temperature during atmospheric passage, after which bubbles and pores are observed due to the evaporation of sulfides (Karwowski, 2012). Thus, troilite content (also that in its crystallographic form displaying α/β transition) is minimal in crust. Troilite that endured an intense increase of temperature changes its structure. Obtained low values of $\Delta H_{\alpha/\beta}$ support this principle, which is also demonstrated in the lowest FeS content in the crust throughout the cross-cut of the meteorite. In the crust samples there was a broad depression in the DSC thermogram indicating two effects of partially oxidized troilite and its α/β transition combined. This is characteristic for specimens of the crust. A significant decrease in the characteristic high peak of α/β transition and its shifting to lower temperature (Fig. 4) also indicate a substantial reduction of troilite in the crust.

The edge of a meteorite is in the intermediate zone in terms of temperature produced during atmospheric friction (Vaz, 1972). Shape of thermogram, i.e. the heat flow curve for the edge is composed of the peak characteristic for α/β transition and, starting at lower temperature, depression characteristic for the crust. Therefore, the edge material is only moderately exposed to high temperature during its passage through the atmosphere. The values of $\Delta H_{\alpha/\beta}$ also indicate the thermal processing. The edge experienced rapid but intense elevation of temperature during atmospheric passage. Despite the fact that the T_{α} of the edge differs slightly as compared to the interior, significant changes of enthalpy ($\Delta H_{\alpha/\beta}$) are observed. Therefore, the content of FeS in the edge (present in the same crystallographic form as in the interior) is three times lower in comparison with the interior of the meteorite.

The interior of a meteorite may not experience thermal changes during atmospheric passage. Well defined peaks of α/β transition of the interior troilite of NWA 6255, a transition temperature similar to the theoretical values, and a significantly higher $\Delta H_{\alpha/\beta}$ than for the crust and edge samples support this hypothesis. The current results are in good agreement with the results of Vaz (1971, 1972) and Sears (1975) who found through TL measurements that temperatures as high as 250°C (523.15 K) have been experienced no futher than 0.5 mm from the present surface, but the materials up to about 5 mm below the crust experienced temperature rise of over 150°C (423.15 K). The lack of a shift in the α/β transition peak of the troilite indicates that the temperature of the interior (10 mm below the fusion crust) did not exceed 150°C (423.15 K).

Troilite concentration

Determined content of troilite in the NWA 6255 meteorite is in relatively good agreement with the previous results from Leco method. It should be added that the DSC measurement were conducted one year after determination of sulphur content by Leco method. This may be the reason why troilite content estimated on the basis of current thermophysical measurement is lower, as troilite tends to oxidize quickly (Velbel, 2014). Nevertheless, the value for interior with standard deviation is in the same range as that by Leco determination. These results (Tab. 2) support our opinion that NWA 6255 has a heterogeneous distribution of FeS in terms of crust, edge and interior of the meteorite. One should bear in mind that estimation of troilite content in the meteorite is only valid for the fresh fall or finds with a low weathering grade (W0−W2), where FeS did not undergo the terrestrial weathering. Moreover, it should be done for ground, homogenized samples from representative parts of the meteorite (avoid shock vein, shock melt pocket as well as part of meteorite generally enriched in metals). Troilite content should be regarded as a valuable complementary method to estimate the composition of samples since troilite constitutes a minor part of a meteorite, and the DSC instrument allows measurement of samples with relatively small masses (2−25 mg).

CONCLUSIONS

We have applied a thermal analytical technique of differential scanning calorimetry for evaluation of thermophysical properties of the ordinary chondrite NWA 6255. We also demonstrated the efficacy of DSC, a highly underrated tool, for determination of thermophysical properties of extraterrestrial rocks. Beside determination of specific heat capacity over a wide range of temperatures, the technique can provide information on thermal transitions of crystallites comprising the specimen, specifically troilite, whose extent may be correlated with the thermal history of the sample, and consequently used as the cosmothermometer, as proposed by Howard and Gooding (1996) and later developed by Szurgot. The applied technique requires that the specimen itself posses flat and thin geometry to allow instant heat transfer within the whole material. Otherwise, it is recommend to grind a complex sample to diminish the influence of porosity, cracks etc. since thermal conductivity and by extension the measured *Cp* are controlled by the physical state of

the material. Grinding may be also advantageous for specimens characterized by high heterogeneity to obtain average values representative of the whole sample. Nevertheless, the measurements are usually conducted using small samples (a few mg), which depending on the specific meteorite, may have limited availability.

Detailed examination of a cross-section of the NWA 6255 meteorite revealed a gradient, along the axis from the surface to the interior, in the enthalpy of troilite transition, which reflects the thermal history of the meteorite in distinct locations. Our research proved that the natural relict temperature inferred from troilite shows values that vary systematically not only with metamorphic and shock grades of the examined samples (Allton et al., 1994) but also with the distance from the crust. As it was expected, the surface experienced the highest temperature (minor heat effect of troilite transition), whereas the site on the edge of the meteorite (1−2 mm below the crust) experienced a much lower temperature as demonstrated by a diminished peak in the DSC heat flow thermogram.

The current results obtained by the DSC can be validated by well-established methods, such as thermoluminescence, and are indeed in good agreement with those. Changes of the *Cp* with temperature were followed, and when compared to that of another chondrite showed high correlation. The *Cp* of the crust was somewhat lower than that of the meteorite's interior, which is due to relatively higher metals content, as metals and others siderophile elements tend to be refractory and so survived the high temperature during ablation.

Knowing the mineral composition and the specific heat capacity of the specimen while then taking into account the temperature and heat effect of transition of the troilite in the meteorite bulk set against, for instance, sulphur content can also provide evidence of the thermal history of the parent body of the meteorite. Therefore, the straightforward method of DSC used for determination of thermophysical properties of meteorites may provide complementary information to better understand the matter of different bodies of the Solar System.

ACKNOWLEDGEMENTS

The analyses were financed by the National Science Center of Poland, grant no. DEC-2011/03/N/ST10/05821, and the internal grant of Wrocław University of Technology "Rozwój potencjału dydaktyczno-naukowego młodej kadry akademickiej Politechniki Wrocławskiej" grant no. MK/SS/84/VI/2013/U. The authors would like to thank reviewers: G.J. Consolmagno and M. Szugot for comprehensive review of this paper and constructive notes.

REFERENCES

Alexeyeva K.N., 1958 – Physical properties of stony meteorites and their interpretation in the light of the hypothesis of the origin of meteorites. *Meteoritika* 16, 67–77.

Allton J.H., Wentworth S.J., Gooding J.L., 1993 – Calorimetric thermometry of meteoritic troilite: Early reconnaissance. *Meteoritics* 28, 315.

Allton J.H., Wentworth S.J., Gooding J.L., 1994 – Calorimetric thermometry of meteoritic troilite: Preliminary thermometer relationship, *XXV Lunar and Planetary Science Conference*. 25–26.

Andresen A.F., Torbo P., 1967 – Phase transition in Fe_xS (x = 0.90–1.00) studied by neutron diffraction, *Acta Chemica Scandinavica* 14, 919–926.

Beech M., Coulson I.M., Wenshuang N., McCausland P., 2009 – The thermal and physical characteristics of the Gao-Guenie (H5) meteorites. *Planetary and Space Science* 57, 764–770.

Bhandari N., Lal D., Rajan R.S., Arnold J.R., Marti K., Moore C.B., 1980 – Atmospheric ablation in meteorites. A study based on cosmic ray tracks and neon isotopes. *Nuclear Tracks* 4, 213–226.

Consolmagno G.J., Schaefer M.W., Schaefer B.E., Britt D.T., Macke R.J., Nolan M.C, Howell E.S., 2013 – The measurement of meteorite heat capacity at low temperature using liquid nitrogen vaporization. *Planetary and Space Science* 87, 146–156.

Chase M.W. Jr., Davies C.A., Downey J.R., Frurip D.J., McDonald R.A., Suverud A.N., 1985 – JANAF Thermochemical Tables. 3rd ed., *Journal of Physical and Chemical Reference Data* 14, Supplement 1, 1194.

Evans H.T., 1970 – Lunar troilite: Crystalography. *Science* 167, 621–623.

Ghosh A., Mc Sween H.Y., 1999 – Temperature dependence of specific heat capacity and its effect on asteroid thermal models. *Meteoritics and Planetary Science* 34, 121–127.

Haraldsen H., 1941 – Über die Hochtemperaturumwandlungen der Eisen(II)-Sulfidmischkristalle. *Zeitschrift für anorganische und allgemeine Chemie* 246, 195–226.

Hägg G., Sucksdorff I., 1933 – Die Kristallstruktur von Troilit und Magnetkies. *Zeitschrift für Physikalische Chemie* 2, 444–452.

Henke S., Gail H.P., Trieloff M., Schwarz W.H., Kleine T., 2012 – Thermal evolution and sintering of chondritic planetesimals. *Astronomy and Astrophysics* 537, A45, 19 p.

Horwood J.L., Townsend M.G., Webster A.H., 1976 – Magnetic susceptibility of single-crystal $Fe_{1-x}S$. *Journal of Solid State Chemistry* 17, 35–42.

Howard V.L., Gooding J.L., 1996 – Troilite cosmothermometer: Application to L-chondrites. *Lunar and Planetary Science XXVII*, 731.

Höhne G.W.H., Hemminger W., Flammersheim H.J., 1996 – Differential Scanning Calorimetry. An Introduction for Practitioners. Springer, Berlin.

Hutchison R., 2006 – Meteorites a petrologic, chemical and isotopic synthesis. Cambridge University Press, New York.

Karwowski Ł., 2012 – Sołtmany meteorite. *Meteorites* 2, 15–30.

King H.E., Prewitt C.T., 1982 – High pressure and high temperature polymorphism of iron sulfide (FeS). *Acta Crystallographica B* 38, 1877–1887.

Kruse O., 1992 – Phase transitions and kinetics in natural FeS measured by X-ray diffraction and Mössebauer spectroscopy at elevated temperatures. *American Mineralogist* 77, 391–398.

Kruse O., Ericsson T., 1988 – A Mössebauer investigation of natural troilite from the Agpalilik meteorite, *Physics and Chemistry of Minerals* 15, 509–513.

Lang K.R., 2011 – The Cambrigde Guide to the Solar System. Part IV: Remants of creation: small worlds in the solar system, chapter 12: Asteroids and meteorites, Cambridge University Press, UK, second edition, 374.

Lauer H.V. Jr., Gooding J.L., 1996 – Troilite cosmothermometer: application to L-chondrites. *XXVII Lunar and Planetary Science Conference*, 731–732.

Łuszczek K., 2012 – Chemical composition of L chondrites group and potential natural resources of their parent bodies. In: Drzymała J., Ciężkowski W. [eds.] – *Interdyscyplinarne zagadnienia w górnictwie i geologii* 3, Wrocław, 161–173.

Matsui T., Osako M., 1979 – Thermal property measurement of Yamato meteorites. *Memoirs of National Institute of Polar Research Special Issue* 15, 243–252.

McSween H.Y., Huss G.R., 2010 – Cosmochemistry. Cambrigde University Press, Cambridge.

Moldenhauer W., Brückner W., 1976 – Physical properties of nonstoichiometric iron sulfide $Fe_{1-x}S$ near the α-phase transition. *Physica Status Solidi A* 34, 565–571.

Opeil C.P., Consolmagno G.J., Safarik D.J., Britt D.T., 2011 – Stony meteorite thermal properties and their relationship with meteorite chemical and physical states.*Meteoritics* & *Planetary Science* 47 (3), 319–329.

Ozawa K., Anzai S., 1966 – Effect of pressure on the α-transition point of iron monosulphide. *Physica Status Solidi* 17, 697–700.

Sears D.W., 1975 – Temperature gradients in meteorites produced by heating during atmospheric passage. *Modern Geology* 5, 155–164.

Sears D.W.G., 2004 – The orgin of chondrules and chondrites. Cambridge University Press, Cambrigde.

Szurgot M., 2003 – Thermophysical properties of meteorites, Specific heat capacity. *2nd Meteorite Seminar in Olsztyn*, 136–145 (in Polish).

Szurgot M., 2011a – On the specific heat capacity and thermal capacity of meteorites. *42nd Lunar and Planetary Science Conference,* Abstract #1150.pdf.

Szurgot M., 2011b – Thermal conductivity of meteorites. *Meteoritics* & *Planetary Science* 46, Supplement, A230.

Szurgot M., 2012a – On the heat capacity of asteroids, satellites and terrestrial planets. *43rd Lunar and Planetary Science Conference.* Abstract #2626.pdf.

Szurgot M., 2012b – Mean specific heat capacity of Mars, moons and asteroids. *75th Annual Meteoritical Society Meeting*. Abstract #5035.pdf.

Szurgot M., 2012c – Thermal capacity of Mars, Martian crust, mantle and core. *75th Annual Meteoritical Society Meeting*. Abstract #5094.pdf.

Szurgot M., 2012d – Heat capacity of Mars. *Workshop on the Mantle of Mars*. Abstract #6001.pdf.

Szurgot M., 2014 – Modal abundance of minerals in Sołtmany L6 chondrite. *Meteoritics* & *Planetary Science* 49, Supplement, #5031.pdf.

Szurgot M., Polański K., 2011 – Investigations of HaH 286 eucrite by analytical electron microscopy. *Meteorites* 1, 29–38.

Szurgot M., Wojtatowicz T.W., 2011 – Thermal diffusivity of meteorites. *Meteoritics* & *Planetary Science* 46, Supplement, A230.

Szurgot M., Rożniakowski K., Wojtatowicz T.W., Polański K., 2008 – Investigation of microstructure and thermophysical properties of Morasko iron meteorites. *Crystal Research and Technology* 43, 921–930.

Szurgot M., Wach R.A., Przylibski T.A., 2012 – Thermophysical properties of Sołtmany meteorite, *Meteorites* 2, 53–65.

Szurgot M., Wach R.A., Bartoschewitz R., 2014 – Thermophysical properties of Braunschweig meteorite. *Meteoritics* & *Planetary Science* 49, Supplement, #5015.pdf.

Töpel-Schadt J., Müller W.F., 1982 – Transmission electron microscopy on meteorite troilite. *Physics and Chemistry of Minerals* 8, 175–179.

Vaz J.E., 1971 – Lost City meteorite: Determination of the temperature grandient induced by atmospheric friction using thermoluminescence. *Meteoritics* 6 (3), 207–216.

Vaz J.E., 1972 – Ucera meteorite: Determination of differential atmospheric heating using its natural thermoluminescence. *Meteoritics* 7 (2), 77–86.

Velbel M.A., 2014 – Terrestrial weathering of ordinary chondrites in nature and continuing during laboratory storage and processing: Review and implications for Hayabusa sample integrity. *Meteoritics* & *Planetary Science* 49 (2), 154–171.

Wach R.A., Adamus A., Szurgot M., 2013 – Specific heat capacity of Sołtmany and NWA 4560 meteorites. *Meteoritics* & *Planetary Science* 48, Supplement, #5017.pdf.

Waples D.W., Waples J.S., 2004 – A review and evaluation of specific heat capacities of rocks, minerals, and subsurface fluids. Part 1: Minerals and nonporous rocks. *Natural Resources Research* 13 (2), 97–122.

Yomogida K., Matsui T., 1981 – Physical properties of some Antarctic meteorites. *Memories of the National Institute of Polar Research., Special Issue* 20, 384–394.

Yomogida K., Matsui T., 1983 – Physical properties of ordinary chondrites. *Journal of Geophysical Research* 88, 9513–9533.

www.lpi.usra.edu, 7.04.2014.

www.mindat.org, 7.04.2014.

Publishers: Wrocław University of Technology, Faculty of Geoengineering, Mining and Geology
Polish Meteorite Society

Meteorites
Vol. 3, Nos. 1–2, 2014, 45–58
www.meteorites.pwr.wroc.pl
DOI 10.5277/met140104

NORTHWEST AFRICA 7915: A NEW APPROVED LL5 CHONDRITE FROM MOROCCO

Maciej BRAWATA[1], Ryszard KRYZA[1], Tomasz JAKUBOWSKI[2], Tadeusz Andrzej PRZYLIBSKI[3], Jacek ĆWIĄKALSKI[1], Katarzyna ŁUSZCZEK[3]

[1] University of Wrocław, Institute of Geological Sciences, ul. Cybulskiego 30, 50-205 Wrocław, Poland
[2] ul. Drzewieckiego 44/7, 54-129 Wrocław, Poland
[3] Wrocław University of Technology, Faculty of Geoengineering, Mining and Geology, Division of Geology and Mineral Waters, Wybrzeże S. Wyspiańskiego 27, 50-370 Wrocław, Poland

Abstract: A 415 g single meteorite was purchased in 2010 by T. Jakubowski from a dealer in Morocco. The meteorite was isometric in shape, ca. 8 cm in size, with distinct regmaglypts on the original ablated surface, and covered mostly in primary crust with one broken surface. The weight of the sample studied was 69 g. The meteorite is composed of several types of chondrules including porphyritic-Ol-Px, barred-Ol, radial-Px, granular and cryptocrystalline with distinct and diffused (not sharp) boundaries, and opaque grains and aggregates, enclosed in a very fine-grained matrix. The average compositions of minerals are: *olivine* (both in chondrules and matrix) – $Fo_{70.4}Fa_{29.1}Te_{0.5}$, *pyroxenes,* represented by Mg-Fe (Ca-poor) orthopyroxene (and minor clinopyroxene?) – $En_{73.9}Fs_{24.1}Wo_{2.0}$, *feldspars* (small in the matrix and in barred chondrules), with $An_{12\text{-}37}$, and $Or_{\sim 3\text{-}4}$, *taenite* – Fe 70.80, Ni 25.50 and Co 1.67 wt. %, *troilite* – $Fe_{0.98}S_{1.00}$, *chromite* $(Fe^{2+}_{0.96}Mg_{0.12}Mn_{0.01}Zn_{0.01})$ $(Cr_{1.52}Al_{0.23}Fe^{3+}_{0.02}Ti_{0.10}Si_{0.02})O_4$; altered accessory minerals including *apatite* and *iron-rich secondary phases* have also been identified and analyzed.

The meteorite is of petrologic type 5, as evidenced by the observed recrystallization of the matrix, relatively good preservation of the chondrule structures, homogeneous composition of olivine and pyroxene, and the presence of only secondary small feldspar grains. The shock stage, S2, is based on the presence of undulatory extinction and irregular fractures in olivine crystals. The weathering grade, W3, is confirmed by the observation that kamacite is totally altered into secondary iron phases, whereas Ni-rich taenite, and troilite are only partly weathered.

The specimen shows many bulk- and mineral-chemical parameters corresponding, mostly, to the LL chondrite group (e.g., Fe/SiO_2 0.49, SiO_2/MgO 1.62, Fa in olivine 29.05). However, concentrations of several other elements, including REE, are not fully consistent with the average values for the LL ordinary chondrites. Apparently, the parent body of the studied NWA 7915 meteorite was depleted in Dy, Tm, and Yb, compared to typical LL-type ordinary chondrite parent bodies. Also, relatively high concentrations of other elements, including Ba and Sr, have been measured, which may result from terrestrial weathering in hot desert conditions.

The meteorite has been classified as LL5 ordinary chondrite, S2, W3, and registered in the Meteoritical Society database as NWA 7915. The type specimen is deposited in the Mineralogical Museum of the University of Wrocław.

Keywords: chondrite, NWA 7915, Morocco, chondrule, chondrite chemistry, chondrite weathering

INTRODUCTION

This study aimed at mineralogical, petrographic and geochemical characterization of a new ordinary chondrite from Morocco which was formally registered in the Meteoritical Society database. The results of the study extend our knowledge on the mineral chemistry and bulk chemical composition of ordinary

Corresponding author: Tadeusz A. PRZYLIBSKI, Tadeusz.Przylibski@pwr.edu.pl

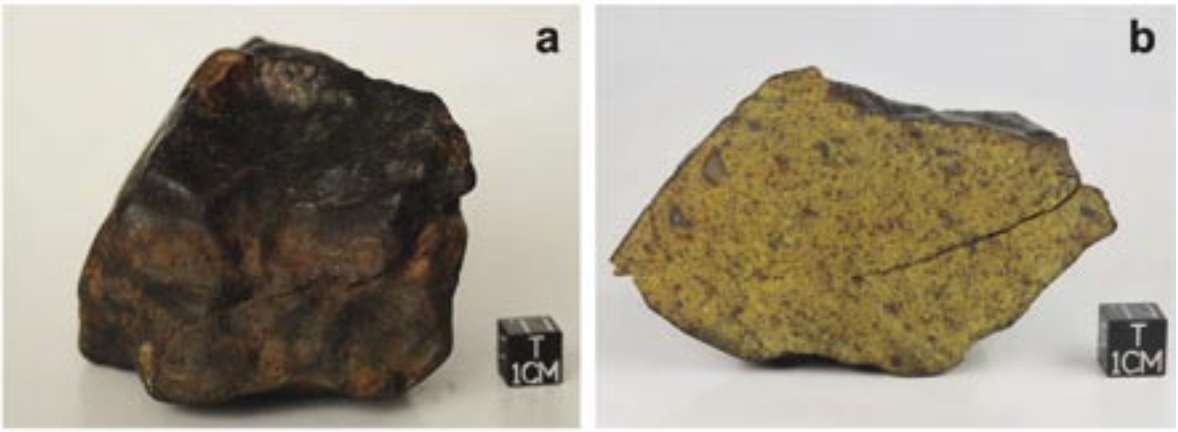

Fig. 1. Original (415 g) specimen of NWA 7915 meteorite (a), and polished cut face of this chondrite (b)

chondrites and their parent bodies that formed in the young Solar System. Though this subject has been studied intensively by many authors (i.e. Grossman & Larimer, 1974; Wanke & Dreibus, 1988; Kallemeyn et al., 1989; Brearley & Jones, 1998; Davis & Richter, 2004; Yin, 2005; Ebel, 2006; Alexander et al., 2008), our knowledge remains incomplete.

The studied meteorite (Fig. 1) comes from the collection of Tomasz Jakubowski who purchased it in Morocco in 2010. The geographic coordinates of the find and the name of the finder are unknown. The type specimen is deposited in the collection of the Mineralogical Museum of the University of Wrocław.

The studied meteorite, now registered as NWA 7915, is a yellowish-brown colored stone, broadly isometric in shape, ca. 8 cm in size (Fig. 1a). Its original surface is ablated, with distinct regmaglipts. It is moderately magnetic. The total weight (TKW) was 415 g, the weight of the sample studied was 69 g (Fig. 1b).

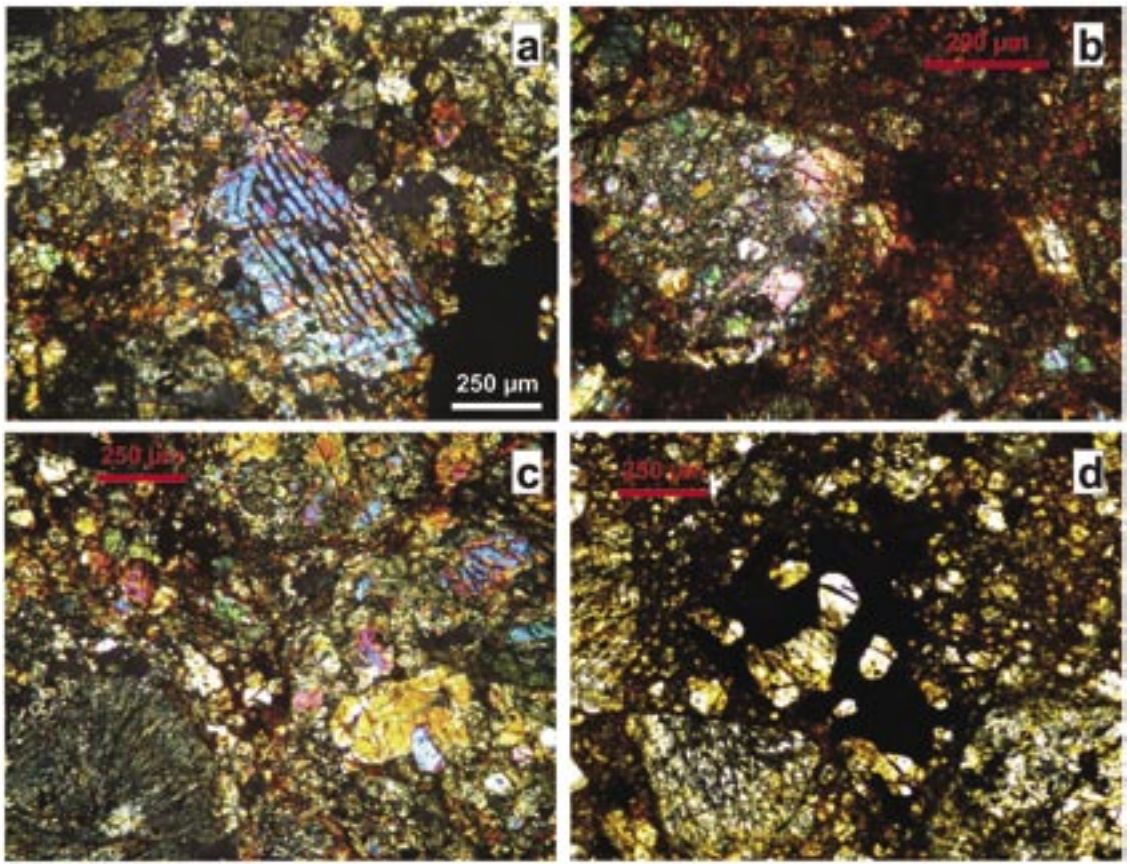

Fig. 2. NWA 7915: textures and composition: (a) – barred-olivine chondrule and opaque in a fine-grained matrix; (b) – porphyritic chondrule in a couloured matrix; (c) – radial-pyroxene chondrule in a grainy matrix; (d) – opaque aggregate enclosing olivine crystals; (a–c – crossed nicols, d – one nicol)

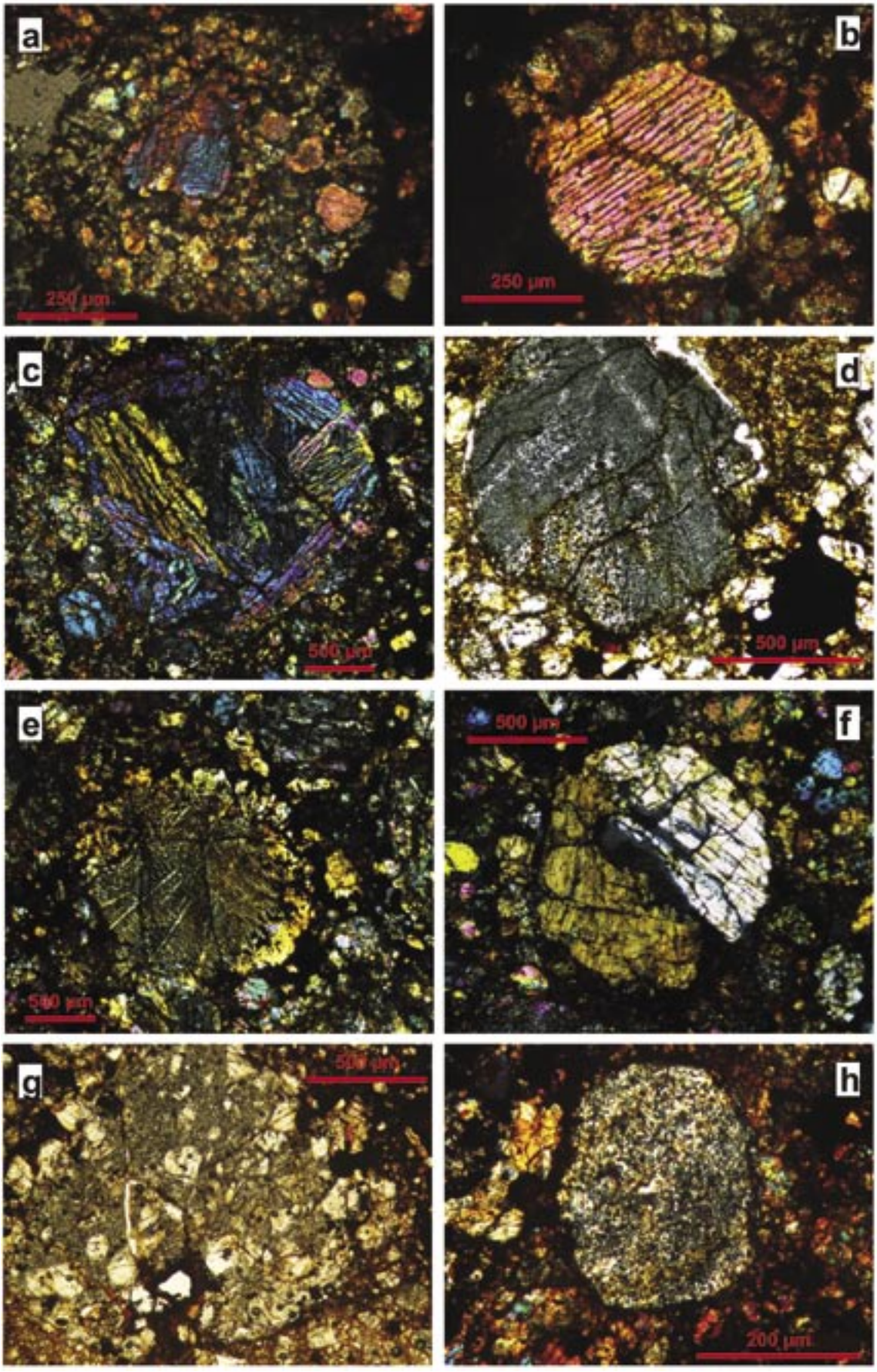

Fig. 3. Various types of chondrules in NWA 7915: (a) – porphyritic-olivine; (b, c) – barred-olivine; (d, e) – radial-pyroxene; (f) – orthopyroxene; (g) – porphyritic-cryptocrystalline; (h) – cryptocrystalline (g – one nicol, all others – crossed nicols)

METHODS

Conventional mineralogical and petrographic investigations were made in three polished thin sections, using the polarizing microscope, in transmitted and reflected light. Chemical compositions of minerals were determined with the electron microprobe Cambridge M9 at the Department of Mineralogy and Petrology, University of Wrocław (instrument donated by the Free University of Amsterdam). Both EDS and WDS techniques were used. WDS quantitative analyses were performed at the following analytical conditions: 15 kV accelerating voltage, 50 nA beam current, 20 s counting time, a set of natural mineral and synthetic standards, and ZAF correction.

Part of the sample studied, 11 g in weight, was ground in an agate mortar and used for bulk chemical analysis of major and trace elements. The analyses were performed in ACME Analytical Laboratories Ltd, Canada, by means of ICP-MS and XRF analysis. ICP-MS was used to determine the content of the major and trace elements (including REE). XRF analysis was used to measure the nickel content which was too high to be accurately determined by the ICP-MS. The content of volatile elements (C and S) was measured by means of the Leco method (see ACME web site: http://acmelab.com/).

RESULTS

Petrography

On the cut surface of the meteorite (Fig. 1b), chondrules and shiny metal grains are distinguishable within an orange-gray, fine-grained matrix. The grains are uneven with serial and directionless texture (Fig. 2). The matrix grains vary from sub-microscopic to several tens of μm in size, but individual grains attain ca. 0.5 mm in size. Olivine dominates over pyroxene, both in the chondrules and matrix. Minor components include metal phases, largely replaced by secondary iron oxides/hydroxides, occasional troilite and chromite, and partly altered apatite. The rock is rather

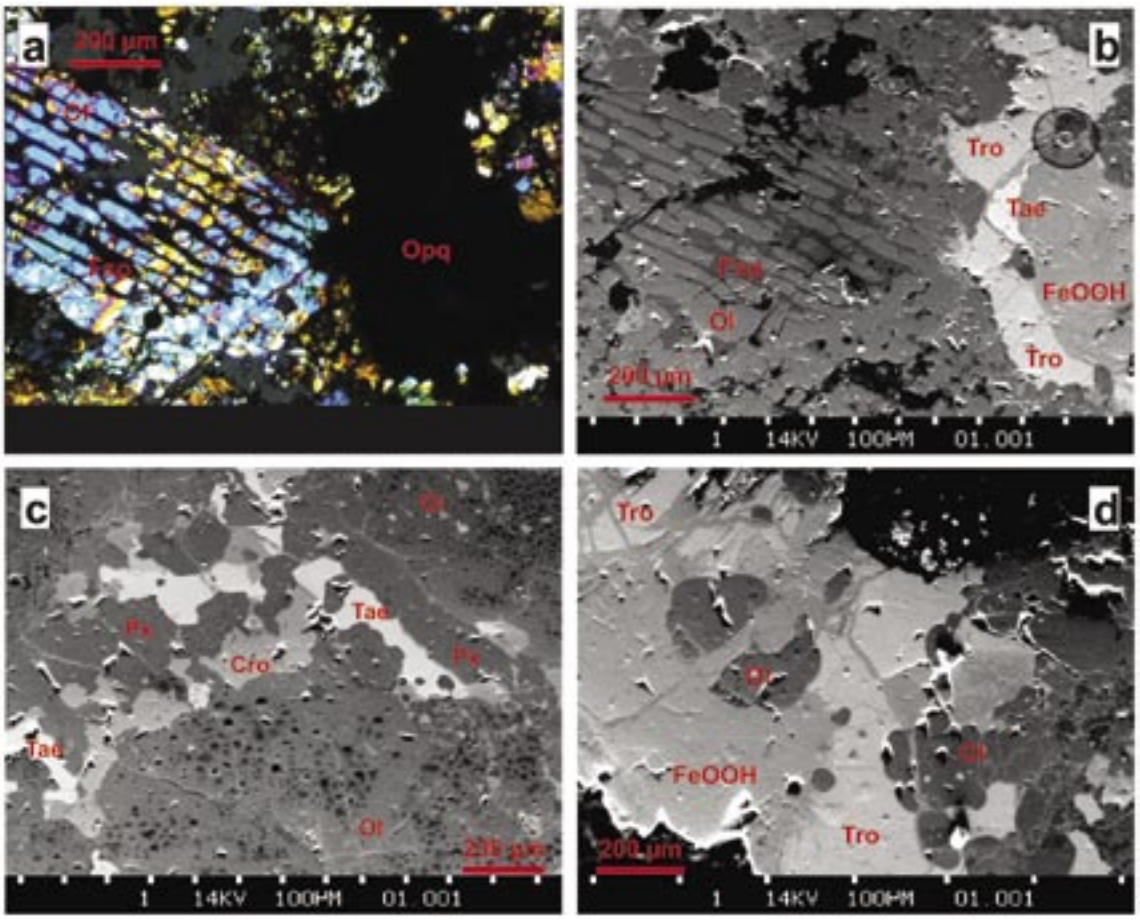

Fig. 4. (a) – barred-olivine chondrule with feldspar intercalations (crossed nicols); (b) – BSE image of the same field; (c, d) – BSE images showing opaques among silicates; Cro – chromite, FeOOH – iron oxide/hydroxide, Fsp – feldspar, Ol – olivine, Opq – opaques, Px – pyroxene, Tae – taenite, Tro – troilite

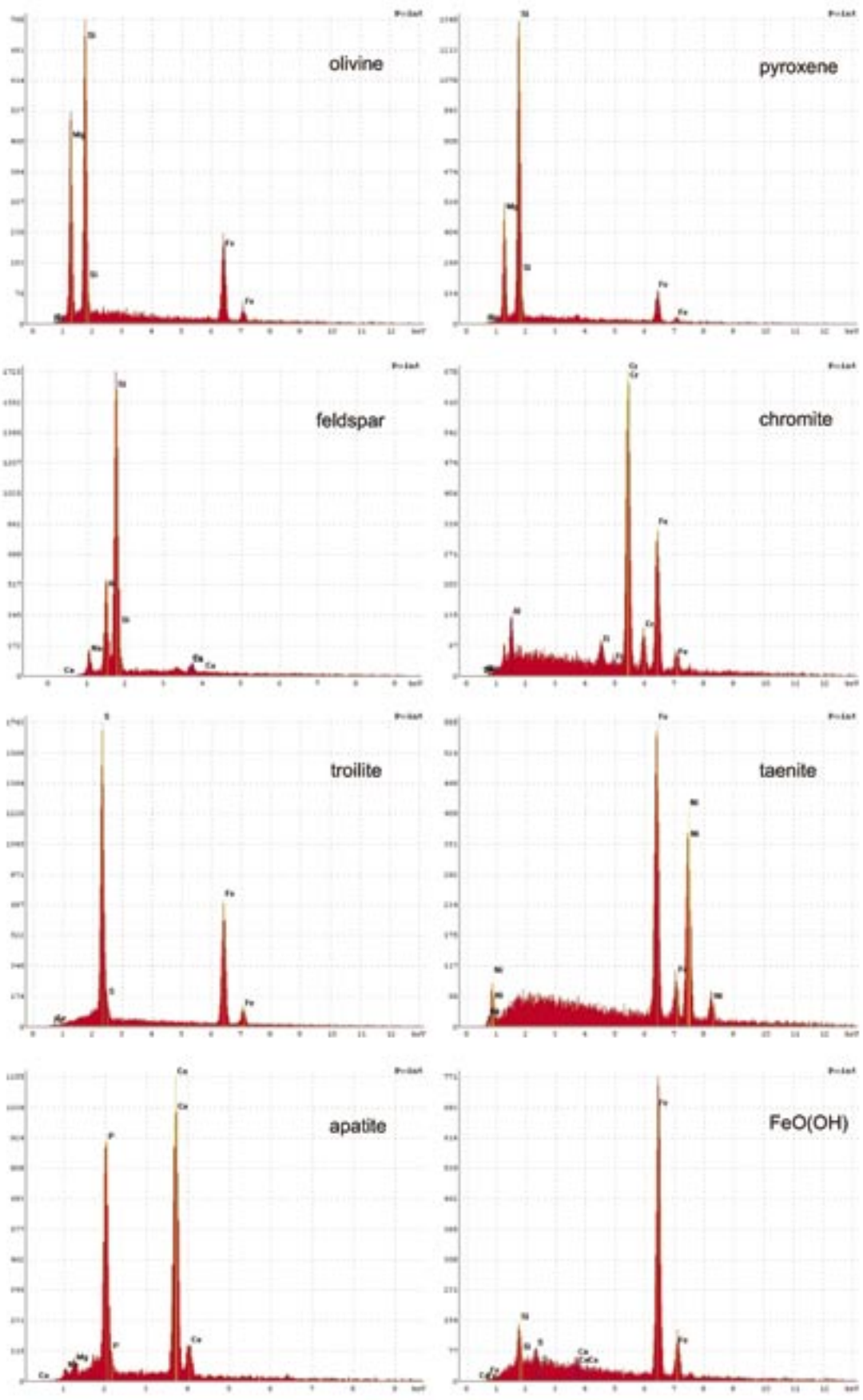

Fig. 5. EDS spectra of minerals of NWA 7915

massive (compact) and pores observed in thin sections are most likely the result of grinding and polishing of the brittle material.

The relatively well-defined component of the meteorite are chondrules (Fig. 3) composed mainly of olivine and pyroxene, and displaying several types of textures (c.f. Lauretta et al., 2006): POP – porphyric-olivine-pyroxene, BO – barred-olivine, RP – radial-pyroxene, G – granular, and CC – cryptocrystalline. All types of chondrules are found in the studied meteorite (Table 1). Their size varies between 0.2 and 4 mm. Some of them have regular spherical shape, but most display various degree of deformation: brecciation, flattening or veining. Many chondrules have distinct outlines but quite often, in particular in porphyritic chondrules, their borders against the matrix are not sharp (Fig. 3g).

The common porphyritic chondrules (Fig. 3a) are composed of relatively large olivine and, less frequently, pyroxene crystals dispersed in a microscopically translucent mesostasis. Olivine is clearly dominant.

The barred-olivine chondrules (Fig. 3b, c), 0.4–4.0 mm in size and having well defined borders, are formed of olivine crystals, all showing the same crystallographic orientation (single skeletal crystals) and sparse mesostasis. In BSE images, the olivine crystals appear to be separated by feldspar mesostasis, which was confirmed by EDS and WDS analyses (c.f. compositional EDS profiles in Figs. 6 and 7).

The radial-pyroxene chondrules (Fig. 3d, e), ranging between 0.5 and 2 mm, are formed of thin acicular pyroxene crystals most commonly arranged into several distinct fans within one chondrule. The observed low birefringence suggests that orthopyroxene is more common than clinopyroxene in these chondrules. Locally, thin olivine lamellae and opaque veinlets are observed. Rather scarce chondrules are formed of typically two or three large orthopyroxene crystals (Fig. 3f).

Table 1. Size of chondrule types in NWA 7915

Chondrule type	size (mm)		
	min	max	average
Porphyritic Ol-Px	0.5	1.2	0.9
Porphyritic Ol	0.4	4.0	1.1
Porphyritic Px	0.4	2.0	0.9
Radial Px	0.5	2.0	1.2
Barred Ol	0.3	4.0	1.1
Granular	0.5	1.2	0.6
Cryptocrystalline	0.2	1.5	0.8
All	0.2	4.0	0.9

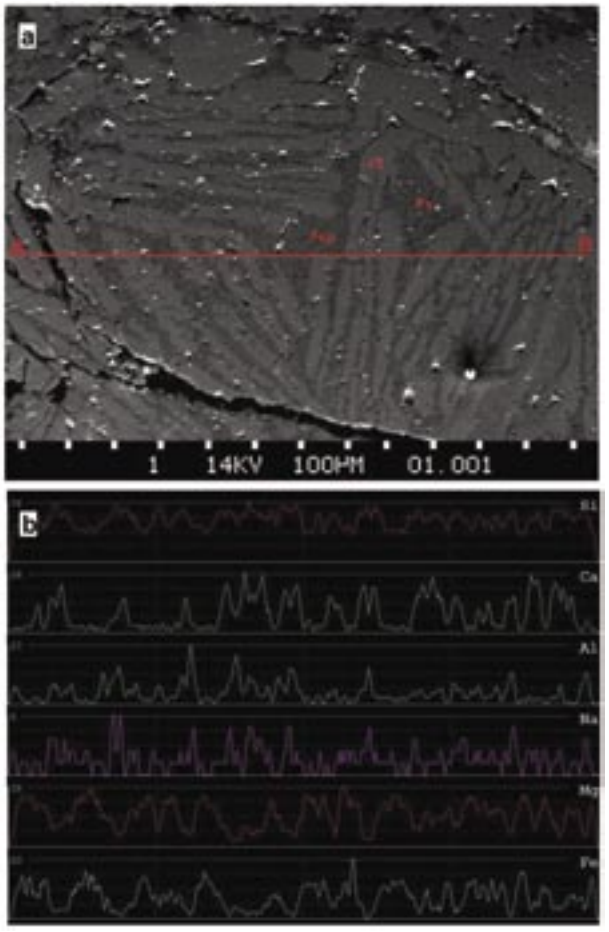

Fig. 6. (a) – BSE image of barred-olivine chondrule with mesostasis composed of feldspar and pyroxene; (b) – EDS compositional profiles. Notice coinciding peaks of Na, Ca and Al corresponding to feldspar intercalations in the chondrule

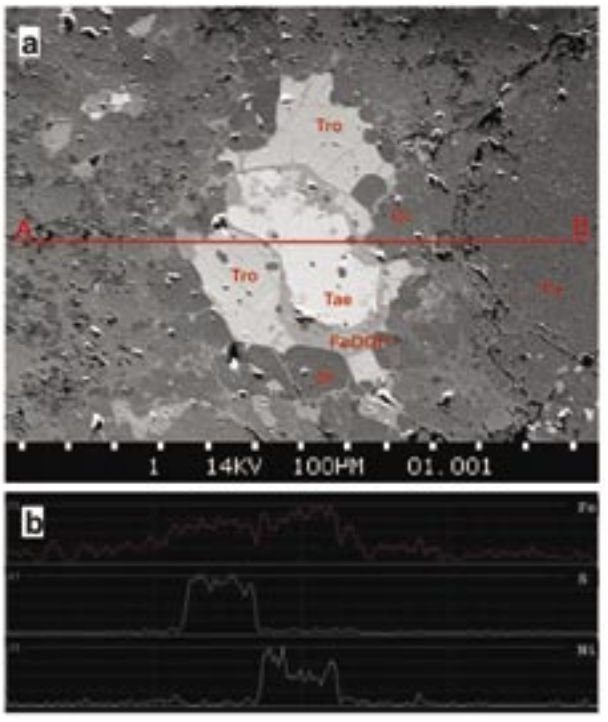

Fig. 7. (a) – BSE image of an opaque cluster composed of taenite (Tae) (partly replaced by secondary FeOOH) and troilite (Tro); Ol – olivine, Px – pyroxene; (b) – EDS compositional profile A–B; notice variable Ni content in taenite

Table 2a. Average chemical analyses of silicates and chromite in NWA 7915 (n – number of analyses, nd – not determined, sd – standard deviation, FeO* – all Fe as Fe^{2+})

olivine (n6)		sd	pyroxene (n3)		sd	feldspar (n2)		sd	chromite (n4)		sd
SiO_2	36.940	0.998	SiO_2	54.714	0.858	SiO_2	62.062	2.409	SiO_2	0.426	0.197
TiO_2	0.039	0.029	TiO_2	0.158	0.003	TiO_2	0.239	0.061	TiO_2	3.631	0.160
Al_2O_3	0.298	0.266	Al_2O_3	0.979	0.718	Al_2O_3	18.387	2.710	Al_2O_3	5.446	0.119
Cr_2O_3	0.066	0.094	Cr_2O_3	0.236	0.190	Cr_2O_3	nd		Cr_2O_3	52.499	1.059
Fe_2O_3			Fe_2O_3	0.476	0.578	Fe_2O_3	1.968	0.369	Fe_2O_3	0.694	0.636
FeO*	26.067	1.235	FeO	14.670	0.329	FeO			FeO	31.452	0.413
MnO	0.456	0.035	MnO	0.444	0.030	MnO	0.008	0.011	MnO	0.467	0.052
NiO	0.158	0.170	NiO	0.037	0.020	NiO	nd		NiO	0.209	0.144
MgO	35.460	0.708	MgO	26.776	1.097	MgO	2.254	2.355	MgO	2.249	0.169
CaO	0.044	0.028	CaO	0.996	0.148	CaO	5.424	3.969	CaO	0.032	0.008
Na_2O	0.097	0.075	Na_2O	0.267	0.361	Na_2O	8.566	1.816	Na_2O	nd	
K_2O	0.001	0.002	K_2O	0.016	0.026	K_2O	0.636	0.158	K_2O	nd	
CoO	0.071	0.045	CoO	nd		CoO	nd		CoO	nd	
ZnO	0.024	0.040							ZnO	0.385	0.096
Total	99.719	0.706	Total	99.770	0.756	Total	99.543	0.013	Total	97.490	0.512
Si^{4+}	0.985	0.015	Si^{4+}	1.976	0.015	Si^{4+}	2.803	0.062	Si^{4+}	0.016	0.007
Ti^{4+}	0.001	0.001	Al^{4+}	0.022	0.017	Ti^{4+}	0.008	0.002	Ti^{4+}	0.100	0.004
Al^{3+}	0.009	0.008	T site	1.999	0.002	Al^{3+}	0.978	0.128	Al^{3+}	0.234	0.005
Fe^{2+}	0.582	0.035	Al^{+6}	0.019	0.031	Fe^{3+}	0.067	0.014	Cr^{3+}	1.516	0.024
Mn^{2+}	0.010	0.001	Ti^{4+}	0.004	0.000	Mn^{2+}	0.000	0.000	Fe^{3+}	0.019	0.018
Mg^{2+}	1.410	0.012	Cr^{3+}	0.007	0.005	Mg^{2+}	0.153	0.161	Fe^{2+}	0.961	0.013
Ca^{2+}	0.001	0.001	Fe^{3+}	0.013	0.016	Ca^{2+}	0.264	0.197	Mn^{2+}	0.014	0.002
Na^{+}	0.005	0.004	Fe^{2+}	0.443	0.007	Na^{+}	0.749	0.146	Mg^{2+}	0.122	0.009
K^{+}	0.000	0.000	Mn^{2+}	0.014	0.001	K^{+}	0.037	0.010	Ca^{2+}	0.001	0.000
Co^{2+}	0.002	0.001	Ni^{2+}	0.001	0.001	Total	5.059	0.048	Ni^{2+}	0.006	0.004
Zn^{2+}	0.000	0.001	Mg^{2+}	1.442	0.056	O^{2-}	8.000	0.000	Zn^{2+}	0.010	0.003
Ni^{2+}	0.003	0.004	Ca^{2+}	0.039	0.006				Total	3.000	0.000
Cr^{3+}	0.001	0.002	Na^{+}	0.019	0.025	An	24.668	17.313	O^{2-}	4.000	0.000
Total	3.011	0.016	K^{+}	0.001	0.001	Ab	71.855	18.041			
O^{2-}	4.000	0.000	M1,M2	2.001	0.002	Or	3.477	0.727			
			O^{2-}	6.002	0.003						
Fo	70.440	1.311									
Fa	29.046	1.294	Wo	1.986	0.367						
Te	0.514	0.038	En	73.927	0.515						
			Fs	24.088	0.311						

A rarer type of porphyritic chondrules, granular/cryptocrystalline chondrules (Fig. 3g), are composed mainly of very fine-grained olivine in a cryptocrystalline mesostasis. The composition of the cryptocrystalline aggregates (Fig. 3h) is difficult to determine under the microscope.

The opaque grains in the meteorite matrix are often oval and rounded in shape and variable in size, from microcrystalline to larger ones, clustering in places into aggregates up to 4 mm in diameter. Locally, they concentrate around chondrules or form small inclusions inside them. Ni-rich taenite is associated with rather fresh troilite and secondary iron oxide/hydroxide phases, the latter apparently formed mostly after totally altered kamacite (Figs. 4 and 7). Sparse chromite appears to cluster with taenite (Fig. 4).

The matrix is totally recrystallized into a very fine-grained aggregate and no traces of glass have been detected. The yellowish-brown coloration comes from secondary iron-rich compounds likely due to terrestrial weathering.

Table 2b. Average chemical analyses of troilite and taenite in NWA 7915 (n – number of analyses, sd – standard deviation)

	troilite (n6)	sd	taenite (n6)	sd
Na	0.09	0.05	0.06	0.05
Mg	0.05	0.01	0.16	0.25
Al	0.03	0.02	0.05	0.06
Si	0.09	0.06	0.25	0.37
S	34.39	0.73	0.02	0.02
Ti	0.01	0.01	0.01	0.01
Cr	0.00	0.01	0.00	0.00
Mn	0.01	0.01	0.00	0.00
Fe	63.46	0.54	70.88	2.62
Co	0.16	0.05	1.67	0.27
Ni	0.18	0.13	25.50	1.48
Zn	0.04	0.06	0.03	0.06
Total	98.52	0.91	98.65	0.99

Mineralogy and mineral chemistry

EDS spectra of the most common mineral components are shown in Fig. 5. Average chemical compositions are given in Table 2.

Olivine, both in chondrules and matrix, has a rather constant composition, with the mean value $Fo_{70.4}Fa_{29.1}Te_{0.5}$, and with traces of Ni (0.02–0.42 wt. %).

Pyroxenes are represented by Mg-Fe (Ca-poor) compositions. In larger grains, e.g. in some chondrules, they show orthogonal extinction and low birefringence typical of orthopyroxene, however, it is usually difficult to distinguish between ortho- and clinopyroxene (and olivine) in the fine-grained matrix. Analyses recalculated to cation proportions and the basic end-members give an average of $En_{73.9}Fs_{24.1}Wo_{2.0}$, with only very slight variation (below 0.5 mol. %).

Feldspars form small (10–50 μm) crystals in the matrix; they are also detected in BSE images and EMPA analyses from olivine-feldspar intergrowths in barred olivine chondrules. In Figures 4 and 6, they are visible as thin stripes between barred-shape olivine crystals. Their composition is reflected in the EDS element-distribution profiles, in sections with high concentrations of Na, Ca and Al. Quantitative WDS analyses show relatively high, though variable An contents, between 12 and 37 mol. %, and rather low Or of ca. 3–4 mol. %. The relatively high amounts of Fe and Mn (Table 2) are caused by the small size of the analyzed grains and resulted contamination from neighbouring olivine.

Taenite forms individual grains in the matrix, locally clustered in aggregates, with associated chromite and troilite (Fig. 4). It shows moderate symptoms of replacement by secondary iron phases. The taenite composition varies insignificantly, around the average concentration of Fe 70.80, Ni 25.50 and Co 1.67 wt. %, and with detectable traces of Si and Mg (0.25 and 0.16 wt. %, respectively).

Troilite is moderately abundant, often associated with taenite and secondary iron phases (Fig. 7). The sulphide shows nearly stoichiometric ratios: $Fe_{0.98}S_{1.00}$, with trace admixtures of Ni (up to 0.34 wt. %) and Co (up to 0.24 wt. %).

Chromite is also not very abundant opaque phase, often associated with the Fe-Ni metal (Fig. 4). The chromite composition is very constant, though not ideally stoichiometric, with an average formula: $(Fe^{2+}_{0.96}Mg_{0.12}Mn_{0.01}Zn_{0.01})(Cr_{1.52}Al_{0.23}Fe^{3+}_{0.02}Ti_{0.10}Si_{0.02})O_4$. Ni content is around 0.006±0.004 wt. %.

Apatite, as a rare accessory mineral, is partly altered, but its approximate composition was confirmed by WDS analysis (F and Cl were not analyzed).

Fe secondary phases, replacing the primary Fe-bearing components including apparently common kamacite (?), are fairly abundant; they form rather compact, pseudomorphic aggregates but also penetrate interstitial spaces. Their measured compositions vary considerably, within the range: Fe_2O_3 68.50–77.90 and NiO 3.21–13.00 wt. %, and with variable admixtures of SiO_2, Al_2O_3, and MgO, and minor CoO, CaO and Na_2O.

Bulk chemistry

The consolidated results of NWA 7915 bulk chemical composition analysis are presented in Table 3 and Figs. 8–10. Out of 59 analyzed elements, the content of Be, Hf, Nb, Ta, Th, Cd, Sb, Bi, Ag, and Tl were below the analytical method's detection limits. The chemical data are discussed below.

DISCUSSION

Chondrite group

The above presented results of petrologic investigations, comprising determination of the texture, mineralogy and mineral composition, as well as the bulk chemical composition, provide the basic data for the classification of the meteorite. Further parameters, important for classification of a chondrite, comprise the petrologic type (thermal metamorphic grade), shock stage (S) and weathering grade (W).

The NWA 7915 meteorite has a range of petrologic features typical of the ordinary chondrites: it is composed of various types of olivine and pyroxene chondrules enclosed in a fine-crystalline matrix, and contains opaque phases represented by Fe-Ni metal and troilite.

The bulk chemical composition and the chemical composition of mineral phases are used to define the classification group within the class of ordinary chondrites. Based on the classical systematics of the ordinary chondrites by Van Schmuss & Wood (1967) and Weisberg et al. (2006), the studied NWA 7915 meteorite shows parameters corresponding to the LL group (values in parentheses): Fe/SiO_2 0.49 (0.49±0.03), SiO_2/MgO 1.62 (1.58±0.05), Fa in olivine 29.05 (29±2). Referring to the bulk element ratios reported by Wasson & Kallemeyn (1988), NWA 7915 displays similar values of Al/Si (0.77) and Mg/Si (0.86) to groups L and LL. However, the Ni/Si and Zn/Si ratios in the studied meteorite are considerably different from those in most of the groups of the ordinary chondrites. In the classification of the ordinary

Table 3. Bulk chemical composition of NWA 7915 ordinary chondrite (MDL – Minimum Detection Limit)

element		abundance	MDL	element		abundance	MDL
Si	weight %	18.59	0.01	Ni	ppm	7 417.3	0.1
Al		1.17	0.01	Ba		15	1
Fe		19.57	0.04	Be		<1	1
Mg		14.81	0.01	Co		365.1	0.2
Ca		1.26	0.01	Cs		0.1	0.1
Na		0.68	0.01	Ga		4.4	0.5
K		0.10	0.01	Hf		<0.1	0.1
Ti		0.07	0.01	Nb		<0.1	0.1
P		0.087	0.01	Rb		2.7	0.1
Mn		0.26	0.01	Sn		1	1
Cr		0.361	0.002	Sr		30.3	0.5
LOI		0.2	0.1	Ta		<0.1	0.1
Sum		99.51	0.01	Th		<0.2	0.2
C_{TOT}		0.07	0.02	U		0.1	0.1
S_{TOT}		0.39	0.02	V		54	8

element		abundance	MDL	element		abundance	MDL
W	ppm	9.7	0.5	Sc	ppm	8	1
Mo		0.6	0.1	Y		1.9	0.1
Cu		85.3	0.1	La		0.7	0.1
Pb		1.2	0.1	Ce		1.2	0.1
Zn		21	1	Pr		0.19	0.02
As		1	0.5	Nd		0.6	0.3
Cd		<0.1	0.1	Sm		0.19	0.05
Sb		<0.1	0.1	Eu		0.08	0.02
Bi		<0.1	0.1	Gd		0.27	0.05
Ag		<0.1	0.1	Tb		0.05	0.01
Hg		0.02	0.01	Dy		0.14	0.05
Tl		<0.1	0.1	Ho		0.07	0.02
Se		5.4	0.5	Er		0.2	0.03
Zr		8.1	0.1	Tm		0.02	0.01
Au		0.1237	0.0005	Yb		0.15	0.05
				Lu		0.04	0.01

chondrites by Jarosewich (1990), based on selected major element contents and ratios, NWA 7915 also corresponds to groups L and LL.

The new bulk-chemical results from NWA 7915 (Table 3) allow to compare its composition with the average values found in H, L, LL ordinary chondrites and CI carbonaceous chondrites. The chemical composition of NWA 7915 is slightly inconsistent with typical LL-type ordinary chondrites and also differentiates this meteorite from other ordinary chondrites.

The LL-type ordinary chondrite classification of NWA 7915 was undoubtedly confirmed by the total content of iron (Tables 4 and 5). Table 4 contains additional chemical properties which allowed for NWA 7915's classification as an LL-type chondrite. However, further examination of the chemical data (Table 4) led to the conclusion that, with the exception of Fe, P, as well as Al, and Au, the contents of several other elements are not fully consistent with the average values found in other LL-type ordinary chondrites.

The affiliation of NWA 7915 with other LL-type ordinary chondrites is depicted on Figure 8. The diagram also reveals a low nickel and high iron content. The content of Cr and Ca in NWA 7915 chondrite is more closely aligned with H-type chondrites. On the other hand, the Si, Mn and Mg contents in NWA 7915 chondrite are more closely aligned with L-type chondrites (Table 4). Such differences in particular element concentrations, compared to the values typical of ordinary chondrites, H, L and LL, are not unusual. A good example is, e.g., the Nyirábrany chondrite (Meszaros et al., 2014).

The analysis of data from Fig. 9 and Table 5 reveals further characteristic properties of NWA 7915's bulk chemical composition. The content of major elements (excluding Ni) is typical of LL-type ordinary chon-

Table 4. Bulk chemical composition and selected atomic ratios of NWA 7915 chondrite in relation to the composition and characteristic atomic ratios of ordinary chondrites' groups and CI carbonaceous chondrites (after Hutchison, 2006)

Element		Chondrites				
		H	L	LL	NWA 7915	CI
Si	weight %	16.9	18.5	18.9	18.59	10.5
Ti		0.060	0.063	0.062	0.07	0.042
Al		1.13	1.22	1.19	1.17	0.86
Cr		0.366	0.388	0.374	0.361	0.265
Fe		27.5	21.5	18.5	19.6	18.2
Mn		0.232	0.257	0.262	0.256	0.19
Mg		14.0	14.9	15.3	14.81	9.7
Ca		1.25	1.31	1.30	1.26	0.92
Na		0.64	0.70	0.70	0.86	0.49
K		0.078	0.083	0.079	0.100	0.056
P		0.108	0.095	0.085	0.087	0.102
Ni		1.60	1.20	1.02	0.74	1.07
Co		0.081	0.059	0.049	0.037	0.051
S		2.0	2.2	2.3	0.39	5.9
C		0.11	0.09	0.12	0.07	3.2
Au (ppb)		215	162	140	123.7	144
Atomic ratios		H	L	LL	NWA 7915	CI
Mg/Si		0.957	0.931	0.935	0.920	1.068
Al/Si($\cdot 10^4$)		696	686	655	655	853
Ca/Si($\cdot 10^4$)		518	496	482	475	614
Fe/Si($\cdot 10^4$)		8184	5845	4923	5294	8717
Ca/Al		0.74	0.72	0.74	0.73	0.72
Ni/Si($\cdot 10^4$)		453	310	258	190	488
CI normalized Atomic ratios		H	L	LL	NWA 7915	CI
Mg/Si		0.90	0.87	0.88	0.86	1.0
Al/Si		0.82	0.81	0.77	0.77	1.0
Fe/Si		0.94	0.67	0.56	0.61	1.0

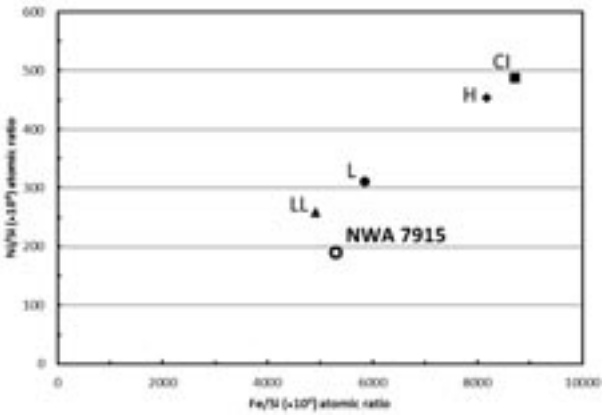

Fig. 8. The diagram of Ni/Si($\cdot 10^4$) versus Fe/Si($\cdot 10^4$) for NWA 7915 chondrite in comparison to CI, H, L and LL chondrites (after Hutchison, 2006). The ratios are atomic

drites and thus confirms the accuracy of NWA 7915's original classification. Among these elements, however, the content of K is slightly higher than the values observed in other LL-type ordinary chondrites (Fig. 9a).

The content of the rare earth elements (REE) in NWA 7915 diverges from the average values observed in LL-type ordinary chondrites (Fig. 9b; Table 5) including higher levels of La (more than twice), Ce and Pr, and lower levels of Dy (less than half), Tm, and Yb. These results are rather surprising and should be verified by additional analyses. The plot of REE abundances in NWA 7915 and CI-type carbonaceous chondrites normalized to LL ordinary chondrites (Fig. 9b) shows a totally different trend. These results indicate the enrichment of LL-type ordinary chondrites in REE in general, and of NWA 7915 in particular, as opposed to CI-type carbonaceous chondrites, excluding Dy, Tm, and Yb in the case of NWA 7915. The three above mentioned elements are present in NWA 7915 in lower concentration than in CI-type carbonaceous chondrites (Fig. 9b). As far as the parent rock on the parent body of NWA 7915 is concerned, it seems that the enrichment had a little bit different origin and character compared to "typical" LL-type ordinary

Table 5. Selected elements' abundances (ppm) in NWA 7915 chondrite in relation to average (McSween & Huss, 2010), maximum and minimum abundances of these elements in LL-type chondrites (based on data after Koblitz, 2010). The maximum and minimum values for LL-type ordinary chondrites were determined on the basis of at least 3 data points for Pb, and up to 188 data points for Fe

element	NWA 7915	average LL	range LL	element	NWA 7915	average LL	range LL
Si	185 928	189 000	93 000–237 600	Pb	1.2	nd	0.058–0.35
Al	11 699	11 800	8 300–25 400	Zn	21	56	16.5–370
Fe	195 664	198 000	78 900–892 000	As	1	1.3	0.08–37.7
Mg	148 130	153 000	57 000–194 800	Cd	<0.1	0.04	0.00039–1.248
Ca	12 580	13 200	6 400–27 400	Sb	<0.1	0.075	0.0345–2.460
Na	6 825	6 840	34–11 900	Bi	<0.1	<0.03	0.00069–0.153
K	996	880	170–12 450	Ag	<0.1	0.075	0.00994–0.554
Ti	659	680	36–2 520	Hg	0.02	0.022	0.098–5.3
P	873	910	170–2 840	Tl	<0.1	<0.03	0.00024–0.114
Mn	2 556	2 600	56–5 950	Se	5.4	9	1.68–21.8
Cr	3 607	3 690	315–6 980	Zr	8.1	7.4	3–10.69
Ni	7417.3	10 600	100–356 000	Au	0.1237	0.146	0.000011–0.00466
Ba	15	4	1.2–7.3	Sc	8	8	5.9–11.6
Be	<1	0.045	0.041–0.062	Y	1.9	2	2–3.58
Co	365.1	480	81.1–13 900	La	0.7	0.330	0.23–0.66
Cs	0.1	0.150	0.009–3.070	Ce	1.2	0.880	0.637–14.1
Ga	4.4	5.3	1.1–19.9	Pr	0.19	0.130	0.109–0.213
Hf	<0.1	0.170	0.14–0.29	Nd	0.6	0.65	0.495–0.998
Nb	<0.1	nd	0.42–0.49	Sm	0.19	0.205	0.161–0.34
Rb	2.7	2.2	0.26–50.8	Eu	0.08	0.078	0.031–0.1
Sn	1	nd	0.083–1.9	Gd	0.27	0.29	0.242–0.458
Sr	30.3	13	9–12.6	Tb	0.05	0.054	0.036–0.087
Ta	<0.1	nd	nd	Dy	0.14	0.36	0.257–0.461
Th	<0.2	0.047	0.032–0.086	Ho	0.07	0.082	0.0615–0.112
U	0.1	0.015	0.0046–0.186	Er	0.2	0.24	0.178–0.327
V	54	76	4–85	Tm	0.02	0.035	0.032–0.052
W	9.7	0.115	0.064–3.28	Yb	0.15	0.23	0.178–0.287
Mo	0.6	1.1	0.86–9	Lu	0.04	0.034	0.025–0.06
Cu	85.3	85	20–4040				

chondrites parent bodies. Parent bodies of LL-type chondrites are enriched with all analyzed REE, while the parent body of NWA 7915 chondrite seems to be depleted in Dy, Tm, and Yb in comparison to respective REE concentrations which are characteristic for CI-type carbonaceous chondrites (Fig. 9b). This is an interesting problem for further and more detailed studies.

The content of the remaining elements in NWA 7915 exhibits a different (even opposite) trend to that observed in CI-type carbonaceous chondrites (Fig. 9c). Among these elements, the average content only of Co, Ga, Rb, Cu, As, Hg, Zr and Au shows the affiliation with other LL-type ordinary chondrites. On the other hand, NWA 7915 exhibits the highest deficiency in Zn, Mo, Se, and V compared to other LL-type ordinary chondrites, whereas the highest noteworthy enrichment exists for Ba and Sr (Fig. 9c). The positive anomaly for Ba and Sr was also observed by Hezel et al. (2011) in meteorites found in the United Arab Emirates (W2–W4); however, they report positive anomaly for Mo while in the case of NWA 7915 it is negative. The higher content of Ba and Sr may be related to higher content of feldspars, that may also be supported by the observed slightly higher content of K. Another reason for the increased concentration of Ba and Sr could be terrestrial weathering, as reported from ordinary chondrites weathered in hot desert climate conditions (Velbel, 2014). It is also noteworthy that meteorites found on the Arabian Peninsula have the tendency to preferentially accumulate Sr whereas the Saharan and Australian meteorites have a stronger Ba signal (Zurfluh et al., 2012). However, the increase in Ba and Sr should be combined with elevated concentration of Rb, which should display a similar trend. However, that is not the case for NWA 7915.

Figure 10 shows the content of selected elements in NWA 7915 in order of decreasing volatility. The content of all these elements best matches their trends typical of LL-type ordinary chondrites. Nevertheless,

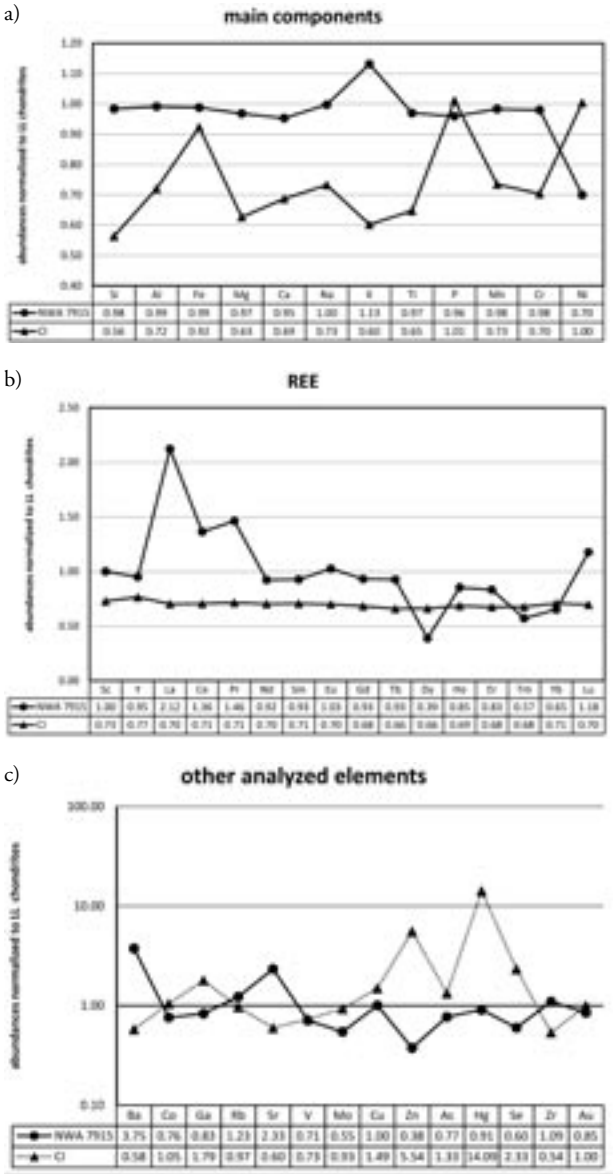

Fig. 9. Abundances of elements analyzed in NWA 7915 chondrite normalized to LL chondrites in comparison to CI chondrites' abundances (after McSween & Huss, 2010).

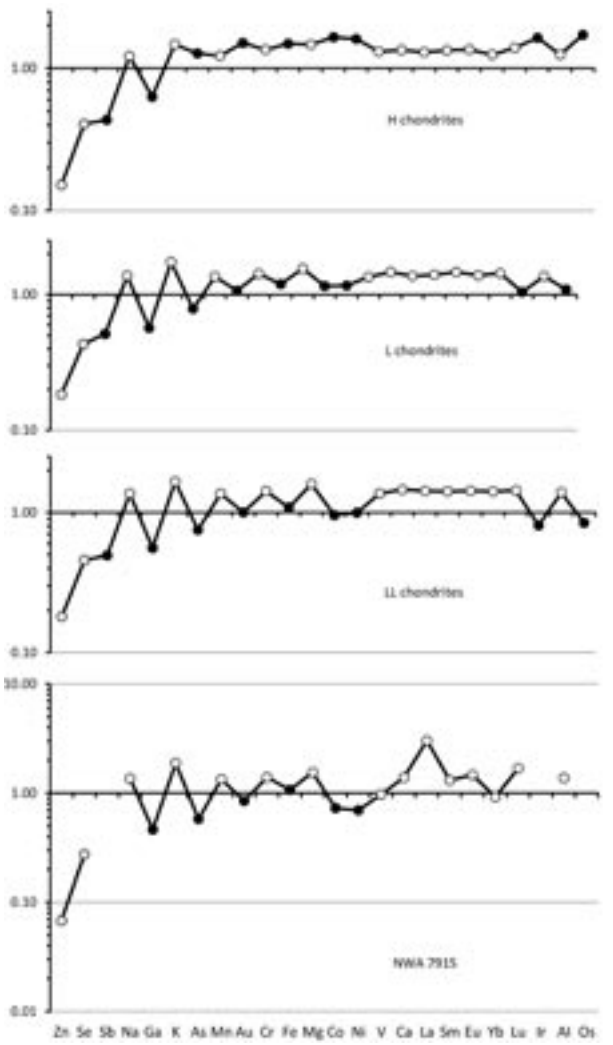

Fig. 10. CI-normalized abundances of lithophile (open symbol), siderophile (black symbol) and chalcophile (gray symbol) elements of NWA 7915 chondrite in relation to H, L and LL chondrites (after McSween & Huss, 2010)

the presence of certain deviations can be identified. As we have already pointed out, the content of Ni is significantly lower, as well as the contents of Co, V, and Yb. The content of La is also higher (Fig. 10).

The content of all the analyzed elements in NWA 7915 is presented in Table 5, along with their average values and the minimum and maximum values observed in other LL-type ordinary chondrites. The content of Mo, Hg, and Dy, as well as Ba, Sr, W, and Pb in NWA 7915 deserves particular attention. The amounts of Mo, Hg, and Dy are lower than the values ever observed in any of the 121 analyzed LL-type chondrites registered in the MetBase® database (Table 5; Koblitz, 2010). On the other hand, the contents of Ba, Sr, W, and Pb are higher than the values ever observed in any of the 121 analyzed LL-type ordinary chondrites registered in the MetBase® database (Koblitz, 2010). The higher concentration of W may be explained by the use for sample grinding a tungsten carbide (WC) mill. NWA 7915 is depleted of Ni due to terrestrial weathering. It is also possible that some other element concentrations present in strongly weathered kamacite grains may be underestimated in this analysis (i.e. Mo?). The content of all other elements may reflect chemical composition of the parent rock of NWA 7915 chondrite. However, it is also possible that some of these chemical inconsistencies result from terrestrial weathering processes that occurred in the hot desert in NW Africa.

Petrologic type

The petrologic type reflects the thermal metamorphic grade of a meteorite (Weisberg et al., 2006). The fol-

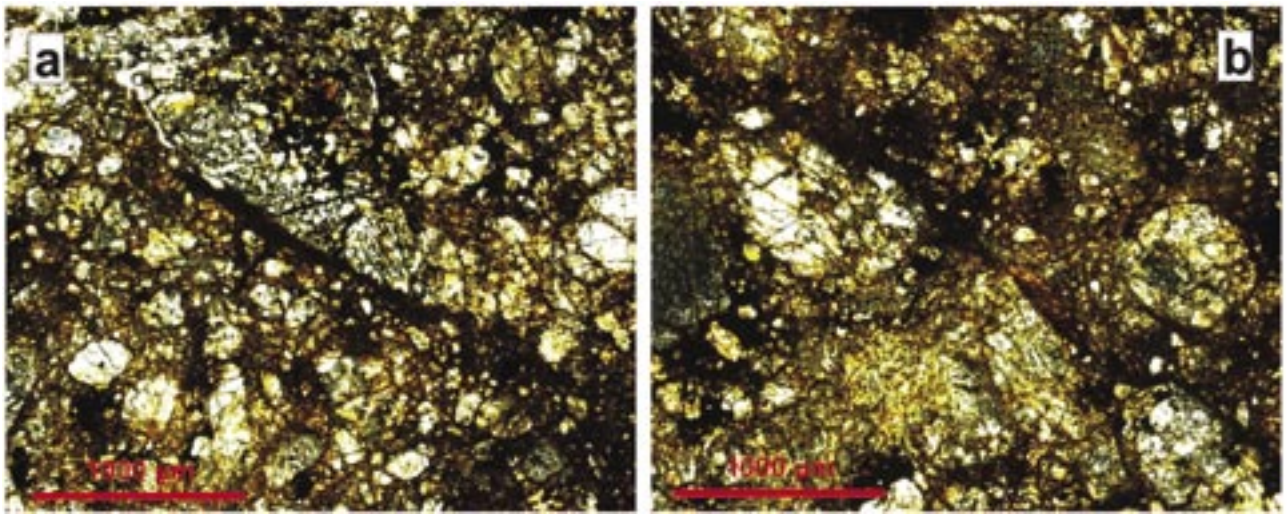

Fig. 11. (a) and (b) – veins cutting the NWA 7915 chondrite (from top left to bottom right in both photos) and adjacent spots filled with iron oxides and hydroxides (opaque, black on the photos), which are possible relics of shock veins and pockets (one nicol)

lowing features observed in NWA 7915 have been used to define its petrologic type:

1. homogeneous olivine and pyroxene composition (type 5-6),

2. large orthopyroxene phenocrysts present (type 5-6),

3. small secondary feldspars discernable only in BSE (type 5),

4. matrix composed of olivine, pyroxene and opaques (no glass preserved) (type 5–6),

5. chondrules with distinct and diffused boundaries (type 4–5).

In conclusion, the NWA 7915 meteorite represents petrologic type 5, i.e. it experienced a strong, but not the highest possible, thermal exposure. The main arguments are the observed recrystallization of the matrix, but moderately good preservation of the chondrule structures, the homogeneous composition of olivine, and the presence of only secondary small feldspar grains.

Shock stage and weathering grade

The shock stage in the NWA 7915 meteorite has been classified as very weak, S2, according to shock classification of chondrites based on effects seen in thin sections, combined by Hutchison (2006) and referring to Stöffler et al. (1991) and Rubin et al. (1997). Among the main argument for this assignment is the undulatory extinction and irregular fractures clearly visible in many of olivine crystals. The evidence for the S2 shock stage comprises also veinlets and cracks observed in chondrules, as well as undulose extinction in some radial pyroxene chondrules. Also, some rare veins and spots filled with iron oxides and hydroxides have been observed (Fig. 11) that may be relics of shock veins and pockets. However, these structures are rare and their origin rather problematic, thus they were not taken into account for defining the shock stage of the stone. It is possible that the shock pressures were close to the upper limit of the S2 stage, i.e. ~10 GPa.

The weathering grade (Wlotzka, 1993) has been estimated at W3. Kamacite has not been found, apparently being totally altered into secondary iron oxide/hydroxide phases, whereas Ni-rich taenite, and troilite are only partly weathered. The matrix and opaque minerals are strongly coloured by secondary rusty Fe-rich compounds. As mentioned above, the observed specific chemical characteristics, e.g. the relatively high abundancy of Ba and Sr, may also reflect terrestrial hot desert weathering processes in the NWA 7915 chondrite.

CONCLUSION

The studied meteorite has been classified as LL5 ordinary chondrite, shock stage S2, weathering grade W3, and approved in the Meteoritical Society database as NWA 7915. The chemical composition of NWA 7915 is somewhat different from the average characteristics of the LL chondrite group, displaying deficiencies in Ni, Co, Zn, Mo, Se, V, Hg, Dy and Yb, and enrichment in Ba, Sr, Pb and La. Some of these chemical characteristics may reflect specific chemical features of the NWA 7915 parent body whose composition is slightly different from that of the main LL chondrite group. However, some chemical anomalies, e.g.

the elevated concentrations of Ba and Sr, may result from terrestrial weathering processes that occurred in hot desert environment. These chemical "anomalies" in weathered ordinary chondrites are potentially interesting problems for more detailed future studies.

ACKNOWLEDGEMENTS

The basic investigations of this study was performed within the MSc project of Maciej Brawata, supervised by Ryszard Kryza. The thesis was supported by the internal Grant of the University of Wrocław, No. 1017/S/ING/13-II. The bulk chemical analyses were performed thanks to the funds from the National Science Centre of Poland and the Polish Ministry of Science and Higher Education, Grant No. 2011/03/N/ST10/05821 awarded to Katarzyna Łuszczek.

REFERENCES

Alexander C.M.O., Grossman J.N., Ebel D.S., Ciesla F.J., 2008 – The formation conditions of chondrules and chondrites. *Science* 320, 1617–1619.

Brearley A.J., Jones R.H., 1998 – Chondritic meteorites. *Planetary Materials, Reviews in Mineralogy and Geochemistry* 36, 3.1–3.398.

Davis A.M., Richter F.M., 2004 – Condensation and evaporation of solar system materials. [in:] Davis A.M. (ed.) – *Treatise on Geochemistry*, Vol 1., Meteorites, Comets and Planets, Elsevier, Oxford, 407–430.

Ebel D.S., 2006 – Condensation of rocky material in astrophysical environments. [in:] Lauretta D.S., McSween H.Y. Jr. (eds.) – *Meteorites and the Early Solar System II*, University of Arizona Press, Tucson, 253–277.

Grossman L., Larimer J.W., 1974 – Early chemical history of the solar system. *Reviews of Geophysics and Space Physics* 12, 71–101.

Hezel D.C., Schlüter J., Kallweit H., Jull A.J.T., Al Fakeer O.Y., Al Shamsi M., Strekopytov S., 2011 – Meteorites from the United Arab Emirates: Description, weathering, and terrestrial ages. *Meteoritics & Planetary Science* 46 (2), 327–336.

Hutchison R., 2006 – *Meteorites. A Petrologic, Chemical and Isotopic Synthesis*. Cambridge University Press, Cambridge, UK.

Jarosewich E., 1990 – Chemical analyses of meteorites: a compilation of stony and iron meteorite analyses. *Meteoritics* 25, 323–337.

Kallemeyn G.W., Rubin A.E., Wang D., Wasson J.T., 1989 – Ordinary chondrites: bulk chemical composition, classification, lithophile-element fractionations, and composition-petrographic type relationships. *Geochimica et Cosmochimica Acta* 53, 2747–2767.

Koblitz J., 2010 – MetBase®, ver. 7.3, Meteorite Data Retrieval Software. Ritterhude, Germany.

Lauretta D.S., Nagahara H., Alexander C.M.O'D., 2006 – Petrology and Origin of Ferromagnesian Silicate Chondrules. [in:] Lauretta D.S., McSween H.Y. Jr. (eds.) – *Meteorites and the Early Solar System II*, University of Arizona Press, Tucson, 431–459.

McSween H.Y., Huss G.R., 2010 – *Cosmochemistry*. Cambridge University Press, New York, USA.

Mészáros M., Kereszturi Á., Ditrói-Puskás Z., 2014 – A new classification of Nyirábrany, an ordinary chondrite from Hungary. *Meteorites* 3 (1–2), 19–32.

Rubin A.E., Scott E.R.D., Keil K., 1997 – Shock metamorphism of enstatite chondrites. *Geochimica et Cosmochimica Acta* 61 (4), 847–858.

Stöffler D., Keil K., Scott E.R.D., 1991 – Shock metamorphism of ordinary chondrites. *Geochimica et Cosmochimica Acta* 55, 3845–3867.

Van Schmuss W.R., Wood J.A., 1967 – A chemical-petrologic classification for the chondritic meteorites. *Geochimica et Cosmochimica Acta* 31 (5), 747–765.

Velbel M.A., 2014 – Terrestrial weathering of ordinary chondrites in nature and continuing during laboratory storage and processing: Review and implications for Hayabusa sample integrity. *Meteoritics & Planetary Science* 49 (2), 154–171.

Wanke H., Dreibus G., 1988 – Chemical composition and accretion history of terrestrial planets. *Phylosophical Transactions of the Royal Society of London* A325, 545–557.

Wasson J.T., Kallemeyn G.W., 1988 – Composition of chondrites. *Phylosophical Transactions of the Royal Society of London* A325, 535–544.

Weisberg M.K., McCoy T.J., Krot A.N., 2006 – Systematics and evaluation of meteorite classification. [in:] Lauretta D.S., McSween H.Y. Jr. (eds.) – *Meteorites and the Early Solar System II*, University of Arizona Press, Tucson, 19–52.

Wlotzka F., 1993 – A Weathering Scale for the Ordinary Chondrites. *Meteoritics* 28 (3), 460–460.

Yin Q.Z., 2005 – From dust to planets: the tale told by moderately volatile elements. [in:] Krot A.N., Scott E.R.D., Reipurth B. (eds.) – Chondrites and the Protoplanetary Disk, *ASP Conference Series* 341, Astronomical Society of the Pacific, San Francisco, 632–644.

Zurfluh F.J., Hofmann B.A., Gnos E., Eggenberger U., Greber N.D., Villa I.M., 2012 – Weathering and strontium contamination of meteorites recovered in the Sultanate of Oman. *Meteorite*, February 2012, 34–38.

Publishers: Wrocław University of Technology, Faculty of Geoengineering, Mining and Geology
Polish Meteorite Society

GUIDELINES FOR AUTHORS

Meteorites publishes only original works that have not been previously published in any journal, joint publication, conference materials, on the Internet, or in any other citable form, and that are not under consideration by other publications at the time of submission. Authors must own the copyright to the data, tables, figures and appendices. Manuscripts accepted for publication in Meteorites (and excerpts) must not be published in any periodical in any language without the permission of the editor-in-chief.

Authors are asked to communicate their contact details (including their e-mail addresses) to the editorial staff and two potential reviewers. Papers must be written in English. Authors are expected to have the papers reviewed linguistically prior to submitting. Papers should be prepared using Microsoft Word 97 or a later version. Figures must be provided in a jpg format with a printable version of at least 400 dpi. Only electronic submissions through e-mail will be accepted.

Italics should be used for equations and formulas only. Decimals should be separated with a point instead of a comma, and a space should be used as a thousands separator. Double or triple line spacing should be used and ample margins of at least 3 cm should be employed. The text should be justified and words should not be divided at the end of a line.

Tables and figures must be prepared on separate pages and not included as part of the main text. They must be numbered in Arabic numerals according to their sequence in the text. Captions to tables and figures must be placed at the end of the manuscript, after the references.

Appendices will be published by way of exception only and may include, but are not limited to, large tables with numerical or analytical results, or the sources of data used for the analysis. Equations and formulas must be centered and numbered consecutively and their numbers must be written on the right, justified in parentheses. Variables and constants should be defined under equations and formulas. Refer to the example below.

$$v > \sqrt{\frac{2MG}{r}} \tag{1}$$

where:

v – escape velocity, $m \cdot s^{-1}$,

M – mass of body from which object is projected, kg,

G – universal gravitational constant, $N \cdot m^2 \cdot kg^{-2}$,

r – radius of body from which object is projected, m.

The manuscript title should be bold and capitalized, e.g.: **ACHONDRITES AND THEIR PARENT BODIES**. Full name of the author(s) should be given below the title, followed by their affiliation(s), and exact postal address. In the case of a paper with more than one author, correspondence concerning the paper will be sent to the first author unless the editorial staff is advised otherwise by an underlining of the relevant name(s). First name should be given first and the initials of middle names and the surname, thereafter, e.g.: Tadeusz A. PRZYLIBSKI.

The abstract of up to 300 words and keywords of up to 9 words must be provided. Paper should be divided into sections, described by short headings. Section headings should be capitalized, e.g.: INTRODUCTION, EXPERIMENTAL / METHODS, DISCUSSION, CONCLUSIONS, etc. Acknowledgments may be included after the body of the text before the references.

Mineral and meteorite names used in the paper must conform to the current nomenclature guidelines of the International Mineralogical Association and the Meteoritical Society. If the name of a particular meteorite has not been officially recognized yet, an announcement will have to be published in Meteorites following its approval.

The "0.0" value must not be used for immeasurably small amounts of particles. The "n.d." (not detected or no data) or "n.a." (not available) abbreviations should instead be used.

CITING SOURCES

Cited sources should be enclosed within parentheses. The author's name and the year of publication should be separated by a comma. Papers with more than two authors should be cited by the first author's last name followed by „et al.", and then the year of publication. If the particular author has two or more texts published in the same year, add a letter after the year to distinguish between them. The same letter should be included in the list of works cited at the end of the paper. See the examples below which will be further used in the bibliography section.

(Rubin, 2003)
(Hutchison, 2004)
(Consolmagno & Britt, 2004)
(Przylibski et al., 2005)

PREPARING REFERECNES

References should be arranged alphabetically. Multiple citations of the same author should be listed chronologically. Works by two authors should be cited by using their last names and should be arranged alphabetically by the names of the authors. Multiple papers by the same author having the same publication date should be distinguished by consecutive letters of the alphabet commencing with "a". Multiple publications with the same co-author should be listed chronologically. See the examples below.

Rubin A.E., 2003 – Chromite-Plagioclase assemblages as a new shock indicator; implications for the shock and thermal histories of ordinary chondrites. *Geochimica et Cosmochimica Acta*, 67 (14), 2695–2709.

Hutchison R., 2004 – Meteorites: A petrologic, chemical and isotopic synthesis. Cambridge University Press, New York.

Consolmagno G.J., Britt D.T., 2004 – Meteoritical evidence and constraints on asteroid impacts and disruption. *Planetary and Space Science*, 52 (12), 1119–1128.

Przylibski T.A., Zagożdżon P.P., Kryza R., Pilski A.S., 2005 – The Zakłodzie enstatite meteorite: Mineralogy, petrology, origin, and classification. *Meteoritics & Planetary Science*, 40 (9), Supplement, A185–A200.

Please refer to the latest issue in case of any doubts regarding the preparation of the manuscript.
Proofs will be sent as a PDF file to the e-mail address of the corresponding author. Only minor changes that do not alter the arrangement of the text and corrections of editorial errors will be allowed at this stage. Substantial changes to the text will not be accepted. Proofs should be returned to the editorial staff within seven calendar days. A PDF file of the article will be sent free of charge to the corresponding author immediately after publication.

COPYRIGHT INFORMATION

The author retains the larger portion of the copyright. The following applications of the article are not subject to the editorial staff's opinion or approval:

- making hard and electronic copies of the article for the personal use of the author, including the personal use connected with teaching,
- making copies of the article for the personal use of the author's colleagues from similar fields of research,
- presentation of the article to any forum (conference, symposium or other official meeting) and the document's distribution among its participants,
- obtaining patents based on information contained in the article,
- re-use of all or part of the published article in the author's doctoral thesis or other scientific papers,
- re-use of all or part of the published article in compilations of the author's publications,
- re-use of all or part of the published article in books on the condition that a reference is made to the first publication of the article.

Crew

EDITOR-IN-CHIEF:
Tadeusz A. Przylibski
Wrocław University of Technology
Faculty of Geoengineering, Mining and Geology
ul. Na Grobli 15, 50-421 Wrocław, Poland
tadeusz.przylibski@pwr.edu.pl

MANAGING EDITOR:
Tomasz Jakubowski
illaenus@gmail.com

STATISTICAL EDITOR:
Katarzyna Łuszczek
katarzyna.luszczek@pwr.edu.pl

ARTICLES TECHNICAL EDITOR
Marek J. Battek
marek@silez.pl

WEB PAGE TECHNICAL EDITOR:
Tomasz Stawarz
tomssmot@gmail.com

NATIVES:
Jason Utas
meteoritekid@gmail.com
Mendy Ouzillou
ouzillou@yahoo.com

LINGUISTIC EDITOR:
Jakub Radwan
jakub@meteorites.pl

Table of Contents

www.meteorites.pwr.wroc.pl